DEMOCRATIC AND POPULAR REPUBLIC OF ALGERIA
MINISTRY OF HIGHER EDUCATION AND SCIENTIFIC RESEARCH

Abou Bekr Belkaid University

Faculty of Sciences

Department of Physics

Laboratoire de Physique Théorique
Option: Matière Condensée

Numerical study of ground state properties of magnetic disordered systems: Application of Density Matrix Renormalization Group

by

Mohamed MEBROUKI

A thesis submitted to the faculty of sciences
for the degree of Doctorate

Defended: **April 14, 2013**

Pr. **Gouti Merad**	Professor at Tlemcen University	**Chairman**
Pr. **Ahmed Houari**	Professor at Tlemcen University	**Supervisor**
Pr. **Noureddine Zekri**	Professor at Oran University	**Examinator**
Pr. **Mostefa Kameche**	Professor at Oran University	**Examinator**
Dr. **Smain Bekhechi**	Maître de conf. at Tlemcen University	**Examinator**
Dr. **Houda Faraoun**	Maître de conf. at Tlemcen University	**Examinator**

Academic year : 2012-2013

Numerical study of ground state properties of magnetic disordered systems: Application of Density Matrix Renormalization Group.

A Thesis Presented to
the Faculty of Science, Department of Physics
University of AbouBekr Belkaid Tlemcen

In Partial Fulfillment
of the requirements for the Degree of
Doctor in Physics

by
Mebrouki Mohamed
2012

This thesis is submitted in partial fulfillment of
the requirements for the degree of

Doctor of Physics in condensed matter

MEBROUKI Mohamed

Pr. Houari Ahmed
Thesis Advisor

To Selmane, Sarah and Soheib

Table of Contents

This page is intentionally left blank.

List of Tables

List of Figures

ABSTRACT

In 1975, K. Wilson has succeeded, through a new numerical method, called renormalization group, to solve Kondo problem. This was a major breakthrough in the domain at a point that K. Wilson was awarded the Nobel prize in 1982. This success has inspired him, and many others, to apply the renormalization group method to quantum systems. Unfortunately, the results were not so encouraging, due to their weak accuracy. In order to overcome this drawback, many attempts was made by physicists: one of them was S. White, who, apparently, was already working on the subject. He was able, after many attempts, to localize the source of failure of Wilson method; it is the criteria of choosing the states that must represent each block to form bigger ones. In 1993, S. White suggested, in his famous paper, to use density matrix concept. Thus, instead of choosing the lowest energy states, he has to build a density matrix of a block, diagonalize it and then choose states corresponding to its highest eigenvalues. This allows him to pick up the "best" states that can represent a block as a part of a superblock. And it works!

Since then, the Density Matrix Renormalization Group (DMRG) has become a powerful tool to investigate the ground state properties of a large panel of quantum systems, with all variations these systems could present. The method was also combined to other numerical methods to better understand the behaviour of those systems. There were attempts to apply it even to cultural domain!

Like any other numerical method, DMRG has its own limitations: the most in sight is that the method itself was firstly designed to deal with 1-dimensional systems, even though, attempts was, later, made to extend it to higher dimensions.

In this thesis, I will first introduce the DMRG method by going back to its origin. Then, technical details of the involved computations are given. I also use DMRG to investigate the ground state properties of spin chains within Heisenberg model with spin site lacking.

En 1975, Kenneth Wilson a parvenu à l'aide d'une nouvelle méthode numérique, à savoir, le groupe de renormalisation, à résoudre le problème de Kondo. Ce qui a été considéré en son temps comme une percée dans son domaine; au point que K. Wilson lui même a reçu le prix nobel en 1982. Ce succès lui a inspiré, et à bien d'autres physiciens, d'appliquer la méthode de groupe de renormalisation aux systèmes quantiques. Malheureusement, les résultats n'étaient pas si encourageantes, à cause de leurs faibles précisions. Pour y remédier, plusieurs physiciens se sont mis à la besogne. Steve White, qui travaillait déjà sur le sujet, a été en mesure, après plusieurs tentatives, à déceler la source du problème: le critère qu'adoptait Wilson pour le choix des états qui devaient représenter chaque bloc du système afin de construire une bloc plus grand n'était pas correct. Pour cela, White a suggéré, dans un article, devenu célébré depuis, d'utiliser le concept de la matrice densité. Ainsi, au lieu de choisir les états des énergies les plus bas, la matrice densité d'un bloc doit être construite, puis diagonalisée. Cette procédure permet d'utiliser les états qui représentent le mieux chaque bloc pour ensuite construire un superbloc.

Depuis, la méthode de groupe de renormalisation par la matrice densité est devenue un outil puissant dans l'étude des propriétés de l'état fondamental d'une panoplie de systèmes quantiques, avec toutes les variétés que peuvent présenter ces derniers. La méthode est

aussi combinée à d'autres méthodes numériques pour mieux comprendre le comportement physiques de ces systèmes. C'est ainsi que même les sciences sociales n'ont pas échappées à l'application de la méthode!

Comme toute méthode numérique ayant ses propres limites, la présente méthode ne fait pas exception. En effet, son application exclusive à des systèmes unidimensionnels était de son propre nature, et présentait un inconvénient majeur pour le traitement des systèmes plus réalistes; bien que beaucoup d'effort a été fait dans ce sens.

Dans ce travail, Je fais une introduction à la méthode du groupe de renormalisation par la matrice densité en retraçant son histoire. Ensuite, je donne les détails techniques de l'implémentation de la méthode. Celle-ci est aussi utilisée pour l'étude des propriétés physiques de l'état fondamental des systèmes de spins.

Numerical study of ground state properties of magnetic disordered systems:
Application of Density Matrix Renormalization Group.

This work has a twofold goal: on one hand, I attempt to extend the Density Matrix Renormalization Group (DMRG) method to be applied to systems with geometries other than one dimension. Thus, a system composed of two crossed chains is investigated within the simple Anderson model. An appropriate DMRG procedure is then applied. Results are so encouraging, with high accuracy. The drawback is that the model itself, in its present form, has no physical utility. It remains a toy model!

On the other hand, I use DMRG method to investigate ground state properties of spin chains where a spin site is lacking (disordered systems). I use next nearest-neighbours interactions to keep the spin chain assembled. The idea is new, and the results have brought some light on the behaviour of ground state and first excited states energies when a spin site is missing.

Chapter 1

Introduction

In quantum mechanics, diagonalizing the Hamiltonian of a system to obtain its eigenvalues and eigenvectors plays a fundamental role in the investigation of its physical properties, especially at low temperatures. The larger the system, the more efficient is the investigation of its properties. However, increasing the size of the system will terribly increases the corresponding Hilbert space. More and more memory and running time on computers are then needed, and, unfortunately, these facilities become rapidly prohibitive, even for small systems. For example, a one-band Hubbard chain of just 10 sites (which is 'nothing' compared to a realistic structure) is represented in a Hilbert space of $4^{10} = 1048576$ states, which is enormous, at least for us!

The use of symmetry properties of the system to investigate desired states with defined quantum numbers can reduce the Hilbert space, and then smaller matrices are diagonalized. Still, this reduction is not so helpful in many cases!

Helped by the rapid increase of the computational power of the computers, physicists have proposed computational techniques for computing the low-lying states of strongly correlated systems; with mainly two types of approximations. The first class is based on the projection of a huge Hilbert space on a smaller basis by means of truncation. Lanczos method, Configuration Interaction schemes, and more recently the Density Matrix Renormalization Group are the most representative. The second branch of these approximations uses the sampling of the full Hilbert space. The most in sight is the Monte carlo method.

In this thesis I will focus on one particular type of numerical methods, the Density Matrix Renormalization Group (DMRG). This numerical method, invented by Steve White in 1992, and which has its origin back to Kenneth Wilson works on renormalization group, has proven to be the most accurate tool for the numerical solution of one-dimensional models. It was firstly applied to solve the ground state of the spin 1/2 Heisenberg chain. Since then, the method has been applied to many models; from one dimensional fermionic systems, ladder models and some two dimensional models both in real-space and momentum space. In addition, generalization of the DMRG algorithm has been proposed for the calculation of thermodynamic properties, 2D classical systems, phonons models, dynamical correlation functions and even for social culture evolution!

In chapter 1, I revisit the remote origin of the DMRG, back to K. Wilson work on Kondo problem, and see how he had solved it and why the renormalization group (RG) failed when applied to other quantum systems. Then, I will revise some of the ideas that led S. White to invent the DMRG.

In chapter 2, more technical insights on the DMRG method is given. Details about the DMRG technique are abundant in literature, and the reader is invited to consult it.

In chapter 3, I first review different applications of the DMRG to quantum system models. Then I will give examples of DMRG implementation to some strongly correlated system models. The formalism to calculate expectation values of dynamic operators is also presented.

Finally, in chapter 4, my work on DMRG method and its applications is presented. Thus, the toy model of single quantum mechanics particle in box is extended to investigate a two-crossed-chains model. Then, I will present a method using DMRG to compute ground state energy for chains with lacking spin within spin-$\frac{1}{2}$ Heisenberg model. I also present results of entanglement entropy of the spin-$\frac{1}{2}$ Heisenberg chains with and without a single lacking spin site with next nearest neighbours interactions.

Chapter 2

Renormalization group method

2.1 Historical facts

In 1982, Kenneth. G. Wilson was awarded the Nobel prize of physics for his work on Kondo problem. Inspired by ideas from field theory [1] and scaling ideas from condensed matter, he had developed a non-perturbative powerful numerical tool, called since then *the numerical renormalization group method* (NRG) [2], to calculate critical exponents, and later to solve the Kondo problem [3]. This success opened the door to generalizing Wilson's results to deal with more realistic models for magnetic impurities, such as the non-degenerate Anderson model.

In fact, the history of the Kondo problem [4] goes back to the 1930's when a resistance minimum was found at very low temperatures in seemingly pure metals [5].

As a matter of fact, in most metals, when the temperature is lowered, the electrical resistivity decreases as a result of the decreasing amplitude of the thermal ionic vibrations. When small amounts of iron, chromium, manganese, molybdenum, rhenium, or osmium are added to copper, silver, gold, magnesium, or zinc, for example, the resistivity generally exhibits a *minimum*.

In fact, the magnetic impurities can be found in transition metals, such as manganese and iron, rare earths, such as cerium, and the actinides, of which the most important is uranium. The magnetic character of these elements is due to their partially filled inner shells, even though the outer valence states also contain electrons, which influences their electronic density of states [4].

The explanation for this effect was provided by J. Kondo in 1964 [6], within a perturbative calculation for the $s-d$ (or Kondo) model (a model for magnetic impurities in metals), by examining a system of noninteracting electrons undergoing spin flip scatterings by external local moments. He realized that when magnetic impurities are present the conduction electrons may suffer a change of spin as they scatter, and that higher orders of perturbation theory than the first have to be treated very carefully.

Kondo successfully explained the resistance minimum within a perturbative calculation for the $s-d$ (or Kondo) model [6]. He had shown that second-order contributions to the resistivity $\rho(T)$ increased logarithmically with T as T was lowered ($\rho(T) \propto \ln T$). However, Kondo's result implies a divergence of $\rho(T)$ for $T \to 0$, in contrast with the saturation found experimentally. The problem of finding a solution valid in low temperature regime $T \to 0$ is called the 'Kondo problem'.

In his calculations, Kondo started with the part of the perturbing potential containing the magnetic interaction, $\mathbf{s} \cdot \mathbf{S}$, where $\mathbf{s}$ and $\mathbf{S}$ are, respectively, the spin of the conduction electron and the spin of the localized electron in the d or f shell of the impurity. The localized spin can have a total spin different from 1/2. Kondo assumed that the spins of the localized and conduction electrons are uncorrelated and have independently equal probability of initially being either up or down. While this will directly reveal the onset of the resistance minimum as the temperature is lowered, it will fail as the temperature is decreased further; since at the lowest temperatures conduction and localized spins form bound singlet pairs.

Kondo suggested that the resistance minimum is rather a consequence of the interaction between the spins of the localized and conduction electrons, than a fact of the interaction with impurities.

It is worthy to note that impurities in transition metals cannot be treated by the well-known self-consistent field approach [7] due to a strong local Coulomb interaction, and also because we are interested in the behavior of the system as a function of temperature rather than ground state properties. Instead, simpler model Hamiltonians are derived to describe the low energy excitations associated with the impurity.

Conduction electrons in wide bands can be assumed to behave approximately as independent particles moving within a periodic potential. The long range Coulomb interaction between the electrons is screened (contributing to plasma excitations, which are of too high an energy to concern us) so that the electrons are essentially quasi-particles, electrons together with their screening cloud.

One of the most important ways in which impurities affect the behaviour of a metal is their contribution to the electrical resistivity at low temperatures. The conductivity is infinite for electrons in a perfect lattice as there is no scattering, and consequently no current dissipation. At finite temperatures the scattering with phonons usually provides the most important mechanism for the dissipation of the electron current. At low temperatures there are few phonons, so the scattering by impurities and defects becomes more important, and becomes the dominant dissipative mechanism as $T \to 0$, leading to a finite conductivity in this limit.

2.2 How Wilson solved the Kondo problem?

In 1974, K. G. Wilson [2] succeeded to solve the Kondo problem, where, as he himself remarked, "it was the first example where the renormalization group program had been carried out in full". In fact, the solution was based on the division of the whole lattice into *shells* around the impurity, in such a way that the further shell was from the center, the nearer to the Fermi surface the electrons were supposed to be. Shells were integrated in an iterative way, starting from the center, so the external ones only saw the impurity sheltered by the inner shells. It is important to remark that the solution required a strong amount of numerical computations (in 1974 terms) and it was considered to be a great success with an error in the observables of a few percent.

In fact, the usage of mixed real space and momentum space techniques is one of Wilson's great ideas. Electrons which are far away from the impurity only contributed to the magnetic

susceptibility (his main target) if they were so near to the Fermi surface that their ability to be excited could compensate.

In both Kondo model and impurity Anderson model, the impurity couples to a free conduction band with a density of states which is, for simplicity, assumed to be constant within the band-edges $-D$ and D. The technical steps described in the following are mainly designed to deal with the arbitrarily low energies (measured relatively to the Fermi level) present in the free conduction band (for more details see [2, 4, 8]).

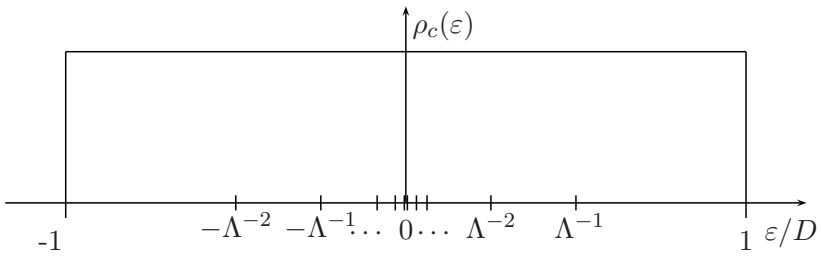

Figure 2.1: Logarithmic discretization of the conduction band

The first step to set up the renormalization group transformation is a logarithmic discretization of the conduction band (see Fig.2.1): the continuous conduction band is divided into infinite intervals $[\xi_{n+1}, \xi_n]$ and $[-\xi_n, \xi_{n+1}]$ with $\xi_n = D\Lambda^{-n}$ and $n = 0, 1, 2, \cdots, \infty$. D is half of the bandwidth of the conduction band and Λ the NRG discretization parameter (typical values used in the calculations are $\Lambda = 1.5, \cdots, 2$). The conduction band states in each interval are then replaced by a *single state*. While this approximation by a discrete set of states involves some coarse graining at higher energies, it captures arbitrarily small energies near the Fermi level.

In a second step, this discrete model is mapped on a semi-infinite chain form via a tridiagonalization procedure (for details, see [8] and section 4.2 in [4]). The Hamiltonian of the semi-infinite chain has the following form (see also Fig. 2.2):

$$H = \sum_\sigma \varepsilon_f f_\sigma^\dagger f_\sigma + U f_\uparrow^\dagger f_\uparrow f_\downarrow^\dagger f_\downarrow + \sum_\sigma V(f_\sigma^\dagger c_{0\sigma} + c_{0\sigma}^\dagger f_\sigma) + \sum_{\sigma,n=0}^{\infty} \varepsilon_n (c_{n\sigma}^\dagger c_{n+1\sigma} + c_{n+1\sigma}^\dagger c_{n\sigma}), \quad (2.1)$$

This form is valid for a general symmetric conduction band density of states. The impurity now couples to a single fermionic degree of freedom only (the $c_{0\sigma}^\dagger$) with a hybridization V. Due to the logarithmic discretization, the hopping matrix elements decrease as $\varepsilon_n \propto \Lambda^{-n/2}$. This means that in going along the chain, the parameters in the Hamiltonian evolve from high energies (given by D and U) to arbitrarily low energies (given by $D\Lambda^{-n/2}$). The renormalization group transformation is now set up in the following way.

We start with the solution of the isolated impurity, that is, the knowledge of all eigenstates, eigenvalues, and matrix elements. The first step of the renormalization group transformation is to add the first conduction electron site, set up the Hamiltonian matrices for

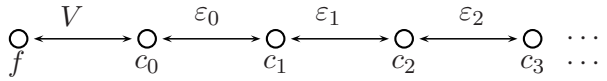

Figure 2.2: Semi-infinite chain form of the single impurity Anderson model

the enhanced Hilbert space, and obtain the information for the new eigenstates, eigenvalues, and matrix elements by diagonalizing these matrices. This procedure is then iterated.

An obvious problem occurs after only a few steps of the iteration. The Hilbert space grows as 4^N (with N the size of the cluster), which makes impossible to keep all the states in the calculation. Therefore, Wilson devised a very simple truncation procedure in which only those states (typically a few hundreds) with the lowest energies are kept. This truncation scheme is very successful but relies on the fact that the hopping matrix elements are falling off exponentially. Higher-energy states therefore do not change the very low frequency behaviour and can be neglected. This procedure gives for each cluster a set of eigenvalues and matrix elements from which a number of physical properties can be derived.

The basic idea of this scheme is that only the low-energy eigenstates obtained for a system of size L will be important in making up the low-energy states of a system of size $L+1$. Note that in isolating the block of length L, one has to decide how to treat the boundaries of the block. The simplest thing to do is to neglect connections to surrounding sites, which corresponds to applying open boundary conditions to the system being diagonalized. This procedure worked well in Wilson's original work on the single impurity Kondo problem and, with minor variations, is still used today for a variety of single and two Kondo and Anderson impurity problems. In his original paper, Wilson has very carefully justified the truncation by perturbatively calculating the error [2]. In addition, he compared the numerical results with analytical analysis of the behaviour near the fixed points. However, when this procedure is applied to other systems for which the model does not include an intrinsic separation of energy scales, the accuracy becomes quite poor after just a few iterations [15].

In general, Wilson's numerical RG procedure then proceeds as follows:

1. Isolate a portion of the system, containing L sites. Here L is chosen to be small enough so that the Hamiltonian $\mathbf{H}_L$ can be diagonalized exactly.

2. Diagonalize $\mathbf{H}_L$ numerically, obtaining the m lowest eigenvalues and eigenvectors.

3. Transform $\mathbf{H}_L$ and other operators in the "block" of length L, to a new basis consisting of the m lowest eigenvectors of $\mathbf{H}_L$, i.e. form $\overline{\mathbf{H}}_L = \mathbf{O}_L^T \mathbf{H}_L \mathbf{O}_L$, , where the columns of $\mathbf{O}_L$ contain the m lowest eigenvectors of $\mathbf{H}_L$. Note that $\overline{\mathbf{H}}_L$ is a diagonal matrix with m elements,.i.e.:

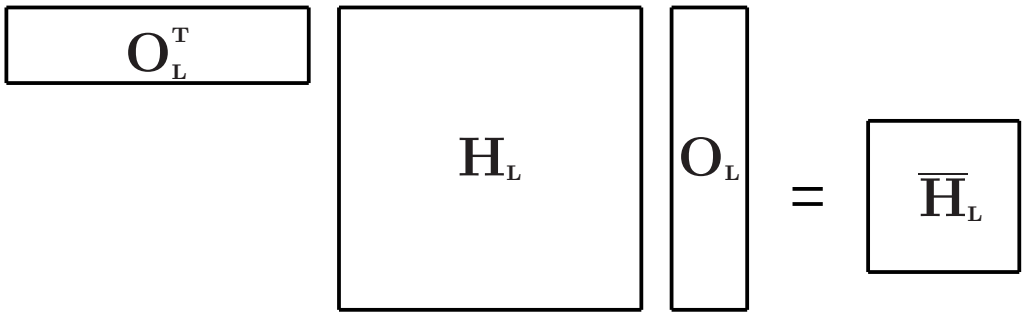

Figure 2.3: Step three of the Wilson RG procedure.

4. Add a site to $\mathbf{H}_L$ to form $\mathbf{H}_{L+1}$. In order to do this, the interaction between the block of length L and the additional site added must be reconstructed.

5. Repeat starting with step (2), substituting $\mathbf{H}_{L+1}$ for $\mathbf{H}_L$.

2.3 What is Renormalization?

The study of electronic properties of quantum lattice systems requires the diagonalization of their Hamiltonians. If the lattice has N sites and there are k possible states per site then the dimension of the corresponding Hilbert space $\mathcal{H}$ is simply k^N. For example, $k = 4$ for the Hubbard model, $k = 3$ for the $t - J$ model and $k = 2$ for the Heisenberg model. However, when N is large enough, it is impossible, at least in the immediate future, to solve the corresponding eigenvalue problem, unless the system itself has an analytic solution. This impasse opens the door to a variety of approximate methods which are more or less accurate with different domain of excellency. Among them, the renormalization group (RG) approach is one of the most relevant, especially its numerical version.

The basic idea of renormalization is to transform a lattice system to a bigger lattice which is apparently the same as the original one. This is done by eliminating number of its degrees of freedom (keep relevant information of a physical system, and neglect or integrate out irrelevant one) followed by an iteration which reduces, step by step, the number of variables until a more manageable situation is reached (see [9, 10, 11] and references therein). In fact, it is a matter of symmetry that the system keeps its *appearance* as we move from one scale to another. During the transformation parameters (coupling constants between components) describing the components (electrons, atoms, atomic spins) of the system will slightly change.

A deeper understanding of the physical meaning of the renormalization group came from the image given by Leo P. Kadanoff. In his paper in 1966 [9], Kadanoff proposed the "block-spin" renormalization group, with a fundamental idea: a spin block behaves, after the coupling constants being appropriately readjusted, in the same way as a single spin does. He proved that this transformation explains some empirical relations among the scaling exponents. A breakthrough was made when, in 1974, Kadanoff and his collaborators worked out the first results for one of the most significative problems: 2D and 3D Ising models [12] [13].

Technically, there are mainly two procedures to reduce the size of the lattice. The first one, introduced by Kadanoff, consists in dividing the lattice into blocks. This can be applied to 2D and 3D systems.

Thus, in 2D Ising systems where each site is occupied by a single atom spin with two degree of freedom, the renormalization process consists in aggregating, for example, four sites together to make a square and then choose for them a single degree of freedom. How could that value be chosen? The mean value of spins seems to be the natural solution, except that it does not provide us with a value when the sum of spins is zero.

To lift this inconvenience, we may allow random values of spins to represent blocks, or adopt more than one degree of freedom for each block, allowing a more refined analysis. This transformation process, called flow, has some fixed points which determine the macroscopic physics of the system.

The second approach, introduced by Wilson [2], starts with a small system whose Hamiltonian can be exactly diagonalized. The system size is then increased without increasing the size of the Hilbert space (the Hilbert space is truncated to a numerically reasonable size) until the desired system size is reached. It is intrinsically restricted to deal with one-dimensional lattices, and was used by Wilson in his treatment of the Kondo problem. The success of the renormalization approach rests on scale separation: for continuous phase transitions, the diverging correlation length sets a natural long-wavelength low-energy scale which dominates the physical properties, and fluctuations on shorter length scales may be integrated out and summed up into quantitative modifications of the long-wavelength behaviour. In the Kondo problem, the width of the Kondo resonance sets an energy scale such that the exponentially decaying contributions of energy levels far from the resonance can be integrated out. This is the essence of the numerical renormalization group RG.

In fact, after two small blocks are linked to form a twice larger block, the Hamiltonian of this latter is then exactly diagonalized and its eigenstates are used as base states. Only eigenstates whose energy lies below a certain threshold are kept. The states which are kept characterize the new block that is again linked to an identical block, and the process is iterated. During this process of block forming the Hamilton operator of the systems must not change. Also, physical quantities like the partition function for thermal phase transitions or the density of states for the Anderson model [14] are not changed, while the coupling constants are varying according to their own trajectories, for different initial values, in the corresponding space. Another version of the Wilson approach is to start from an exact representation of a small subsystem and build effective representations of larger subsystems iteratively, adding one site at every iteration.

In systems where the degrees of freedom can be cast in terms of the Fourier modes of a given field, the so-called momentum-space RG can be used. It proceeds by integrating out a

certain set of high momentum (high spatial frequency) modes, since high spatial frequency is related to short length scales.

2.4 The Renormalization Group mathematically

The renormalization group is a mapping R of a Hamiltonian $H(\mathbf{K})$, which is specified by a set of interaction parameters or couplings $\mathbf{K} = (K_1, K_2, \cdots)$ into another Hamiltonian of the same form with a new set of coupling parameters $\mathbf{K'} = (K_1', K_2', \cdots)$. This is expressed formally

$$\mathbf{R}\{\mathbf{H}(\mathbf{K})\} = \mathbf{H}(\mathbf{K'}), \tag{2.2}$$

or equivalently,

$$\mathbf{R}(\mathbf{K}) = \mathbf{K'}. \tag{2.3}$$

The transformation is in general non-linear. Such transformations were generated in the scaling approach to eliminate higher energy states. The new effective Hamiltonian is then valid over a reduced energy scale. In applications to critical phenomena the new Hamiltonian is obtained by removing short range fluctuations to generate an effective Hamiltonian valid over larger length scales. The transformation is usually characterized by a parameter, say α, which specifies the ratio of the new length or energy scale to the old one. A sequence of transformations,

$$\mathbf{K'} = \mathbf{R}_\alpha(\mathbf{K}), \qquad \mathbf{K''} = \mathbf{R}_\alpha(\mathbf{K'}), \qquad \mathbf{K'''} = \mathbf{R}_\alpha(\mathbf{K''}), \quad \text{etc.} \tag{2.4}$$

generates a sequence of points or a *trajectory* in the parameter space $\mathbf{K}$, where α is a continuous variable. The transformation is constructed so that it satisfies

$$\mathbf{R}_{\alpha'}\{\mathbf{R}_\alpha(\mathbf{K})\} = \mathbf{R}_{\alpha+\alpha'}(\mathbf{K}). \tag{2.5}$$

In applications, as the transformations are generated either by a reduction in energy scale or a coarse graining of space, inverse transformations do not exist so that, strictly speaking, the transformations constitute a mathematical semi-group rather than a group.

One of the key concepts of the renormalization group is that of a **fixed point**. This is a point $\mathbf{K}^*$ which is invariant under the transformation,

$$\mathbf{R}_\alpha(\mathbf{K}^*) = \mathbf{K}^*. \tag{2.6}$$

The trajectories generated by the repeated application of the renormalization group tend to be drawn towards or expelled from the fixed points. The behaviour of the trajectories near a fixed point can usually be determined by linearizing the transformation in the neighbourhood of the fixed point. If in the neighbourhood of a particular fixed point $\mathbf{K} = \mathbf{K}^* + \delta\mathbf{K}$ then, expanding $\mathbf{R}_\alpha(\mathbf{K})$ in powers of $\delta\mathbf{K}$,

$$\mathbf{R}_\alpha(\mathbf{K}^* + \delta\mathbf{K}) = \mathbf{K}^* + \mathbf{L}_\alpha^* \delta\mathbf{K} + O(\mathbf{K}^2), \tag{2.7}$$

where $\mathbf{L}^*_\alpha$ is a linear transformation. If the eigenvectors and eigenvalues of $\mathbf{L}^*_\alpha$ are $\mathbf{O}^*_n(\alpha)$ and $\lambda^*_n(\alpha)$, and if these are complete (there is in general nothing to ensure this, so it is an assumption) then they can be used as a basis for a representation of the vector $\delta\mathbf{K}$,

$$\delta\mathbf{K} = \sum_n \delta K_n \mathbf{O}^*_n(\alpha), \tag{2.8}$$

where δK_n are the components.

How the trajectories move in the region of a particular fixed point depends on the eigenvalues $\lambda^*_n(\alpha)$. If we act m times on a point $\mathbf{K}$ in the neighbourhood of a fixed point $\mathbf{K}^*$ then, from (2.7), we find

$$\mathbf{R}^m_\alpha(\mathbf{K}^* + \delta\mathbf{K}) = \mathbf{K}^* + \sum_n \delta K_n \lambda^{*\,m}_n(\alpha)\mathbf{O}^*_n(\alpha), \tag{2.9}$$

provided all the points generated by the transformation are in the neighbourhood of the fixed point so that the linear approximation (2.7) remains valid.

For eigenvalues $\lambda^*_n(\alpha) > 1$, which are termed *relevant*, the corresponding components of $\delta\mathbf{K}$ in (2.9) increase with m. Those corresponding to eigenvalues $\lambda^*_n(\alpha) < 1$, termed *irrelevant* (this is a technical term and should not be always taken literally), get smaller with m. Eigenvalues $\lambda^*_n(\alpha) = 1$ are termed *marginal* and the corresponding components in (2.9) do not vary with m. The eigenvalues of the linearized equation lead to a classification of the fixed points. *Stable* fixed points have only *irrelevant* eigenvalues so $\delta\mathbf{K} \to 0$ and the trajectories in their neighbourhood are drawn in towards the fixed point. If there are one or more relevant eigenvalues then the fixed points are *unstable* and the trajectories are eventually driven away from the fixed point in a direction largely determined by the most relevant eigenvector. A fixed point is *marginal* if it has no relevant eigenvalues and at least one marginal one. In this case the behaviour of the trajectories in the neighbourhood of the fixed point cannot be determined solely from the linearized form (2.7) and the non-linear corrections have to be examined. There may be competitive influences on a trajectory due to several fixed points. The region in which a trajectory passes from the sphere of influence of one fixed point to that of another is known as a *crossover* region.

Transformations are then generated to find how the interaction between blocks varies as the size of the block increases, on the assumption that the interblock interaction can always be described by a model of the same form (at least approximately). The critical exponents are then deduced from these scaling transformations in the limit in which the block size tends to infinity (it is the interactions between the very large blocks that determine the long range fluctuations that determine the critical behaviour). These transformations are essentially renormalization group transformations, and are such that the trajectories for very large blocks are controlled by an unstable fixed point.

2.5 Numerical RG for a Particle in a Box

In order to understand why the Wilson numerical renormalization group procedure breaks down for interacting quantum chemical systems, it is useful to consider first its application

to a simple non interacting problem, e.g. a linear chain of H-atoms. The Hamiltonian that we will consider is the simple Hückel Molecular Orbital (HMO) approximation:

$$H = \alpha \sum_{i=1}^{L} c_i^\dagger c_i + \beta \sum_{i=1}^{L-1} (c_i^\dagger c_{i+1} + c_{i+1}^\dagger c_i) \tag{2.10}$$

where $c_i^\dagger$ and c_i are respectively the creation and annihilation operators for an orbital on site i. The matrix elements $H_{ij} = \langle i|H|j\rangle$ are then

$$H_{ij} = \begin{cases} \alpha = 0 & i = j \\ \beta = -1 & |i-j| = 1 \\ 0 & otherwise \end{cases} \tag{2.11}$$

The values: $\alpha = 2$ and $\beta = -1$ are chosen so that this operator is just the discretization of the second derivative operator, $\frac{\partial^2}{\partial x^2} \Rightarrow \frac{\partial^2 f(x)}{\partial x_l^2} \approx \frac{2f(x_l) - f(x_{l-1}) - f(x_{l+1})}{h^2}$.

The Wilson procedure described in the previous section can be carried out on this system with just a few minor modifications. First, since this is a one-particle problem, the dimension of the Hilbert space for a grid of length L is L, rather than $exp(L)$ as in an interacting system. Since the Hilbert space grows less rapidly with system size for the non-interacting systems, we will add two equal-sized blocks in the real-space blocking step, rather than adding a site at a time. Secondly, the formalism of putting the blocks together is a little simpler.

In step (1) of the Wilson's procedure, we isolated a block of length L. We can understand how this is done for the non-interacting system by considering a semi-infinite system broken up into blocks of length L. The Hamiltonian can then be written:

$$\mathbf{H} = \begin{pmatrix} \mathbf{H}_L & \mathbf{T}_L & 0 & 0 & \cdots \\ \mathbf{T}_L^\dagger & \mathbf{H}_L & \mathbf{T}_L & 0 & \cdots \\ 0 & \mathbf{T}_L^\dagger & \mathbf{H}_L & \mathbf{T}_L & \cdots \\ \vdots & \vdots & \vdots & \vdots & \end{pmatrix} \tag{2.12}$$

For $L = 1$, the $\mathbf{H}_1$ is a 1×1 matrix with value 2 and $\mathbf{T}_1$ is a 1×1 matrix with value -1. For larger L, $\mathbf{H}_L$ just has the form of Eq. (2.11), and $\mathbf{T}_L$ just has a -1 in the lower left corner, and just connects the sites on the block boundaries. Isolating a block then consists of neglecting the $\mathbf{T}_L$, and therefore applies fixed boundary conditions to $\mathbf{H}_L$. Here we use the term "fixed" boundary conditions rather than the equivalent "open" boundary conditions to emphasize that the single-particle wavefunction vanishes at the boundary. In step (2), we diagonalize $\mathbf{H}_L$ and form

$$\mathbf{O}_L = \begin{pmatrix} | & & | \\ \bar{v}_1 & \cdots & \bar{v}_m \\ | & & | \end{pmatrix} \tag{2.13}$$

where $\bar{v}_1 \cdots \bar{m}$ are the eigenvectors corresponding to the $m \leq L$ lowest eigenvalues of $\mathbf{H}_L$. In step (3), we form the diagonal $m \times m$ matrix $\overline{\mathbf{H}}_L = \mathbf{O}_L^t \, \mathbf{H}_L \, \mathbf{O}_L$ and transform the connection between $\mathbf{H}_L$ and the rest of the system $\mathbf{T}_L$ to the new basis by forming $\overline{\mathbf{T}}_L = \mathbf{O}_L^t \, \mathbf{T}_L \, \mathbf{O}_L$.

We now increase the size of the system, step (4), by putting two blocks of size L together to form a system of size $2L$ with

$$\mathbf{H}_{2L} = \begin{pmatrix} \overline{\mathbf{H}}_L & \overline{\mathbf{T}}_L \\ \overline{\mathbf{T}}_L^\dagger & \overline{\mathbf{H}}_L \end{pmatrix} \tag{2.14}$$

and

$$\mathbf{T}_{2L} = \begin{pmatrix} 0 & 0 \\ \overline{\mathbf{T}}_L & 0 \end{pmatrix} \tag{2.15}$$

The procedure can then be repeated starting with step (2) by substituting $\overline{\mathbf{H}}_{2L}$ and $\overline{\mathbf{T}}_{2L}$ for $\mathbf{H}_L$ and $\mathbf{T}_L$. The size of the system therefore doubles at each step, but the size of the matrix to be diagonalized is at most $2m \times 2m$. Notice that since we transform to a truncated basis at each step, the matrix elements of $\overline{\mathbf{H}}_L$ and $\overline{\mathbf{T}}_L$ can no longer be easily related to the original real-space basis. However, if m were equal to L at each step, the procedure would be exact; it would just be a complicated reshuffling of the original Hamiltonian.

This scheme is depicted pictorially in Fig. 2.4. For a Hamiltonian represented in a real-space basis, the RG step is a real-space blocking scheme. Typically, the number of states m kept at each step is held constant, so the time and memory required for each diagonalization stays the same, and the computer time needed is linear in L.

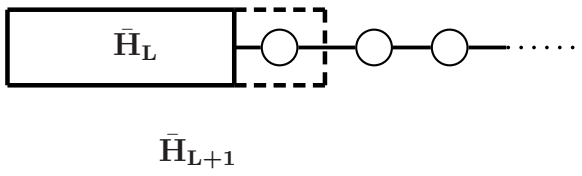

Figure 2.4: A pictorial depiction of the Wilson numerical RG procedure.

This procedure performs quite badly as soon as $m < L$. There are large errors in the energies of the lowest few states after only the first few truncating steps. This failure was pointed out by Wilson at an informal seminar at Cornell University in 1986 as an example of a numerical RG procedure which does not work. He also, pointed out that in this simple system it is easy to understand why the procedure fails. In the continuum limit, the linear H-atom chain model with fixed boundary conditions describes a particle-in-a-box of length L with an infinitely high potential at the walls. The eigenfunetions are therefore particle-in-a-box eigenfunctions: $\psi_n(x) \propto \sin(\frac{n\pi x}{L})$ with n a positive integer, and vanish at the boundaries of the box. In the RG procedure, the lowest few eigenstates of a system of length L are combined to form the low-lying eigenstates of a system of length $2L$. Clearly, a combination of the ground states of two systems of length L is a bad approximation to the ground state for a system of length M. Since the wave vectors of the discrete system take on

small but finite values on the first and last sites of the system, the "kink" at the boundary between the blocks can be removed, but only by using almost all of the eigenstates of the smaller block.

2.6 Real-Space Numerical Renormalization Group (NRG) Algorithm for a 1D Quantum Lattice

In the standard real-space NRG, one begins by breaking the 1D chain into finite identical blocks. It is usually convenient to start at the first iteration with blocks consisting of just one site. We will label the blocks, "B" and the block Hamiltonian "H_B" . H_B contains all terms of H involving only sites contained in B. H_B is represented as an $m \times m$ matrix where m is the number of states of the block B. The information describing the interactions between blocks is also needed. Now, the standard procedure is as follows:

1. At the beginning of an iteration, one forms the Hamiltonian for two blocks joined together, H_{BB}. BB has m^2 states.

2. The lowest-lying eigenstates $u^{\alpha}_{i_1 i_2}, \alpha = 1, \cdots, m$ of H_{BB} are the states used to describe B' ($BB \rightarrow B'$), obtaining by diagonalization of H_{BB}

3. Then one forms matrix representations of boundary operators corresponding to the interactions between neighbouring blocks for BB from the corresponding matrices for B.

4. The new block Hamiltonian matrix $H_{B'}$ is evidently diagonal in this basis; but in the more general case where the states kept, the u^{α}, are not eigenstates of H_{BB} we can use this transformation where the $m \times m^2$ matrix O is made out of the basis in such a way that the rows of O are the states kept. If O were square, this would be a unitary transformation. Since O is not square, the transformation truncates away the high-energy states. Moreover, in order to obtain new matrices for boundary operators at this stage, it is necessary to use O again.

5. Now we can replace B by B' and start the next iteration. The iteration is continued until the system is large enough to represent properties of the infinite system.

Many authors applied the real-space approach described below to quantum systems : 1D Hubbard model [15], 1D Heisenberg model [16], 2D Anderson localization [17]. The results are more or less discouraging, and the standard numerical RG approach generally performs poorly.

2.7 Why Wilson Renormalization group fails?

While the Wilson approach of renormalization leads to solve accurately the Kondo problem, it fails to give accurate results when applied to strongly correlated systems like Hubbard model, t-J model and Heisenberg model [15, 18, 19, 16]. The most important difference between the Kondo system and a 1D system is that the couplings between adjacent layers

or "sites" decreases exponentially in the Kondo system, whereas it remains constant for a 1D system. This exponential decrease is the key to the success of the method for the Kondo system and related impurity systems.

Technically, the failure of Wilson's RG lies in the way each method deals with entanglement. Typically the ground state of a lattice system exhibits quantum correlations. In order to represent the state of an isolated portion of lattice sites, say A, it is necessary to take into account the correlations between A and the rest of the lattice, say C. Due to the nonlocal nature of the entanglement responsible for the correlations, it is impossible to represent the state of AC using only the local degrees of freedom of A. Thus Wilson's RG cannot represent the correlations of A with C unless a full exact diagonalization is performed. Thus, neglecting all connections to neighbouring blocks during the diagonalization of the block Hamiltonian introduces large errors which cannot be corrected by any reasonable increase in the number of states kept.

In quantum information language, the failure is due to the fact that the ground state of an interacting lattice is typically entangled, and thus a subsystem of the total lattice cannot be assigned a definite state.

This can be understood in detail by considering a toy model, a single particle on a tight-binding chain which is equivalent in the continuum limit to a 1D particle in a box with the Hamiltonian matrix like that:

$$H = \begin{cases} 2, & i = j, \\ -1, & |i-j| = 1 \\ 0 & \text{otherwise} \end{cases} \tag{2.16}$$

Applying the outlined real-space NRG approach to this problem, gives very poor results.

2.8 The way towards Density Matrix Renormalization Group (DMRG)

In order to improve the performance of the real-space RG, many authors were bended over. Thus, instead of doubling the block size, Xiang and Gehring [16] used to add a single site to a block at each iteration. The result was more encouraging, but still with low accuracy.

Wilson himself was convinced that the truncation of the interactions leading to discontinuities at the edge of a block was unjustified, because ignoring them means that the retained states vanish at the edge of the blocks, and any subsequent states. Thus, he proposed, in an informal talk in 1986, that attempts to fix the approach should pass first through the solution of the particle-in-a-box problem of real space RG before trying out many particle systems [20]. Steve R. White was among the assistance and decided to take care of the problem .

In fact, few years after, S. White and R. Noack [21] had succeeded to formulate two types of RG procedures which solve these problems and work quite well for the single-particle problem. Both are based on choosing a new basis for H_L which is not the eigenbasis of H_L.

In the first procedure, called the combination of boundary conditions (CBC) method, the new basis is formed from the low-lying eigenstates of several different block Hamiltonians. The Hamiltonians are formed by applying a number of different boundary conditions to the edge of the block. For example, fixed and free (for free boundary conditions the derivative

of the wave function vanishes at the boundary) boundary conditions can be applied. One can form $H_L^{bb'}$ with $b, b' =$ fixed or free. For example,

$$H_{L=2}^{\text{free,fixed}} = \begin{pmatrix} 1 & -1 \\ -1 & 2 \end{pmatrix} \tag{2.17}$$

One diagonalizes $H_L^{bb'}$ for all 4 combinations of boundary conditions, and then form $\mathbf{O}_L$ from the $m/4$ eigenvectors associated with the lowest eigenvalues from each combination of boundary conditions. Since the columns of $\mathbf{O}_L$ are not orthogonal, we must explicitly orthogonalize them using e.g. the Gram-Schmidt procedure. We then form $\overline{\mathbf{T}}_L = \mathbf{O}_L^t \, \mathbf{T}_L \, \mathbf{O}_L$. Note that $H_L^{bb'}$ is not diagonal. The Hamiltonian of the system of size $2L$ is then

$$H_{2L=}^{bb'} \begin{pmatrix} \overline{\mathbf{H}}_L^{\text{b,fixed}} & \overline{\mathbf{T}}_L \\ \overline{\mathbf{T}}_L^{\dagger} & \overline{\mathbf{H}}_L^{\text{fixed,b}'} \end{pmatrix} \tag{2.18}$$

Fixed boundary conditions must be used at the boundaries between the blocks in order to make the procedure exact when all states are kept. The matrix T_{2L} is formed as in Eq. (2.15). The fixed-free CBC procedure works amazingly well. The state energy can be obtained to 10 digit accuracy keeping $m = 8$ states and performing 10 iterations so that $L = 2048$. The CBC procedure can also be formulated with other combinations of boundary conditions such as periodic and antiperiodic. While the periodic-antiperiodic CBC procedure is not as accurate as the fixed-free procedure, it performs much better than the Wilson procedure with periodic or antiperiodic boundary conditions.

The second type of procedure developed by S. White and R. Noack [21], called the superblock method, consists in choosing a new basis for $\overline{\mathbf{H}}_{2L}$ and $\overline{\mathbf{T}}_{2L}$ based on the idea that they will eventually be used to make up part of a larger system. In order to do this, a "superblock" (with periodic boundary conditions) made up of $p > 2$ blocks is formed and diagonalized. For example,

$$\mathbf{H}_{2L}^{p=4} = \begin{pmatrix} \overline{\mathbf{H}}_L & \mathbf{T}_L & 0 & \mathbf{T}_L^t \\ \mathbf{T}_L^t & \overline{\mathbf{H}}_L & \mathbf{T}_L & 0 \\ 0 & \mathbf{T}_L^t & \overline{\mathbf{H}}_L & \mathbf{T}_L \\ \mathbf{T}_L & 0 & \mathbf{T}_L^t & \overline{\mathbf{H}}_L \end{pmatrix} \tag{2.19}$$

The transformation $\mathbf{O}_{2L}$ is then made up by projecting the m lowest-lying eigenstates of $\mathbf{H}_{2L}^p$ onto the coordinates of the first two blocks, and then orthogonalizing its columns. This new basis is used to transform $\overline{\mathbf{H}}_{2L} = \mathbf{O}_{2L}^t \, \mathbf{H}_{2L} \, \mathbf{O}_{2L}$ and $\overline{\mathbf{T}}_{2L} = \mathbf{O}_{2L}^t \, \mathbf{T}_{2L} \, \mathbf{O}_{2L}$, as defined in Eqs. (2.14) and (2.15). The idea is that the fluctuations in the additional blocks surrounding the system to be blocked effectively apply general boundary conditions, or equivalently, provide the conditions at the boundaries that the transformed blocks would see as part of a larger system. As p becomes large, this procedure becomes exact because it reduces to an exact diagonalization of the complete final system. Another interesting feature of this procedure is that the diagonalization step is decoupled from the real-space blocking step; a different size system is diagonalized than is blocked together. This procedure yields accurate results for the particle-in-a-box eigenstates, although not quite as accurate as the fixed-free CBC procedure.

The standard *real-space renormalization group* procedure is as follows:

1. Interactions on an initial sublattice ("block") A of length l are described by a block Hamiltonian $\hat{H}_A$ acting on an M-dimensional Hilbert space.

2. Form a compound block AA of length $2\,l$ and the Hamiltonian $\hat{H}_{AA}$, consisting of two block Hamiltonians and interblock interactions. $\hat{H}_{AA}$ has dimension M^2.

3. Diagonalize $\hat{H}_{AA}$ to find the M lowest-lying eigenstates.

4. Project $\hat{H}_{AA}$ onto the truncated space spanned by the M lowest-lying eigenstates, $\hat{H}_{AA} \longrightarrow \hat{H}^{\rm tr}_{AA}$.

5. Restart from step 2, with doubled block size: $2\,l \longrightarrow l, AA \longrightarrow A$, and $\hat{H}^{\rm tr}_{AA} \longrightarrow \hat{H}_{AA}$, until the box size is reached.

This success pushed Steven White to try his numerical technique to interacting quantum systems; in vain. However, as White himself said, this led him to the conclusion that extra boundary sites are needed, which were not part of the block, in order to induce the right boundary conditions. This led to the idea of solving a "superblock" system, and then projecting the superblock state onto the block [20].

Then, he realized that the projection idea of the superblock onto a block was actually equivalent to a singular value decomposition:

$$\psi_{ij} = U_{i\alpha} D_{\alpha\alpha} V_{\alpha j} \tag{2.20}$$

where i denotes states of the block, and j denotes states of the remainder of the superblock.

The very decomposition was actually equivalent to diagonalizing a density matrix, a concept borrowed from Feynman's lectures [22]:

$$\rho_{ii'} = \psi_{ij}\psi_{i'j} = U_{i\alpha} D^2_{\alpha\alpha} U_{i'\alpha}. \tag{2.21}$$

Indeed, for a system which is strongly coupled to the outside universe, it is much more appropriate to use the eigenstates of the density matrix to describe the system rather than the eigenstates of the systems Hamiltonian. In other words, to analyze which states have to be retained, the block has to be embedded in some environment and we can view the rest of the lattice as a heat bath at an effective inverse temperature b to which the system is coupled. And the density matrix tells us which states are the most important ones.

Therefore, we come up with the key idea of DMRG namely: rather than keeping the lowest-lying eigenstates of the Hamiltonian in forming a new effective Hamiltonian of a block of sites, one should keep the most significant eigenstates of the block density matrix, obtained from diagonalizing the Hamiltonian of a larger section of the lattice which includes the block.

Thus, infinite-system DMRG method for the Heisenberg spin 1/2 chain was the first application of the new technique, and nice results were obtained when compared with the exact Bethe ansatz solution.

Chapter 3

Density Matrix Renormalization Group

3.1 Introduction

The dramatic success of the DMRG method [21, 23, 24] has changed the picture of real-space RG techniques completely and became in few years a powerful numerical technique for finding accurate approximations to the ground state and the low-lying excited states of strongly interacting quantum lattice systems such as the Heisenberg, $t-J$, and Hubbard models. DMRG is remarkable in the accuracy that can be achieved for one dimensional systems.

Thus, DMRG has been applied until now in very different fields of scientific research [25, 26, 27]. The method itself is a rather complicated algorithm and a detailed description together with some examples is given by S.R. White in [23].

3.2 The Density Matrix Projection

In this chapter, I will attempt to introduce DMRG in a pedagogical manner and discuss how to generalize the projection of the superblock described in the previous section for the noninteracting system to interacting systems. The main material is taken from [28]. The procedure involves forming the reduced density matrix for the system block as part of the superblock. I will show that the basis obtained using this density matrix projection is the optimal basis in a particular sense.

First, let us briefly review the properties of density matrices. An excellent treatment is given in Feynman's book on statistical mechanics [22]. The term "density matrix" is used to refer to a number of different, but related mathematical objects, both in quantum mechanics and quantum statistical mechanics. Here I consider a quantum mechanical system in a definite pure state, and consider the properties of a part of that system. Since I will later use this procedure as part of a superblock algorithm, I will label the entire system the *superblock*, the part that we are interested in constructing a basis for the *system block*, and the remainder of the system the *environment block*, as depicted in Fig.5.1. Let $|i\rangle$ labels the states of the system block, and $|i\rangle$ labels the states of the environment block, i.e. the

rest of the superblock. If $\psi\rangle$ is a state of the superblock,

$$|\psi\rangle = \sum_{ij} \psi_{ij} |i\rangle |j\rangle \tag{3.1}$$

The reduced density matrix for the system block is defined as

$$\rho_{ii'} = \sum_{j} \psi^*_{ij} \psi_{i'j}. \tag{3.2}$$

by normalization, $\mathrm{Tr}\rho = 1$. The density matrix contains all the information needed from the wavefunction ψ to calculate any property restricted to the system block. If the operator A acts only on the system block, then

$$\langle A \rangle = \sum_{ii'} A_{ii'} \rho_{i'i} = \mathrm{Tr}\rho\mathrm{A} \tag{3.3}$$

Now let us diagonalize the density matrix. Let ρ have eigenstates $|u^\alpha\rangle$ and eigenvalues $w_\alpha \geq 0$. Since $\mathrm{Tr}\rho = 1$, $\sum_\alpha w_\alpha = 1$. Then for any system block operator A,

$$\langle A \rangle = \sum_{\alpha} w_\alpha \langle u^\alpha | A | u^\alpha \rangle. \tag{3.4}$$

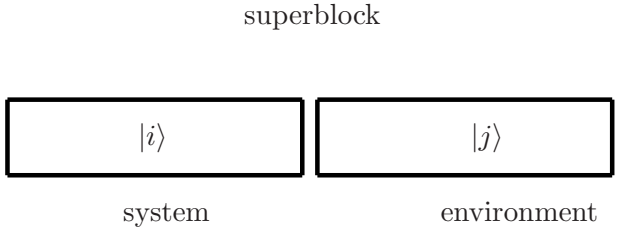

Figure 3.1: A superblock divided into a system block and an environment block.

Equation (3.3) will apply immediately to our numerical renormalization group procedure. Suppose we wish to throw away some states from the system block. If for a particular α, $w_\alpha \approx 0$, we make no error in $\langle A \rangle$, for any A, if we discard $|u^\alpha\rangle$. We have found a way to find which states to keep (those with significant w_α) and which to discard.

This argument can be made much more precise. In particular, we can show that keeping the most probable eigenstates of the density matrix gives the most accurate representation of the state of the superblock, i.e., the system block plus the environment block. Let us assume we have diagonalized the superblock and obtained one particular state $|\psi\rangle$, typically the ground state. We wish to define a procedure for producing a set of states of the system block $|u^\alpha\rangle, \alpha = 1, \cdots, m$, with $|u^\alpha\rangle = \sum_i u^\alpha_i |i\rangle$, which are optimal for representing ψ in some

sense. Because we allow only m states, we cannot represent $|\psi\rangle$ exactly if $l > m$, where l is the number of system block states $|i\rangle$. We wish to construct an accurate expansion for $|\psi\rangle$ of the form

$$|\psi\rangle \approx |\bar{\psi}\rangle = \sum_{\alpha,j} a_{\alpha,j} |u^\alpha\rangle |j\rangle. \tag{3.5}$$

In other words, we wish to minimize

$$\mathcal{S} = \left| |\psi\rangle - |\bar{\psi}\rangle \right|^2 \tag{3.6}$$

by varying over all $a_{\alpha,j}$ and u^α, subject to $\langle u^\alpha | u^{\alpha'} \rangle = \delta_{\alpha\alpha'}$. Without loss of generality, we can write

$$|\bar{\psi}\rangle = \sum_\alpha a_\alpha |u^\alpha\rangle |v^\alpha\rangle \tag{3.7}$$

where $v_j^\alpha = \langle j | v^\alpha \rangle = N_\alpha a_{\alpha,j}$, with N_α chosen to set $\sum_j \left| v_j^\alpha \right|^2 = 1$. Switching the matrix notation, we have

$$\mathcal{S} = \sum_{ij} (\psi_{ij} - \sum_{\alpha=1}^{m} a_\alpha \, u_i^\alpha \, v_j^\alpha)^2, \tag{3.8}$$

and we minimize $\mathcal{S}$ over all u^α, v^α, and a_α, given the specified value of m. The solution to this minimization problem is known from linear algebra. We now think of ψ_{ij} as a rectangular matrix. The solution is produced by the singular value decomposition of ψ [**?**],

$$\psi = U \, D \, V^T, \tag{3.9}$$

where U and D are $l \times l$ matrices, V is an $l \times J$ matrix (where $j = 1, ..., J$,and we assume $J \geq l$), U is orthogonal, V is column-orthogonal, and the diagonal matrix D contains the singular values of ψ. Linear algebra tells us that the u^α, v^α, and a_α which minimize $\mathcal{S}$ are given as follows: the m largest-magnitude diagonal elements of D are the a_α and the corresponding columns of U and V are the u^α and v^α. (We emphasize that the singular value decomposition is not being used here as a numerical method, only as a convenient factorization which allows us to use a theoretical result from linear algebra.)

These optimal states u^α are also eigenvectors of the reduced density matrix of the block as part of the system. This reduced density matrix for the block depends on the state of the system, which in this case is a pure state $|\psi\rangle$ (the system could also be in a mixed state or at finite temperature.) The density matrix for the block in this case, where ψ_{ij} is assumed real, is given by

$$\rho_{ii'} = \sum_j \psi_{ij} \psi_{i'j}. \tag{3.10}$$

We see that

$$\rho = U \, D^2 \, U^T, \tag{3.11}$$

i.e. U diagonalizes ρ. The eigenvalues of ρ are $w_\alpha = a_\alpha^2$ and the optimal states u^α are the eigenstates of ρ with the largest eigenvalues. Each w_α represents the probability of the block being in the state u^α, with $\sum_\alpha w_\alpha = 1$. The deviation from of $P_m \equiv \sum_{\alpha=1}^m w_\alpha$ from unity, i.e. the "discarded weight" of the density matrix eigenvalues, measures the accuracy of the truncation to m states.

We can also consider the superblock to be in a mixed state. This is the natural assumption for a system at finite temperature, and it is also useful to assume a mixed state when one wishes to obtain several of the lowest lying states: if we put the superblock with equal probability into each of several states, then the system block states obtained from the density matrix will equally well represent each of these superblock states. We represent the mixed case by saying that the superblock has probability W_k to be in state $|\psi^k\rangle$. If the superblock is at a finite temperature, then the W^k are normalized Boltzmann weights. In this case the appropriate definition for the error in the representation is

$$\mathcal{S} = \sum_k W_k \sum_{ij} (\psi_{ij}^k - \sum_{\alpha=1}^m a_\alpha^k \, u_i^\alpha \, v_j^{k,\alpha})^2, \tag{3.12}$$

Note that we are interested in determining a single set of optimal u^α, whereas we allow the rest of the system additional freedom to choose a different v^α for each state k. Minimizing over the u_i^α, $v_j^{k,\alpha}$ and a_α^k , we find

$$\rho^\alpha = w_\alpha u^\alpha \tag{3.13}$$

with

$$\rho_{ii'} = \sum_k W_k \sum_j \psi_{ij}^k \psi_{i'j}^k \tag{3.14}$$

and

$$w_\alpha = \sum_k W_k (a_\alpha^k)^2. \tag{3.15}$$

This equation for ρ is the definition of the reduced density matrix when the superblock is in a mixed state, and the u^α are the eigenstates of ρ.

3.3 DMRG Algorithms

In this section, I will describe how to combine the superblock procedure with the density matrix projection in order to define efficient DMRG algorithms. There are three main ingredients needed to form a DMRG algorithm: first, we have to decide how to add degrees of freedom to the system, i.e. how to build up the system block; second, we have to determine the configuration of the superblock; and finally, we must choose which superblock eigenstate or eigenstates to use to construct the density matrix.

For interacting systems, it is clear that one wants to add the minimum number of degrees of freedom at once to the system block in order keep as large a fraction of the system block states as possible, and to keep the size of the Hilbert space of the superblock as small as

possible. Therefore, one usually wants to build up the system block one site at a time in a procedure similar to that described for the Wilson numerical RG.

The algorithms then fall into two classes, depending on how the environment block is chosen to form the superblock: the infinite system algorithm and the finite system algorithm. We will discuss these algorithms in detail below.

The superblock state or states used to form the reduced density matrix for the system block are called *target states*. If only ground state properties are desired, it is most accurate to target just the ground state of the superblock. (The Hamiltonian is usually block diagonal in particular quantum numbers such as S_z; by ground state we will mean ground state for a particular quantum number.) If excited states or matrix elements between different states are required, more than one target state can be used. However, for fixed number of states kept m, the accuracy with which the properties of each individual state can be determined goes down as more states are targeted. For simplicity, we will assume that only the ground state is targeted in the following.

3.3.1 The infinite system algorithm

The infinite system algorithm is the most straightforward extension of the Wilson procedure described before that incorporates the superblock concept. We build up the system block one site at a time, just as in the Wilson procedure, but must choose some sort of environment block. The simplest way of forming the environment block is to use a reflection of the system block. The superblock configuration is shown in Fig.3.2. Here $\overline{H}_l$ is the Hamiltonian for the system block in the reduced basis, as before, and the solid dots represent single sites. The right block, $\overline{H}_l^R$, is formed by relabelling the sites in the system block so that they are reflected onto the right part of the lattice.

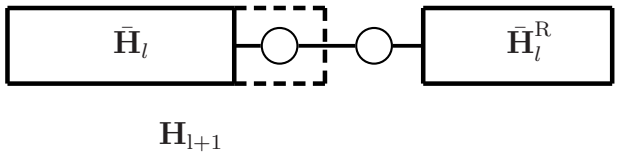

Figure 3.2: A superblock configuration for the infinite-system algorithm.

The infinite system algorithm then proceeds as follows:

1. Form a superblock containing L sites which is small enough to be exactly diagonalized.
2. Diagonalize the superblock Hamiltonian H_L^{super} numerically, obtaining *only* the ground state eigenvalue and eigenvector $|\psi\rangle$ using the Lanczos or Davidson algorithm.
3. Form the reduced density matrix $\rho_{ii'}$ for the new system block from $|\psi\rangle$ using (3.10). Note that $l' = l = L/2 - 1$.

4. Diagonalize $\rho_{ii'}$ with a dense matrix diagonalization routine to obtain the m eigenvectors with the largest eigenvalues.

5. Construct H_{l+1} and other operators in the new system block and transform them to the reduced density matrix eigenbasis using $\bar{H}_{l+1} = O_L^\dagger \, H_{l+1} \, O_L$, $\bar{A}_{l+1} = O_L^\dagger \, A_{l+1} \, O_L$, etc.,where the columns of O_L contain the m highest eigenvectors of $\rho_{ii'}$, and A_{l+1} is an operator in the system block.

6. Form a superblock of size $L+2$ using $\bar{H}_{l+1}$, two single sites and $\bar{H}^R_{l+1}$.

7. Repeat starting with step 2, substituting $H^{\rm super}_{L+2}$ for $H^{\rm super}_L$.

It is clear that this algorithm is very much in the spirit of the original Wilson procedure in that the system being diagonalized grows at each step. There are, however, a few important differences. First, as in the noninteracting superblock procedure, the diagonalization step and the real-space blocking step take place on different size systems. Therefore, the energy and various expectation values are calculated during the superblock diagonalization, while the density matrix diagonalization rather than a Hamiltonian diagonalization is used to determine the new basis for the system block. Second, the size of the superblock grows by two sites rather than one site at every step. Third, we have assumed that the system is reflection symmetric. It is possible to formulate algorithms that do not assume reflection symmetry, but this is done most easily in the context of the finite system algorithm described below.

3.3.2 The finite system algorithm

In the finite size algorithm, the environment block is chosen in a different way: it is chosen so that the size of the superblock is kept fixed at each step. Suppose that we have run the infinite system algorithm until the superblock reaches size L, but have stored all the $\bar{H}^R_{l'}$ for $l = 1, \cdots, L/2-2$ as well as all the additional operators needed to connect the blocks at each step. We can then continue to build up the system block, but keep $L = l + l' + 2$ fixed by using the appropriate previously stored $\bar{H}^R_{l'}$. The finite size algorithm then proceeds as follows:

1. Carry out the infinite system algorithm until the superblock reaches size L, storing $\bar{H}_l$ and the operators needed to connect the blocks at each step.

2. Carry out steps 3-5 of the infinite system algorithm to obtain $\bar{H}_{l+1}$. Store it. (Now $l \neq l'$.)

3. Form a superblock of size L using $\bar{H}_{l+1}$, two single sites and $\bar{H}^R_{l'+1}$. The superblock configuration is given by Fig. 6, where $l' = L - l - 2$.

4. Repeat steps 1-2 until $l = L-3$ (i.e. $l' = 1$). This is the *left to right* phase of the algorithm.

5. Carry out steps 3-5 of the infinite system algorithm, reversing the roles of $\bar{H}_l$ and $\bar{H}^R_{l'}$, i.e. switch directions to build up the right block and obtain $\bar{H}^R_{l'+1}$. Store it.

6. Form a superblock of size L using $\bar{H}_{l-1}$, two single sites and $\bar{H}^R_{l'+1}$.

7. Repeat steps 4-5 until $l = 1$. This is the *right to left* phase of the algorithm.

8. Repeat starting with step 1.

Note that since the left block and the right blocks are stored independently, we do not have to assume that the lattice is reflection symmetric. Since the same size superblock is always diagonalized, the algorithm is less dependent than the infinite system algorithm on translational invariance,i.e. on the optimum representation of different size superblocks being similar.

If reflection symmetry is present, it can be used at the point at which $l = l'$ to shorten the length of the zips. One way of formulating the algorithm in this case is to build up the left blocks from $l = 1$ to $l = L/2 - 1$, and build up the right blocks from $l' = L/2$ to $l' = L - 3$, i.e. to only zip from the left side of the superblock to the middle and then back to the left side. The fact that we have used reflection symmetry in the infinite system phase, step 0, is usually not important. However, it is also possible to formulate infinite system algorithms that do not use reflection symmetry. This issue will be discussed in more detail below in the context of algorithms for two-dimensional and fermion systems.

For a given system size L, the finite system algorithm almost always gives substantially more accurate results than the infinite system algorithm, and is therefore usually preferred unless there is a specific reason to go to the thermodynamic limit.

3.4 Details for interacting systems

Up to now, we have not considered in detail how to store and transform the operators necessary to carry out the renormalization group transformation for an interacting system. In this section, we will discuss how to do this efficiently. In order to construct the Hamiltonian of the system, a block must have various operators stored as matrices connecting these states. For example, for the Heisenberg model with exchange terms

$$\mathbf{S}_i \cdot \mathbf{S}_{i+1} = S^z_i S^z_{i+1} + \frac{1}{2}(S^+_i S^-_{i+1} + S^-_i S^+_{i+1}) \tag{3.16}$$

one needs to store $m \times m$ matrix representations of S^z_i, S^+_i and S^-_i for i equal to the left or right end sites of the block. (In practice, one needs not store S^-_i, since it can be obtained by taking the Hermitian conjugate of S^-_i). For a Hubbard model one would have to store matrices for $c_{i\sigma}$, with $\sigma =\uparrow$ and $\downarrow$, in order to reconstruct the hopping term $\sum_\sigma (c^\dagger_{i+1\sigma} c_{i\sigma} + c^\dagger_{i\sigma} c_{i+1\sigma})$.

Consider joining two blocks B_1 and B_2 together in a Heisenberg system. In the Wilson procedure, B_2 will typically consist of a single site, and for the DMRG algorithms, it is sufficient to consider how to compose two blocks. If B_1 has m_1 states, and B_2 has m_2 states, the combined block B_1B_2 has m_1m_2 states. We label the combined states by two indices, ij. The matrix representing the Hamiltonian of B_1B_2 is then given by

$$\begin{aligned}[H_{B_1B_2}]_{ij;i'j'} = [H_{B_1}]_{ii'}\,\delta_{jj'} + [H_{B_2}]_{jj'}\,\delta_{ii'} + [S^z_l]_{ii'}\left[S^z_{l+1}\right]_{jj'} \\ + \frac{1}{2}\left[S^+_l\right]_{ii'}\left[S^-_{l+1}\right]_{jj'} + \frac{1}{2}\left[S^-_l\right]_{ii'}\left[S^+_{l+1}\right]_{jj'}\end{aligned} \tag{3.17}$$

where H_{B_1} is the Hamiltonian matrix of block B_1, and l is its rightmost site. In order for the connections in the Hamiltonian to be restored when the two blocks are combined, each block must contain each of the matrices appearing in (3.17).

The most time-consuming part of a DMRG calculation is the diagonalization of the system Hamiltonian, which occurs once for every step. Only the ground state or a few low-lying states are needed, and so the Lanczos or Davidson iterative algorithms should be used. These algorithms both require repeated multiplications of superblock vectors ψ by the superblock Hamiltonian H^{super}. However, the actual Hamiltonian matrix should not be constructed and stored. Instead, the following procedure to directly multiply $H^{\text{super}}\psi$ uses much less memory and is also much faster. Consider again, for simplicity, a system formed from two blocks. The superblock Hamiltonian can be written in the general form

$$[H^{\text{super}}]_{ij;i'j'} = \sum_{\alpha} A^{\alpha}_{ii'}\, B^{\alpha}_{jj'}. \tag{3.18}$$

Then the product $H^{\text{super}}\psi$ can be written as

$$\sum_{i'j'} [H^{\text{super}}]_{ij;i'j'}\, \psi^{\alpha}_{i'j'} = \sum_{\alpha} \sum_{i'} A^{\alpha}_{ii'} \sum_{j'} B^{\alpha}_{jj'} \psi_{i'j'}. \tag{3.19}$$

For each α the last sum is performed first, as a matrix-matrix multiplication of B^{α} and ψ^T, to form a temporary matrix $C^{\alpha}_{ji'}$. Then a matrix-matrix multiplication of A^{α} and $[C^{\alpha}]^T$ forms a partial result, which is added into the result vector, giving a sum on α.

Whenever a site is added onto a block, or more generally two blocks are added, the operator matrices must be updated. The eigenstates of the density matrix can be written in the form u^{α}_{ij}, which we write as $O_{ij;\alpha}, \alpha =, \cdots, m$. Here i and j represent state indices of the two blocks that are being added together. Then for each operator A that is needed, $A_{ij;i'j\prime}$, is replaced by $A_{\alpha\alpha'}$, where

$$A_{\alpha\alpha'} = \sum_{iji'j'} O_{ij;\alpha} A_{ij;i'j'} O_{i'j';\alpha'}. \tag{3.20}$$

The terms appearing in (3.17) show the various ways operators $A_{ij;i'j'}$, can be formed from single-block operators $A_{ii'}$.

Any efficient DMRG program must make use of quantum numbers to speed up the calculation and reduce storage. For example, in order to construct the system Hamiltonian it may be necessary to store for a block the matrix form of the operator $\hat{S}^+_l$, where l is the right-most site of the block. If there are m states in the block, this is an $m \times m$ matrix. However, if states are labelled and grouped by block quantum number S^z , then this matrix is mostly zeroes, with the nonzero parts in rectangular blocks. These blocks connect states with specific quantum numbers, e.g. the states corresponding to the left index of the matrix may have $S_z = 0$, and for the right index $S_z = -1$. It is essential to store only the nonzero elements of this matrix. Although this can done using sparse matrices, the best way to do it is as a set of dense matrices, one for each nonzero rectangular block. The multiplication of $H^{\text{super}}\psi$ described above takes place as described in the previous paragraph, except that now there is an additional sum or loop over quantum numbers, and the dense matrices which are multiplied are much smaller. Keeping track of all the matrices, each of a different

size, can be very well organized in the programming language C++ by defining classes to represent operator matrices, submatrices, etc. The fact that these matrices are all different sizes and have different dimensions at each DMRG step makes it somewhat more difficult to use storage efficiently in Fortran 77, which does not have dynamic allocation of memory.

It is useful at this point to mention typical maximum numbers of states kept, m, for various systems on current computers. For the one-dimensional Hubbard model, $m = 800$ for a system of up to a few hundred sites can be treated on typical workstation, using a few hundred megabytes of main memory [29, 30]. For the Heisenberg model, up to $m = 1100$ states have been kept for the spin-one chain with an impurity [31] and $m = 1700$ for the spin two chain [32].

3.5 Measurements

Measurements are made using the superblock wavefunction $|\psi\rangle$ to evaluate expectation values of the form $\langle\psi|A|\psi\rangle$. Rather complicated operators can be evaluated fairly easily, but dynamical information is more difficult to obtain. In order to measure A, one must have kept operator matrices for the components of A. For example, to measure the on-site spin-density S^z_j for all sites l, one must keep track of matrices $[S^z_l]_{ii'}$, for all each site l in each of the blocks. These operators must be updated using (3.20) at every step of each iteration. We will once again divide superblock into two parts with states labeled by $|i\rangle$ and $|j\rangle$. One then obtains the expectation value using

$$\langle\psi|S^z_l|\psi\rangle = \sum_{i,i',j} \psi^*_{ij}\,[S^z_l]_{ii'}\,\psi_{i'j}, \tag{3.21}$$

This procedure gives *exact* evaluations of $\langle\psi|A|\psi\rangle$ for the *approximate* eigenstate $|\psi\rangle$.

For a correlation function such as $\langle\psi|S^z_l S^z_m|\psi\rangle$, the evaluation depends on whether l and m are on the same block or not. If they are on different blocks, then one needs only have kept track of $[S^z_l]_{ii'}$,and $[S^z_m]_{jj'}$, and one has

$$\langle\psi|S^z_l S^z_m|\psi\rangle = \sum_{i,i',j,j'} \psi^*_{ij}\,[S^z_l]_{ii'}\,[S^z_m]_{jj'}\,\psi_{i'j'} \tag{3.22}$$

If l and m are on the same block, one *should not* use

$$\langle\psi|S^z_l S^z_m|\psi\rangle \approx \sum_{i,i',i'',j} \psi^*_{ij}\,[S^z_l]_{ii'}\,[S^z_m]_{i',i''}\,\psi_{i''j} \tag{3.23}$$

This expression does not evaluate the correlation function exactly within the approximate state $|\psi\rangle$. The sum over it should run over a complete set of states, but does not, whereas the sums over the other variables need run only over those states needed to represent $|\psi\rangle$, since they appear as a subscript in either the $|\psi\rangle$ on the left or on the right.

To evaluate this type of correlation function, one needs to have kept track of $[S^z_l\,S^z_m]_{ii'}$ throughout the calculation. One then evaluates

$$\langle\psi|S^z_l\,S^z_m|\psi\rangle = \sum_{i,i',j} \psi^*_{ij}\,[S^z_l\,S^z_m]_{ii'}\,\psi_{i'j} \tag{3.24}$$

to obtain the correlation function.

3.6 Wave function transformations

At each DMRG step, two sites are added inbetween the left and right blocks, previously obtained by truncation process. Meanwhile, one can keep track of the wavefunction in an appropriate basis for the new block [33]. The new basis is defined by the eigenvectors of the density matrix, which is determined from the current system wavefunction. The eigenvectors defining the new basis (which we rewrite as matrices L and R below) can then be used to transform the current system wavefunction into the appropriate basis for the *next* step. Here we consider a finite-system DMRG step, in which we move from left to right, adding a site onto the left block. Let $|\alpha_l\rangle$ be the states of left block l, where l is the rightmost site of the block. The two sites in the middle are $l+1$ and $l+2$. Let $|s_l\rangle$ be the states of site l, $|s_{l+1}\rangle$ for site $l+1$, etc. Then the basis states for the new left block are given by

$$|\alpha_{l+1}\rangle = \sum_{s_{l+1},\alpha_l} L^{l+1}\left[s_{l+1}\right]_{\alpha_{l+1},\alpha_l} |\alpha_l\rangle \otimes |s_{l+1}\rangle. \tag{3.25}$$

The transformation matrix $L^{l+1}\left[s_{l+1}\right]_{\alpha_{l+1},\alpha_l}$ is a slightly rewritten form of the truncated matrix of density matrix eigenvectors $u^{\alpha_{l+1}}$: specifically, $L^{l+1}\left[s_{l+1}\right]_{\alpha_{l+1},\alpha_l} = u^{\alpha_{l+1}}_{s_{l+1}\alpha_l}$. L includes only the eigenvectors which are retained, i.e. whose corresponding eigenvalues are above a cutoff. Let the states of the right block be $|\beta_{l+3}\rangle$, where we note that $l+3$ is the leftmost site of the block. These states were formed at an earlier right-to-left DMRG step, using a different set of density matrix eigenvectors, which we write in terms of a transformation matrix R^{l+3}:

$$|\beta_{l+3}\rangle = \sum_{s_{l+3},\beta_{l+4}} R^{l+3}\left[s_{l+3}\right]_{\beta_{l+3},\beta_{l+4}} |s_{l+3}\rangle \otimes |\beta_{l+4}\rangle. \tag{3.26}$$

Note that reflection symmetry is not assumed here: the L and R matrices are independent.

The wavefunction is written in a basis for the two block plus two site superblock. This superblock basis has basis states of the form

$$|\alpha_l s_{l+1} s_{l+2} \beta_{l+3}\rangle = |\alpha_l\rangle \otimes |s_{l+1}\rangle \otimes |s_{l+2}\rangle \otimes |\beta_{l+3}\rangle. \tag{3.27}$$

A system wavefunction $|\psi\rangle$ is written in this basis as

$$|\psi\rangle = \sum_{\alpha_l s_{l+1} s_{l+2} \beta_{l+3}} \psi(\alpha_l s_{l+1} s_{l+2} \beta_{l+3}) |\alpha_l s_{l+1} s_{l+2} \beta_{l+3}\rangle. \tag{3.28}$$

One needs to transform this wavefunction into the basis appropriate for the next DMRG step, in which the superblock is shifted by one site, with basis states of the form $\alpha_{l+1} s_{l+2} s_{l+3} \beta_{l+4}$. However, the transformation between the two bases cannot be exact, since there is a truncation in going from $\alpha_l s_{l+1}$ to α_{l+1}. However, the states α_{l+1} are formed using the density matrix to be ideally adapted for representing $|\psi\rangle$. This means that the wavefunction can be transformed in an approximate but controlled fashion, with the error in the transformation depending on the truncation error in the DMRG step. Since the error in the density matrix is given by the truncation error, and since the density matrix is, roughly speaking, the

square of the wavefunction, the error in the wavefunction transformation should be roughly the square root of the truncation error.

The simplest way to derive the transformation is to assume, based on the above argument, that for the transformation of the wavefunction only, one can approximate

$$\sum_{\alpha_{l+1}} |\alpha_{l+1}\rangle\langle\alpha_{l+1}| \approx 1. \tag{3.29}$$

With this approximation one readily obtains

$$\psi(\alpha_{l+1}s_{l+2}s_{l+3}\beta_{l+4}) \approx \sum_{\alpha_l s_{l+1}\beta_{l+3}} L^{l+1}\left[s_{l+1}\right]_{\alpha_{l+1},\alpha_l} \psi(\alpha_l s_{l+1}s_{l+2}\beta_{l+3}) R^{l+3}\left[s_{l+3}\right]_{\beta_{l+3},\beta_{l+4}} \tag{3.30}$$

This is the desired transformation.

The most efficient way to implement this transformation numerically is to first form the intermediate wavefunction

$$\psi(\alpha_{l+1}s_{l+2}\beta_{l+3}) = \sum_{\alpha_l s_{l+1}} L^{l+1}\left[s_{l+1}\right]_{\alpha_{l+1},\alpha_l} \psi(\alpha_l s_{l+1}s_{l+2}\beta_{l+3}), \tag{3.31}$$

and then form the final result

$$\psi(\alpha_{l+1}s_{l+2}s_{l+3}\beta_{l+4}) = \sum_{\beta_{l+3}} \psi(\alpha_{l+1}s_{l+2}\beta_{l+3}) R^{l+3}\left[s_{l+3}\right]_{\beta_{l+3},\beta_{l+4}}. \tag{3.32}$$

In this form, the transformation requires very little computer time compared to other parts of the calculation. This transformation is used for one half of the DMRG steps, when a site is being added to the left block. An analogous transformation is used for adding a site to the right block.

Implementing this transformation requires saving all the matrices L and R, which was not necessary in the original formulation of DMRG.

3.7 Extension to two dimensions

A straightforward way to extend the DMRG to two or more dimensional quantum systems would be to replace the single sites added between the blocks with a row of sites. However, for wide systems the extra degrees of freedom in the two center "sites" would make the size of the system's Hilbert space prohibitively large. It is usually better to add single sites by mapping the 2D system onto a 1D system, simply by tracing a path through the lattice. A typical superblock configuration for a ladder system is shown in Fig.(3.3). The site added to the system block is enclosed by a dashed line and the dotted line shows the order in which sites are added in a sweep. An up-down-up-down path is shown. One can see that it is not possible to reflect the left block onto a right block of the proper geometry at every step, so the finite system algorithm must used. With the mapping onto a 1D system, the two-dimensional procedure differs from the one-dimensional finite system procedure only in that there are additional connections between the system and environment blocks along the boundary.

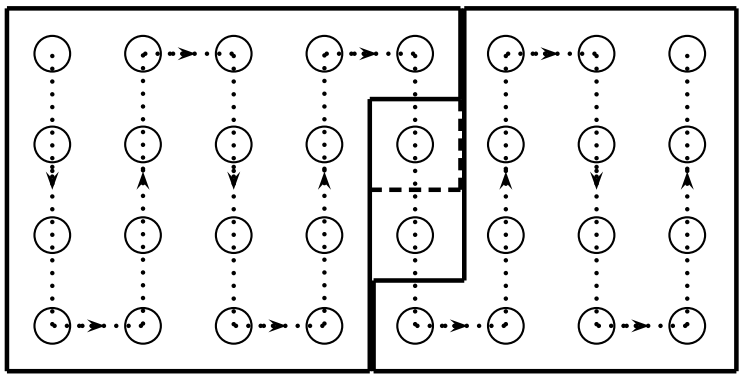

Figure 3.3: The superblock configuration for the two-dimensional algorithm. The order in which sites are added to the system block on a series of iterations is given by the dotted line, and the site added to the approximate system block Hamiltonian is outlined by the dashed line.

The number of states needed to maintain a certain truncation error in the density matrix projection procedure depends strongly on the number of operators connecting the two parts of the system. The best accuracy is obtained when the number of connections between the system and environment blocks is minimized. Therefore, we usually study systems with open rather than periodic or antiperiodic boundary conditions. Also, we find that the number of states m needed to maintain a given accuracy depends strongly on the width and weakly on the length of the system.

Liang and Pang [34] studied the error in the energy as a function of width for a gas of noninteracting spinless fermions and found that the number of states needed to maintain a given accuracy grew exponentially with the width of the system. In an interacting system such as the Hubbard model, the detailed structure of the energy spectrum seems to be important. For systems of more than one dimension, it is important to be able to keep as many states m per block as possible.

3.8 Main restrictions

Like any other numerical method, the DMRG has some important restrictions which are inherent to the method itself and therefore cannot be removed by applying simple changes to the DMRG algorithm. Here we mention the three main restrictions briefly:

1. The most in sight limitation of DMRG is dimensionality. As the method is applied to higher dimensions a declining accuracy appears as the size grows up.

2. The absence of an analytical formulation of the DMRG method.

3. DMRG is restricted to zero temperature and is usually applied for calculating ground state properties. Finite temperature results were obtained only in the low lying spectrum but with very limited accuracy. Recently, based on the idea of Xiang et al, a thermodynamic method was applied successfully, which combines White's DMRG idea [23] with the transfer-matrix technique [35] and which is now called TMRG.

A disadvantage of the DMRG method is that the base states chosen by the algorithm are not intuitive, and the description of the state requires the measurement of observables. For the measurement process, one needs a representation of the operators in the current basis. Consequently each operator that needs to be measured must be stored, and every time the basis is changed all of them have to be transformed. This is expensive in time and memory. Another disadvantage is that dynamical information cannot be easily obtained.

Note that, although its name suggests a connection to renormalization group methods in the analytical sense, the DMRG method should better be viewed as an exact numerical diagonalization technique with a restricted set of Hilbert space states.

Chapter 4

Implementations of the Density Matrix Renormalization Group

In this chapter I will first review briefly the different applications of the density matrix renormalization group method to quantum systems models. Then, I will present, in some details, DMRG implementations for some well-known models that are currently used to investigate strongly correlated systems. Finally, the formalism used to calculate the expectation values of dynamic operators using DMRG method is given.

4.1 DMRG in literature

The development of the density-matrix renormalization-group (DMRG) algorithm by S. White represented an important improvement over previous numerical methods for the study of low dimensional lattice models. It has been applied to a wide variety of systems (gapped ones)[28]. The DMRG approach was first used to study the ground state properties and low-energy excitations of one-dimensional chains [36, 37], ladders [185, 39], Bethe lattice system [40], strongly correlated electron systems [41, 42, 43]. It has been extensively applied to the study of various spin chains. Low-lying excited states of the spin-1 [36, 37] and spin-1/2 Heisenberg antiferromagnets have been calculated [44]. Likewise, spin-1 chains with quadratic and biquadratic interactions [45, 46], a spin-2 antiferromagnetic chain [47, 48, 49], spin-1/2 and spin-1 chains with dimerization and/or frustration (next-nearest-neighbor coupling) [50, 51, 52, 53, 54, 55], and frustrated spin-3/2 and spin-2 chains [56] have all been studied. By using DMRG, the ground-state entanglement in the spin-1/2 isotropic antiferromagnetic Heisenberg chain is studied when there are domain walls generated by a boundary magnetic field [57]. Edge excitations at the ends of finite spin chains and the effects of perturbations such as a weak magnetic field coupled to a few sites have been considered [47, 58, 59, 60]. Randomness in the form of random transverse magnetic field in a spin-1/2 XY model [61], random exchange couplings[62], and random modulation patterns of the exchange [63, 64], has been examined. Also, alternating spin magnitudes [65], the presence of a constant [66] or a staggered [67] magnetic field in a spin-1 chain, bond doping [31], the effects of a local impurity [68], and interactions with quantum phonons [27, 69] have also been considered. Attempts were made to extract critical behavior of gapless systems using the DMRG to generate renormalization transformations

of the coupling constants in the Hamiltonian [70, 71]. Hallberg et al.[72, 73] studied the critical behavior of S = 1/2 and S = 3/2 quantum spin chains with periodic boundary conditions through extensive calculations of ground state correlation functions at different separations and different chain sizes. Spin correlation functions in an open chain have also been calculated and compared with results calculated from low-energy field theory, showing that estimates of the amplitudes can also be obtained [74].

The technique is also applied to models, such as 1D Holstein model [75], 1D Holstein-Hubbard model [76], spin-Peierls model [77], spin-boson model [78, 79, 80, 81, 82] and one-dimensional Kondo lattice model [83].

Xiang have applied the DMRG to models in momentum space [84]. It is then applied to investigate the Hubbard model [85, 84, 86], and other models.

It has proved difficult to extend the density-matrix renormalization-group technique to large two-dimensional systems. Hence, many attempts were made to extend the applicability of DMRG to those systems [87, 88, 171, 86, 90, 91, 92, 84, 86].

DMRG is also used to investigate 1D quantum systems at finite temperatures, using the quantum transfer matrix formulation [93, 169, 95, 96, 97, 167]. Thermodynamic properties of the one-dimensional Kondo model at half-filling are studied by the density matrix renormalization group method applied to the quantum transfer matrix [99]. The density matrix renormalization group (DMRG) method and its applications to finite temperatures and two-dimensional systems are reviewed in [100].

The ground-state dynamical correlation functions calculations in one-dimensional quantum systems based on the density matrix renormalization-group method and the maximum entropy method was developed in [101]. A DMRG method for calculating dynamical properties and excited states in low-dimensional lattice quantum many-body systems is presented in [102].

The DMRG method is also adapted and extended to treat time-dependent problems like: the real-time dynamics of interacting one-dimensional spinless Fermi systems [103, 104, 105, 106], the study of transport properties of quantum-dot systems connected to metallic leads [107], the quantum impurity systems which have a time-dependent Hamiltonian [108], the spin dynamics and transport in one-dimensional spin-1/2 systems at zero temperature [109], the calculation of the zero temperature conductance of nanostructures [110, 111].

The DMRG method has been also applied to the Pariser-Parr-Pople-Peierls model to explore the nature of the ground and low-lying excited states of large polymeric systems [112, 113, 114, 115]. Also, the full configuration interaction problem in quantum chemistry is solved using DMRG [116].

The linear response theory (Kubo) is combined with the DMRG method to evaluate conductance of strongly interacting quantum systems [117]. It is also used to solve the impurity problem in the dynamical mean field theory [118, 119]. The ground-state phase diagram of 2D electrons in a high Landau level (Quantum Hall effect) is studied by the DMRG method in [120]. It is also applied to the BCS pairing Hamiltonian which describes ultrasmall superconducting grains [121].

The DMRG method have been extended to the case where the Hamiltonian has a non-Abelian global symmetry group.[122, 123]

G. Fáth and M. Sarvary have used the DMRG method to establish a theory of cultural evolution [124]!.

In other hand, Martín-Delgado and Sierra have investigated the analytic formulation of DMRG, and have formulated the Correlated Block Renormalization Group (CBRG) [125, 126]. They have also reformulated the DMRG method in terms of a single block, instead of the standard left and right blocks used in the construction of the superblock [127].

F. Verstraete et al. have introduced a picture to analyze the density matrix renormalization group (DMRG) from a quantum information perspective [128]. Also, DMRG is reformulated in terms of Matrix-Product States method (MPS) [129, 130, 131, 132, 133].

After this review of applications of DMRG, it is useful to explore in some detail how DMRG procedure is implemented for some important physical models used to study strongly correlated systems. We begin with Hubbard model.

4.2 DMRG implementation on Hubbard chain

The single-band Hubbard model [134] is widely accepted as a generic and minimal model for one-dimensional strongly interacting electrons. The simplest approximation for the interaction between the electrons is when both electrons are on the same site (on-site Coulomb repulsion), with nearest-neighbour hopping representing the kinetic energy of the system [174, 134]. An exact solution for the Hubbard model is possible for the one-dimensional case using the Bethe Ansatz [136, 137], while it is unsolvable in two and higher dimensions.

4.2.1 Hubbard model

The simplest Hubbard Hamiltonian writes

$$H = -t \sum_{i,\sigma} (c^{\dagger}_{i+1\sigma} c_{i\sigma} + h.c.) + U \sum_{i} n_{i\uparrow} n_{i\downarrow} \tag{4.1}$$

where $c^{\dagger}_{i\sigma}$ creates an electron with spin σ in a Wannier orbital at lattice site i, $n_{i\sigma} = c^{\dagger}_{i\sigma} c_{i\sigma}$, U is the Coulomb repulsion, t is the nearest-neighbor hopping integral and $h.c = c^{\dagger}_{i\sigma} c_{i+1\sigma}$, is the hermitian conjugate.

The hopping term alone leads to a conventional band spectrum and one-electron Bloch levels in which each electron is distributed throughout the entire crystal (a metal). The Coulomb term alone would favour local magnetic moments, since it suppresses the possibility of a second electron (with oppositely directed spin) at singly occupied sites (an insulator). When both terms are present, the competition between them brings about a transition between the metallic phase and the Mott insulating phase (see for example [138]).

A comparison between DMRG results with the exact solution is given in [139]. Thus, the difference between ground states calculated by analytical and numerical methods as the number of iterations and the number of states kept are varying. One can see that after two or three iterations, the error (difference between the exact and the numerical values) saturates. The iteration where saturation happens depends on the number of states kept. The important thing is that the accuracy of the results increases as the number of states kept is increased. However, this accuracy will diminish as the number of sites on the system is increased.

A comparison is also made between the convergence of results using periodic (PBC) or open (OBC) boundary conditions [139]. One finds that convergence is better for (OBC) than for (PBC), which makes reasonable to treat systems with open boundary conditions on large lattices rather than systems with periodic boundaries on small lattices.

As next-nearest neighbors hopping are considered [139], an impurity is introduced [140] or higher dimensions [141] are to be treated, the Hubbard model is no longer integrable [142], i.e., one cannot use Bethe Ansatz to solve it. Also, the weak-coupling treatments no longer work at strong coupling. Therefore, an accurate numerical technique is needed to investigate the low energy behaviour of this system. The DMRG technique seems to be, among other ones, a good candidate to deal with these situations. The investigation involves the calculation of the ground state and few excited states energies, the behaviour of correlation functions of different physical quantities, like spin-spin and charge-charge ones.

One extension of the original Hubbard model is the inclusion of longer-ranged interactions between the electrons on different sites. Then we add the term

$$\sum_j V_j \sum_i n_i n_{i+j} \tag{4.2}$$

where V_j is the interaction term between two electrons on sites far apart of j units.

In order to consider next-nearest neighbours hopping, we have to add the term

$$t' \sum_{i,\sigma} (c^\dagger_{i+2\sigma} c_{i\sigma} + h.c.) \tag{4.3}$$

where t' is the next-nearest-neighbor hopping integral.

The effect of impurities on the ground state of a Hubbard chain is investigated by introducing the term [143]

$$\sum_i (\varepsilon_i - \mu) n_i, \tag{4.4}$$

ε_i (on-site energy) are randomly distributed, $n_i = n_{i\uparrow} + n_{i\downarrow}$, and μ represents the chemical potential which controls the particle density of the system (see, for example, [144]) .

A local site impurity on site j_0 is modeled by [140]:

$$H_{\text{imp}} = V n_{j_0} \tag{4.5}$$

and a hopping impurity by the nonlocal potential

$$H_{\text{imp}} = (t - t') \sum_\sigma (c^\dagger_{j_0+1,\sigma} c_{j_0,\sigma} + c^\dagger_{j_0,\sigma} c_{j_0+1,\sigma}) \tag{4.6}$$

such that the hopping amplitude t is replaced by t' on the bond linking the sites j_0 and $j_0 + 1$.

If a small magnetic field is applied (in the z-direction, for example), an extra term in the site Hamiltonian is then added

$$H_h = -h \sum_i S^z_i, \tag{4.7}$$

with S_i^z is the z-component of electron spin on site i, defined as:

$$S_i^z = n_i - \frac{1}{2} \tag{4.8}$$

In order to examine the properties of a Hubbard model on a two-chain ladder to understand the ground state behaviour of the undoped and doped two-leg ladders, Noack, White and Scalapino [141] used a Hamiltonian of a single-band Hubbard model of two coupled chains of length L,

$$H = -t \sum_{i,\lambda\sigma} (c^\dagger_{i+1,\lambda\sigma} c_{i,\lambda\sigma} + h.c.) - t_\perp \sum_{i,\sigma} (c^\dagger_{i,1\sigma} c_{i,2\sigma} + h.c.) + U \sum_i n_{i,\lambda\uparrow} n_{i,\lambda\downarrow} \tag{4.9}$$

where $c^\dagger_{i,\lambda\sigma}$ and $c_{i,\lambda\sigma}$ create and destroy, respectively, an electron on ring i and chain λ with spin σ, and $n_{i,\lambda\sigma} = c^\dagger_{i,\lambda\sigma} c_{i,\lambda\sigma}$. The hopping integral parallel to the chains is t, the hopping between the chains $t_\perp$, and U is the on-site Coulomb interaction.

A Hamiltonian with particle-hole symmetry and spatial reflection symmetry is used by Eric Jeckelmann [145] to study the phase diagram of the one-dimensional half-filled Hubbard model:

$$H = -t \sum_{i,\sigma} (c^\dagger_{i+1\sigma} c_{i\sigma} + c^\dagger_{i\sigma} c_{i+1\sigma}) + U \sum_i \left(n_{i\uparrow} - \frac{1}{2} \right) \left(n_{i\downarrow} - \frac{1}{2} \right) + V \sum_i (n_i - 1)(n_{i+1} - 1) \tag{4.10}$$

with on-site U and nearest-neighbor V repulsion and hopping term t. Note that at half filling, the number of electrons equals the number of sites of the system.

4.2.2 Implementation details

In this section, I will show in more detail how to implement the DMRG technique on a one-dimensional Hubbard chain. The notation and some ideas about the implementation are borrowed from the work of Dan Bohr, who did himself the calculations [146].

Let's take a simpler version of the Hubbard model for a chain of length L,

$$H = -t_1 \sum_{i,\sigma=\uparrow,\downarrow}^{L-1} (c^\dagger_{i\sigma} c_{i+1\sigma} + c^\dagger_{i+1\sigma} c_{i\sigma}) + U \sum_{i=1}^{L} n_{i\uparrow} n_{i\downarrow}, \tag{4.11}$$

First, we define and label the basis used for a single site as: $|0\rangle \equiv |1\rangle$, $c^\dagger_\uparrow|0\rangle \equiv |\uparrow\rangle \equiv |2\rangle$, $c^\dagger_\downarrow|0\rangle| \downarrow\rangle \equiv |3\rangle$, and $c^\dagger_\uparrow c^\dagger_\downarrow|0\rangle \equiv |\uparrow\downarrow\rangle \equiv |4\rangle$, such that, for example, the element $c^{(1,2)}_{i\uparrow} = \langle 2|c_{i\uparrow}|1\rangle$ is equivalent to $c^{(1,2)}_{i\uparrow} = \langle\uparrow|c_{i\uparrow}|0\rangle$. Using the fact that $|\uparrow\rangle \equiv c^\dagger_\uparrow|0\rangle$ and $\langle i|j\rangle = \delta_{ij}$, we get $c^{(1,2)}_{i\uparrow} = 1$. This procedure can be applied to get matrix elements for all operators in (4.11).

Therefore, the matrix representation, in the already cited fourfold basis, of annihilation operators $c_{i\sigma}$, the on-site repulsion operator $H_U = U n_{i\uparrow} n_{i\downarrow}$ and the total z-spin operator S^i_z for a single site are given by:

$$c_{i\uparrow} = \begin{pmatrix} 0 & 1 & 0 & 0 \\ 0 & 0 & 0 & 0 \\ 0 & 0 & 0 & 1 \\ 0 & 0 & 0 & 0 \end{pmatrix}, \tag{4.12}$$

$$c_{i\downarrow} = \begin{pmatrix} 0 & 0 & 1 & 0 \\ 0 & 0 & 0 & -1 \\ 0 & 0 & 0 & 0 \\ 0 & 0 & 0 & 0 \end{pmatrix}, \tag{4.13}$$

$$H_U = U n_{i\uparrow} n_{i\downarrow} = U c^\dagger_{i\uparrow} c_{i\uparrow} c^\dagger_{i\downarrow} c_{i\downarrow} = U \begin{pmatrix} 0 & 0 & 0 & 0 \\ 0 & 0 & 0 & 0 \\ 0 & 0 & 0 & 0 \\ 0 & 0 & 0 & 1 \end{pmatrix}, \tag{4.14}$$

$$S^z_i = \begin{pmatrix} 0 & 0 & 0 & 0 \\ 0 & \frac{1}{2} & 0 & 0 \\ 0 & 0 & -\frac{1}{2} & 0 \\ 0 & 0 & 0 & 0 \end{pmatrix}. \tag{4.15}$$

Because electrons are fermions, the corresponding site operators, (4.12) and (4.13) and their hermitian conjugates should satisfy the anticommutation relations (see for example [147]),

$$\{c_{i\sigma}, c^\dagger_{j\sigma'}\} = \delta_{i,j}\delta_{\sigma,\sigma'}, \tag{4.16}$$

and

$$\{c_{i\sigma}, c_{j\sigma'}\} = \{c^\dagger_{i\sigma}, c^\dagger_{j\sigma'}\} = 0. \tag{4.17}$$

In the other hand, these operators have to be expressed in the basis of several sites, and hence we must keep track of this anticommutation on this extended basis. This is done using a matrix counting the number of particles on each site, and returning a sign in accordance. For the single site this matrix is

$$P_i = \begin{pmatrix} 1 & 0 & 0 & 0 \\ 0 & -1 & 0 & 0 \\ 0 & 0 & -1 & 0 \\ 0 & 0 & 0 & 1 \end{pmatrix}. \tag{4.18}$$

Let's see how can we maintain these relations when expanding the basis to several sites.

First we expand the basis of operators $c_{1\sigma}$ and $c_{2\sigma}$, related to sites 1 and 2, respectively, to the basis of both sites,

$$\tilde{c}_{1\sigma} = c_{1\sigma} \otimes \delta_2, \tag{4.19}$$

$$\tilde{c}_{2\sigma} = P_1 \otimes c_{2\sigma}, \tag{4.20}$$

where δ_2 is a 4×4 unit matrix. More specifically

$$\tilde{c}_{1\uparrow} = c_{1\uparrow} \otimes \delta_2 = \begin{pmatrix} 0 & \delta_2 & 0 & 0 \\ 0 & 0 & 0 & 0 \\ 0 & 0 & 0 & \delta_2 \\ 0 & 0 & 0 & 0 \end{pmatrix}, \tag{4.21}$$

and

$$\tilde{c}_{2\uparrow} = P_1 \otimes c_{2\uparrow} = \begin{pmatrix} c_{2\uparrow} & 0 & 0 & 0 \\ 0 & -c_{2\uparrow} & 0 & 0 \\ 0 & 0 & -c_{2\uparrow} & 0 \\ 0 & 0 & 0 & c_{2\uparrow} \end{pmatrix}. \tag{4.22}$$

which are 16×16 matrices. Ordinary matrix multiplication yields

$$\tilde{c}^\dagger_{1\uparrow}\tilde{c}_{2\uparrow} + \tilde{c}^\dagger_{2\uparrow}\tilde{c}_{1\uparrow} = \begin{pmatrix} 0 & \delta_2 & 0 & 0 \\ 0 & 0 & 0 & 0 \\ 0 & 0 & 0 & \delta_2 \\ 0 & 0 & 0 & 0 \end{pmatrix} \begin{pmatrix} c^\dagger_{2\uparrow} & 0 & 0 & 0 \\ 0 & -c^\dagger_{2\uparrow} & 0 & 0 \\ 0 & 0 & -c^\dagger_{2\uparrow} & 0 \\ 0 & 0 & 0 & c^\dagger_{2\uparrow} \end{pmatrix} + \begin{pmatrix} c^\dagger_{2\uparrow} & 0 & 0 & 0 \\ 0 & -c^\dagger_{2\uparrow} & 0 & 0 \\ 0 & 0 & -c^\dagger_{2\uparrow} & 0 \\ 0 & 0 & 0 & c^\dagger_{2\uparrow} \end{pmatrix} \begin{pmatrix} 0 & \delta_2 & 0 & 0 \\ 0 & 0 & 0 & 0 \\ 0 & 0 & 0 & \delta_2 \\ 0 & 0 & 0 & 0 \end{pmatrix}$$
$$= \begin{pmatrix} 0 & [c^\dagger_{2\uparrow}, \delta_2] & 0 & 0 \\ 0 & 0 & 0 & 0 \\ 0 & 0 & 0 & -[c^\dagger_{2\uparrow}, \delta_2] \\ 0 & 0 & 0 & 0 \end{pmatrix} \tag{4.23}$$

It is easy to check that

$$[c^\dagger_{2\uparrow}, \delta_2] = \begin{pmatrix} 0 & 0 & 0 & 0 \\ 0 & 0 & 0 & 0 \\ 0 & 0 & 0 & 0 \\ 0 & 0 & 0 & 0 \end{pmatrix} \tag{4.24}$$

Thus, we find $\tilde{c}^\dagger_{1\uparrow}\tilde{c}_{2\uparrow} + \tilde{c}^\dagger_{2\uparrow}\tilde{c}_{1\uparrow} = 0$.

Note that if we had used δ_1 instead of P_1 we would find

$$\tilde{c}^\dagger_{1\uparrow}\tilde{c}_{2\uparrow} + \tilde{c}^\dagger_{2\uparrow}\tilde{c}_{1\uparrow} = \begin{pmatrix} 0 & \{c^\dagger_{2\uparrow}, \delta_2\} & 0 & 0 \\ 0 & 0 & 0 & 0 \\ 0 & 0 & 0 & \{c^\dagger_{2\uparrow}, \delta_2\} \\ 0 & 0 & 0 & 0 \end{pmatrix} \tag{4.25}$$

with

$$\{c^\dagger_{2\uparrow}, \delta_2\} = \begin{pmatrix} 0 & 0 & 0 & 0 \\ 2 & 0 & 0 & 0 \\ 0 & 0 & 0 & 0 \\ 0 & 0 & 2 & 0 \end{pmatrix} \tag{4.26}$$

Thus, $\tilde{c}^\dagger_{1\uparrow}\tilde{c}_{2\uparrow} + \tilde{c}^\dagger_{2\uparrow}\tilde{c}_{1\uparrow} \neq 0$, which is incompatible with the anticommutation relations.

Similarly, we may consider

$$\tilde{c}^\dagger_{2\uparrow}\tilde{c}_{2\uparrow}+\tilde{c}^\dagger_{2\uparrow}\tilde{c}_{2\uparrow}=\begin{pmatrix} c_{2\uparrow} & 0 & 0 & 0\\ 0 & -c_{2\uparrow} & 0 & 0\\ 0 & 0 & -c_{2\uparrow} & 0\\ 0 & 0 & 0 & c_{2\uparrow}\end{pmatrix}\begin{pmatrix} c^\dagger_{2\uparrow} & 0 & 0 & 0\\ 0 & -c^\dagger_{2\uparrow} & 0 & 0\\ 0 & 0 & -c^\dagger_{2\uparrow} & 0\\ 0 & 0 & 0 & c^\dagger_{2\uparrow}\end{pmatrix}+$$
$$\begin{pmatrix} c^\dagger_{2\uparrow} & 0 & 0 & 0\\ 0 & -c^\dagger_{2\uparrow} & 0 & 0\\ 0 & 0 & -c^\dagger_{2\uparrow} & 0\\ 0 & 0 & 0 & c^\dagger_{2\uparrow}\end{pmatrix}\begin{pmatrix} c_{2\uparrow} & 0 & 0 & 0\\ 0 & -c_{2\uparrow} & 0 & 0\\ 0 & 0 & -c_{2\uparrow} & 0\\ 0 & 0 & 0 & c_{2\uparrow}\end{pmatrix}$$
$$=\begin{pmatrix} \{c^\dagger_{2\uparrow},c_{2\uparrow}\} & 0 & 0 & 0\\ 0 & \{c^\dagger_{2\uparrow},c_{2\uparrow}\} & 0 & 0\\ 0 & 0 & \{c^\dagger_{2\uparrow},c_{2\uparrow}\} & 0\\ 0 & 0 & 0 & \{c^\dagger_{2\uparrow},c_{2\uparrow}\}\end{pmatrix} \tag{4.27}$$

where we can easily check that

$$\{c^\dagger_{2\uparrow},c_{2\uparrow}\}=\begin{pmatrix} 1 & 0 & 0 & 0\\ 0 & 1 & 0 & 0\\ 0 & 0 & 1 & 0\\ 0 & 0 & 0 & 1\end{pmatrix} \tag{4.28}$$

and hence indeed $\{\tilde{c}_{2\uparrow},\tilde{c}^\dagger_{2\uparrow}\}=1$, which is also obtained using δ_1 instead of P_1.

It should be noted that the fermionic sign matrix for sites 1 and 2 is

$$P_{12}=P_1\otimes P_2=\begin{pmatrix} P_2 & 0 & 0 & 0\\ 0 & -P_2 & 0 & 0\\ 0 & 0 & -P_2 & 0\\ 0 & 0 & 0 & P_2\end{pmatrix} \tag{4.29}$$

where it is clear that an odd total number of particles on sites 1 and 2 gives a sign, while an even total number of particles does not.

To understand what does this mean, we have to know that the above matrix is a representation of operator P_{12} in the basis $\{|0\rangle|0\rangle,|0\rangle|\uparrow\rangle,\cdots,|\uparrow\rangle|\downarrow\rangle,\cdots,|\uparrow\downarrow\rangle|\uparrow\downarrow\rangle\}$.

Thus, we can, for example, easily check that

$$\langle\uparrow|\langle 0|P_{12}|0\rangle|\uparrow\rangle=-1 \tag{4.30}$$

whereas

$$\langle\uparrow\downarrow|\langle\uparrow\downarrow|P_{12}|\uparrow\downarrow\rangle|\uparrow\downarrow\rangle=1 \tag{4.31}$$

The operator (4.14) is diagonal and remains diagonal after enlargement of the basis. Diagonal matrices commute and hence so does the number operators before and after enlarging the basis. Hence any commutation relations of diagonal matrices are preserved in the process of enlarging the basis. Note that we use δ and not P when enlarging the Hilbert space for bosonic operators.

4.2.2.1 Infinite system sweep

The DMRG procedure is started by constructing the Hamiltonian and other operators for a four site superblock. The basis is enlarged by performing Kronecker tensor products. The Hamiltonian for sites 1 and 2 is constructed first,

$$\begin{aligned} H_{12} &= H_U \otimes \delta_2 + \delta_1 \otimes H_U \\ -t &\left[(c^\dagger_{1\uparrow} \otimes \delta_2)(P_1 \otimes c_{2\uparrow}) + (P_1 \otimes c^\dagger_{2\uparrow})(c_{1\uparrow} \otimes \delta_2)\right] \\ -t &\left[(c^\dagger_{1\downarrow} \otimes \delta_2)(P_1 \otimes c_{2\downarrow}) + (P_1 \otimes c^\dagger_{2\downarrow})(c_{1\downarrow} \otimes \delta_2)\right] \end{aligned} \tag{4.32}$$

where the first line represents the on-site repulsions and the second line represents the hopping between sites 1 and 2. Matrix P_1 is used to maintain anticommutation of fermionic operators.

Other relevant operators are

$$S^z_{12} = S^z_1 \otimes \delta_2 + \delta_1 \otimes S^z_2, \tag{4.33}$$

$$P_{12} = P_1 \otimes P_2, \tag{4.34}$$

$$c^L_\sigma = P_1 \otimes c_{2\sigma}, \tag{4.35}$$

representing the total z-component of the spin, the fermionic sign operator, the annihilation operator for the rightmost site, and the number operator for two sites respectively. Note that c^L_σ is needed to connect the left block to the leftmost central site. All matrices in the combined Hilbert space of sites 1 and 2 have dimensions 16×16.

Completely analogous expressions exist for the right block. Hence, we may construct the Hamiltonian and other operators for the four site superblock,

$$\begin{aligned} H_{1234} &= H_{12} \otimes \delta_{34} + \delta_{12} \otimes H_{34} \\ -t &\left[((c^L_\uparrow)^\dagger \otimes \delta_{34})(P_{12} \otimes c^R_\uparrow) + (P_{12} \otimes (c^R_\uparrow)^\dagger)(c^L_\uparrow \otimes \delta_{34})\right] \\ -t &\left[((c^L_\downarrow)^\dagger \otimes \delta_{34})(P_{12} \otimes c^R_\downarrow) + (P_{12} \otimes (c^R_\downarrow)^\dagger)(c^L_\downarrow \otimes \delta_{34})\right] \end{aligned} \tag{4.36}$$

where c^R_σ is the annihilation operator for the leftmost site in the right block, and where the second line in Eq. (4.36) is the hopping between the left and right blocks.

For realistic calculations, no truncation is done at this stage because the number of states is smaller than the number of states one usually retains. However, for the sake of illustration we will start DMRG process at this system size level (4 sites).

The first step is to compute the ground state eigenvector of the Hamiltonian H_{1234}; a 256×256 sparse matrix represented in the 256-vectors basis
$\{|0,0\rangle|0,0\rangle, |0,0\rangle|\uparrow,0\rangle, \cdots, |0,\uparrow\rangle|0,\downarrow\rangle, \cdots, |\uparrow\downarrow,\uparrow\downarrow\rangle|\uparrow\downarrow,\uparrow\downarrow\rangle\}$. To do this we can use efficiently Lanczos or Davidson routines or even, but in less efficient way, standard routines.

In the process of constructing the superblock, it is useful to profit of the symmetries of the system. This means that the Hamiltonian matrix of the superblock can be made of submatrices corresponding to different numbers of electrons and different numbers of total spin S^z. Consequently, the calculations time may be considerably reduced.

4.2.2.2 Matrix density

The most general wave function, describing a system and the universe surrounding it, can be written [22]

$$|\psi\rangle = \sum_{ij} C_{ij}|\phi_i\rangle|\theta_j\rangle \tag{4.37}$$

where $|\phi_i\rangle$ is a complete set of vectors in the vector space describing the system, and $|\theta_j\rangle$ is a complete set for the rest of the universe.

Let A an operator that acts only on the system, and then it equals to

$$\sum_{ii'j} A_{ii'}|\phi_i\rangle|\theta_j\rangle\langle\theta_j|\langle\phi_{i'}|. \tag{4.38}$$

Then

$$\begin{aligned}\langle\psi|A|\psi\rangle &= \sum_{iji'j'} C^*_{ij}\, C_{i'j'}\langle\theta_j|\langle\phi_i|A|\phi_{i'}\rangle|\theta_{j'}\rangle \\ &= \sum_{iji'} C^*_{ij}\, C_{i'j}\langle\phi_i|A|\phi_{i'}\rangle \\ &= \sum_{ii'}\langle\phi_i|A|\phi_{i'}\rangle\rho_{ii'}\end{aligned} \tag{4.39}$$

where

$$\rho_{ii'} = \sum_j C^*_{ij}\, C_{i'j} \qquad \text{(density matrix)}. \tag{4.40}$$

We define the operator ρ, which operates only on the system, to be such that $\rho_{ii'} = \langle\phi_{i'}|\rho|\phi_i\rangle$.

It is convenient to write $|\psi\rangle$ in a matrix form

$$\psi = \begin{array}{c} \\ \begin{matrix}|\phi_1\rangle|\theta_1\rangle \\ |\phi_1\rangle|\theta_2\rangle \\ \vdots \\ |\phi_N\rangle|\theta_N\rangle\end{matrix} \end{array} \begin{array}{c} \begin{matrix}|\phi_1\rangle|\theta_1\rangle & |\phi_1\rangle|\theta_2\rangle & \cdots & |\phi_N\rangle|\theta_N\rangle\end{matrix} \\ \begin{pmatrix} C_{11} & C_{12} & \cdots & C_{1N} \\ C_{21} & C_{22} & \cdots & C_{2N} \\ \vdots & \vdots & \ddots & \vdots \\ C_{N1} & C_{N2} & \cdots & C_{NN}\end{pmatrix}\end{array} \tag{4.41}$$

so that, it is easy to check from eq.(4.40) that the reduced density matrix (RDM) writes as a simple matrix product

$$\rho = \psi \cdot \psi^\dagger \tag{4.42}$$

The ρ_L (L stands for left side of the superblock, i.e, the system) matrix is diagonalized and m column eigenvectors $\{u_\alpha, \alpha = 1 \cdots m\}$ are retained to construct a matrix,

$$O = (u_1, u_2, \cdots, u_m), \tag{4.43}$$

The block Hamiltonian and all operators needed to reconstruct the superblock Hamiltonian are given by,

$$\tilde{H}_1 = O^\dagger H_{12} O, \tag{4.44}$$

$$\tilde{c}_\sigma^L = O^\dagger c_\sigma^L O, \tag{4.45}$$

$$\tilde{P}_L = O^\dagger P_L O, \tag{4.46}$$

$$\tilde{A} = O^\dagger A O, \tag{4.47}$$

where A is the matrix representation of any operator working on the left block.

In a similar way, we diagonalize ρ_R (R stands for right side of the superblock), to obtain a truncation operator O, through which we calculate $\tilde{H}_4$ and $\tilde{c}_\sigma^R$. The old operators are then replaced by the new ones: $\tilde{H}_1 \to H_1$, $\tilde{c}_\sigma^L \to c_\sigma^L$, $\tilde{P}_L \to P_L$, $\tilde{H}_4 \to H_4$, and $\tilde{c}_\sigma^R \to c_\sigma^R$. Note that the old and the new operators are stored to be used in the finite system algorithm.

At this stage, we add two effective sites (represented in their full real space) in between the right and left blocks. These latter are represented in a truncated basis, and the superblock contains now 6 sites. This procedure is then repeated until the desired chain length L is reached. In the meantime, all operators matrices should be stored.

4.2.2.3 Finite system sweeps

The final picture of the superblock at the end of the infinite system algorithm is: two blocks (left and right), each consisting of $L/2-1$ sites and represented in a truncated basis and two central sites in between them.

Once the superblock Hamiltonian has been constructed the basic step is similar to the infinite system method. Taking the left to right sweep as an example, the basic DMRG step is:

1. Compute the ground state of the superblock Hamiltonian.
2. Construct the RDM ρ_L for the new left block, consisting of the *old* left block, initially of length $L/2-1$, and the leftmost central site.
3. Diagonalize ρ_L.
4. Find the retained eigenbasis by keeping the m most probable eigenstates of ρ_L.
5. Transform all *left* matrices to the eigenbasis of ρ_L and store them.
6. Construct a new superblock Hamiltonian, consisting of the new truncated left block, two central sites, and a new right block containing one site less. At the first finite system step the length of the new left block is $L/2$, and the length of the new right block is $L/2-2$. Matrices defining the new right block were found and stored during the infinite system sweep.

As this procedure is repeated, the position of the two sites is moving along the chain, and a sweep is counted as the left and right blocks are of equal size. Typically 4-6 iterations are sufficient to reach convergence of the ground state value.

4.3 DMRG implementation on Ising model

The Ising model was introduced in the 1920's by H. Lenz and his student E. Ising in order to explain the spontaneous appearance of a magnetization in a ferromagnetic material as it is cooled under its Curie's temperature. It is a matter of a model where spins with only two orientations are arranged on the sites of a multidimensional lattice. L. Onsager in his celebrated paper [148] derived the free energy of the two-dimensional Ising model (2D IM) in the absence of an external magnetic field.

A variation of the model is the Ising model in a transverse field (ITF), used to investigate quantum phase transition on a two-dimensional square lattice. It has the advantage to be exactly soluble in $d = 1$ dimensions; which will help checking accuracies for the method we are using.

To illustrate the infinite system DMRG implementation for Ising model, we pick up an example from the work of A. Juozapavicius [149], where he uses a simple version of the antiferromagnetic Ising spin-1/2 chain in a transverse uniform magnetic field,

$$H = J \sum_{i=1}^{L-1} S_i^z S_{i+1}^z - h \sum_{i=1}^{L} S_i^x, \tag{4.48}$$

where J is a positive coupling constant between the z-components, and h is a uniform magnetic field in x-direction. The basis states on a single site are chosen such that the S_i^z operator is diagonal, and the corresponding states are denoted by: $|\uparrow\rangle$ and $|\downarrow\rangle$, for $S^z = 1/2$ and $S^z = -1/2$, respectively. In this basis, the single-site spin matrices have the following form:

$$S^z = \begin{array}{c} \\ \uparrow \\ \downarrow \end{array} \begin{array}{c} \begin{array}{cc} \uparrow & \downarrow \end{array} \\ \begin{pmatrix} \frac{1}{2} & 0 \\ 0 & -\frac{1}{2} \end{pmatrix} \end{array}, S^x = \begin{array}{c} \\ \uparrow \\ \downarrow \end{array} \begin{array}{c} \begin{array}{cc} \uparrow & \downarrow \end{array} \\ \begin{pmatrix} 0 & \frac{1}{2} \\ \frac{1}{2} & 0 \end{pmatrix} \end{array}. \tag{4.49}$$

4.3.1 Infinite system sweep

Two blocks with two sites each are constructed; then assembled together to form a superblock of 4 sites. Each block has 4 states which are direct products of the single-site states:
$|\uparrow\rangle \otimes |\uparrow\rangle \equiv |\uparrow\uparrow\rangle$,$|\uparrow\rangle \otimes |\downarrow\rangle \equiv |\uparrow\downarrow\rangle$, $|\downarrow\rangle \otimes |\uparrow\rangle \equiv |\downarrow\uparrow\rangle$ and $|\downarrow\rangle \otimes |\downarrow\rangle \equiv |\downarrow\downarrow\rangle$. Thus, the superblock of 4 sites has $(2S+1)^4 = 16$ possible states.

The explicit form of the Hamiltonian of two spins is

$$H_{12} = S_1^z \otimes S_2^z - hS_1^x \otimes \delta_2 - h\delta_1 \otimes S_2^x, \tag{4.50}$$

where δ_1 and δ_2 are 2×2 unit matrices acting in the spaces of the first and the second spins, respectively. Calculation of the direct products gives

$$S_1^z \otimes S_2^z = \begin{pmatrix} \frac{1}{4} & 0 & 0 & 0 \\ 0 & -\frac{1}{4} & 0 & 0 \\ 0 & 0 & -\frac{1}{4} & 0 \\ 0 & 0 & 0 & \frac{1}{4} \end{pmatrix}, \tag{4.51}$$

$$S_1^x \otimes \delta_2 = \frac{1}{2}\begin{pmatrix} 0 & 0 & 1 & 0 \\ 0 & 0 & 0 & 1 \\ 1 & 0 & 0 & 0 \\ 0 & 1 & 0 & 0 \end{pmatrix}, \delta_1 \otimes S_2^x = \frac{1}{2}\begin{pmatrix} 0 & 1 & 0 & 0 \\ 1 & 0 & 0 & 0 \\ 0 & 0 & 0 & 1 \\ 0 & 0 & 1 & 0 \end{pmatrix}, \tag{4.52}$$

and so the matrix of the Hamiltonian is

$$H_{12} = -\frac{1}{4}\begin{pmatrix} -1 & 2h & 2h & 0 \\ 2h & 1 & 0 & 2h \\ 2h & 0 & 1 & 2h \\ 0 & 2h & 2h & -1 \end{pmatrix} \tag{4.53}$$

In a similar way, the Hamiltonian of the right block H_{34} is obtained. We need now a Hamiltonian term that represents the interaction between these two blocks, say H_{23}:

$$H = H_{12} \otimes \delta_{34} + \delta_{12} \otimes H_{34} + \delta_1 \otimes H_{23} \otimes \delta_4, \tag{4.54}$$

where δ_{12} and δ_{34} are 4×4 unit matrices, and $H_{23} = S_2^z \otimes S_3^z$ is given by Eq. (4.51). The superblock matrix H has $16 \times 16 = 256$ elements.

Once H is constructed (we have to choose a value for h), the diagonalization, using numerical methods, is straightforward; and the ground state eigenvector is obtained. Then, we use this ground state eigenvector to construct a 4×4 density matrix ρ for the left side of the system using

$$\rho_{ii'} \equiv \sum_{j=1}^{L} \psi_{ij}^* \psi_{i'j} \tag{4.55}$$

This matrix is also diagonalized, and according to the algorithm, only m states with the largest eigenvalues are kept. In a real calculation it is not useful to start the truncation just after a 2-sites blocks are constructed. We have to extend our blocks to a length such that the number of available states for each block is greater than the number of states we want to keep. This is an illustrative example and we can choose for example $m = 3$. The eigenstates of the lowest energy is then discarded. These three eigenvectors of ρ will form a 3×4 transformation matrix O. This matrix is used to change the basis and truncate the H_{12} Hamiltonian

$$\tilde{H}_{12} = O H_{12} O^T \tag{4.56}$$

The matrix $\tilde{H}_{12}$ represents the Hamiltonian of a 2-spin block, which is projected from its own real effective space (4 basis states) onto a basis with three eigenvectors of ρ with highest eigenvalues. This block is stored to be used later. Similarly, other important matrices of the half-system are truncated. In this case, the matrix of the rightmost spin of the left block is created and truncated: $\tilde{S}_{12R}^z = O(\delta_1 \otimes S_2^z)O^T$. It will be needed to connect the new block to a new single-site in the next iteration. Since the Hamiltonian (4.54) is symmetric with respect to the middle point of the chain, it is possible to number states of the system in such a way, that the right-side matrices are always equal to the left-side ones: $\tilde{H}_{34} = \tilde{H}_{12}$ and $\tilde{S}_{34L}^z = \tilde{S}_{12R}^z$, where the $\tilde{S}_{34L}^z$ matrix represents the z-component of the leftmost spin in the right block. This kind of state numbering is called " reflected numbering". Finally, the matrices are renamed $\tilde{H}_{12} \to H_1$,$\tilde{H}_{34} \to H_4$, $\tilde{S}_{12R}^z \to S_{12R}^z$ etc., and the first DMRG step is finished.

The second step is to insert two new sites between the left and right blocks. The latters are now represented by $m \times m$ truncated Hamiltonian matrices H_1 and H_4, respectively, while the two added sites are described by the on-site 2×2 Hamiltonian $H_2 = -hS^x$, and $H_3 = H_2$, respectively.

To obtain the Hamiltonian matrix of the new superblock, we need at first to construct those of the left and right sides. To do it for the left side, we need H_1 of the block, H_2 of the new site, and a term of interaction between them. Since only nearest neighbor interactions are present in the model, the block-site interaction is equivalent to the interaction between the rightmost spin of the block with the spin of the site. The z-component of the rightmost spin of the block is given by S^z_{12R}, so the interaction term is $H_{Bs} = S^z_{12R} \otimes S^z_2$. Consequently, the Hamiltonian of the left side of the system can be written as

$$H_{12} = H_1 \otimes \delta_2 + H_{Bs} + \delta_1 \otimes H_2, \tag{4.57}$$

which is a $2m \times 2m$ matrix. Due to the "reflected" numbering of states, the Hamiltonian of the right-side is simply $H_{34} = H_{12}$. The total superblock Hamiltonian is easily constructed using the left-side and the right-side matrices, adding a term, which connects the two middle sites:

$$H = H_{12} \otimes \delta_{34} + \delta_{12} \otimes H_{34} + \delta_1 \otimes H_{23} \otimes \delta_4, \tag{4.58}$$

where δ_1 nd δ_4 are $m \times m$, while δ_{12} and δ_{34} are $2m \times 2m$ unit matrices, and the inter-site interaction term $H_{23} = S^z_2 \otimes S^z_3$.

Now the Hamiltonian is diagonalized, the ground state eigenpair is obtained. The reduced DM of the left side is created from the eigenvector using the formula (4.55). ρ is diagonalized, and m states, corresponding to the largest eigenvalues are retained. The m eigenstates of the ρ form the transformation matrix O, which is used to truncate the matrices of the left-side operators: The Hamiltonian $\tilde{H}_{12} = OH_{12}O^T$ and the spin matrix of the rightmost spin of the block $\tilde{S}^z_{12R} = O(\delta_1 \otimes S^z_2)O^T$. The right-side matrices are equal to the corresponding left-side one due to the "reflected" numbering of states. The matrices are renamed $\tilde{H}_{12} \to H_1$,$\tilde{H}_{34} \to H_4$, $\tilde{S}^z_{12R} \to S^z_{12R}$, and the second DMRG step is finished.

Consecutive steps are exactly the same as the second step. They are repeated until the ground state energy o the system converges or until a desirable length of the chain is reached and then the finite-system DMRG may be started to increase accuracy.

4.4 Fermionic DMRG: The Kondo lattice model

The Hubbard model is considered too simple when trying to describe the behaviour of magnetic elements in dilute metallic alloys. Thus, a more sophisticated model is set up to include interactions between the electrons of the localized magnetic ions and the conduction electrons of the host metal. This model is called the periodic Anderson model. Its Hamiltonian is given by

$$\begin{aligned}\mathcal{H} = &-t \sum_{\langle i,j\rangle,\sigma} \left(c^\dagger_{i\sigma} c_{j\sigma} + c^\dagger_{j\sigma} c_{i\sigma} \right) + \varepsilon_f \sum_{i\sigma} f^\dagger_{i\sigma} f_{i\sigma} \\ &+V \sum_{i\sigma} \left(c^\dagger_{i\sigma} f_{i\sigma} + f^\dagger_{i\sigma} c_{i\sigma} \right) + U \sum_i f^\dagger_{i\uparrow} f_{i\uparrow} f^\dagger_{i\downarrow} f_{i\downarrow}\end{aligned} \tag{4.59}$$

where $\sigma = \uparrow$ or $\downarrow$ denotes the spin state, $c_{i\sigma}(f_{i\sigma})$ is the annihilation operator of the conduction (localized) electrons, and $\langle i,j\rangle$ denotes summation over nearest neighbours only. The first sum represents the hopping processes of the conduction electrons, the second one gives the energy of the f electrons, where ε_f is the atomic energy of the f level, the third sum describes the hybridization of the two bands, namely, V is the matrix element of the mixing between the two orbitals. The last term represents the Coulomb repulsion between the f electrons on the same orbital.

Solving the periodic Anderson model is a very complicated problem. However in the limit of large Coulomb repulsion U, the model can be slightly simplified, leading to the Kondo lattice model.

4.4.1 Single-impurity Kondo model

An effective model of the periodic Anderson model can be obtained in the limit, where the number of the localized electrons on a lattice site is fixed, and equal to one. This can happen when the f level is lowered below the d band, or, correspondingly, when the mixing between the two bands V is small compared to the Coulomb repulsion U between f electrons on the same site. The second-order perturbation with respect to V transform the periodic Anderson model Hamiltonian into the Kondo lattice Hamiltonian [150]

$$\mathcal{H} = -t \sum_{\langle i,j\rangle,\sigma} \left(c^{\dagger}_{i\sigma} c_{j\sigma} + c^{\dagger}_{j\sigma} c_{i\sigma} \right) + J \sum_{i} \hat{\mathbf{S}}_{ci} \cdot \hat{\mathbf{S}}_{i}, \tag{4.60}$$

where $\hat{\mathbf{S}}_{ci} = \frac{1}{2} \sum_{\sigma\sigma'} c^{\dagger}_{i\sigma} \tau_{\sigma\sigma'} c_{i\sigma'}$ with τ the Pauli spin matrices. The $\hat{\mathbf{S}}_i$ are spin-1/2 operators for the localized spins. The first sum describes again the motion of the conduction electrons (c-electrons) while each term of the last sum represents the interaction between the localized f spins and the the moving c electrons on a given site. The exchange interaction $J > 0$ is antiferromagnetic: it favors an opposite alignment of the conduction electron spin with the spin of the localized f-electron. It is related to the parameters of the Anderson model U and V.

There are essentially just two parameters in the model: the exchange interaction J (in units of t) and the filling of the c-electrons $n = N_c/N_f$, where N_c is the total number of c-electrons and N_f is the total number of f-electrons (equal to the length of the lattice L). The case $n = 1$ is referred to as half-filling, and $0 < n < 1$ as partial filling.

The Kondo lattice model is considered to be a very good model for number of diverse compounds involving rare-earth or actinide elements. Most of these intermetallic compounds exhibit complex and unusual properties, due to strong many-body effects of the electrons.

The strong correlation is introduced via dynamic scattering by the localized spins. As a conduction electron moves through the lattice, it interacts with the f-spins on each site. If spins of the two electrons are antiparallel, they both flip. Consequently, the conduction electron leaves a trace of its interactions on the lattice. A current spin direction of a given f-electron depends on all those c-electrons that visited in the past. Since a given c-electron might spin-flip on a given lattice site depending on the spin direction of the f-electron on that site, the c-electron lose their independence. This increase of the correlation is a purely

dynamic scattering effect. In contrast, an ordinary potential scattering of electrons would leave them independent.

4.4.2 DMRG application

Contrary to the Ising spin chain, the implementation of the DMRG to the Kondo lattice model has an additional complication due to the fermionic nature of particles (as for Hubbard model). The operators of fermions anticommute and hence a minus sign is introduced whenever places of two operators are interchanged [149].

The single-site basis of the model has 8 states, since the localized electron of spin-1/2 can be in two states, and there are 4 different states of conduction electrons: $|0\rangle$, $|\uparrow\rangle$, $|\downarrow\rangle$ and $|\uparrow\downarrow\rangle$, while the impurity f spin has two states: $|\Uparrow\rangle$ and $|\Downarrow\rangle$. Thus, the local basis $|\eta_k\rangle$, $k = 1, \cdots, 8$, can be chosen so that the z-component of the spin operator is diagonal

$$\{\eta_k\} = \{|0\,\Uparrow\rangle, |\uparrow\Uparrow\rangle, |\downarrow\Uparrow\rangle, |\uparrow\downarrow\Uparrow\rangle, |0\,\Downarrow\rangle, |\uparrow\Downarrow\rangle, |\downarrow\Downarrow\rangle, |\uparrow\downarrow\Downarrow\rangle\}$$

This local basis is a direct product of states of 3 different particles: $|\eta_k\rangle = |n_\uparrow\rangle \otimes |n_\downarrow\rangle \otimes |f\rangle$, where $n_\uparrow = 0, 1$ is the number of electrons with $S^z = \frac{1}{2}$, $n_\downarrow = 0, 1$ is the number of electrons with $S^z = -\frac{1}{2}$, and $f = \Uparrow, \Downarrow$ is the f spin.

While the matrices of the creation and annihilation operators of spin electron in the single particle basis are easy to get from the anticommutation relations, Eqs.(4.16) and (4.17), the extension to several particles is more complicated, for we have keep track of signs. Using the definition $|n_1, n_2, \cdots\rangle = (c_1)^\dagger (c_2)^\dagger \cdots |0\rangle$, where $|0\rangle$ is the vacuum state with no electrons, one obtains

$$\begin{aligned} c_r|\cdots n_r \cdots\rangle &= \begin{cases} (-1)^{\sigma_r}|\cdots n_r - 1 \cdots\rangle & \text{if } n_r = 1, \\ 0 & \text{otherwise} \end{cases} \\ c_r^\dagger|\cdots n_r \cdots\rangle &= \begin{cases} (-1)^{\sigma_r}|\cdots n_r + 1 \cdots\rangle & \text{if } n_r = 1, \\ 0 & \text{otherwise} \end{cases} \end{aligned} \tag{4.61}$$

where the phase factor σ_r is defined by $\sigma_r = \sum_{j=1}^{r-1} n_r$, so to say, a minus sign is introduced whenever the number of electrons "to the left" of the electron r is odd.

Consequently, the matrices of the creation operators in the basis $|\eta_k\rangle$ of a single Kondo lattice site are given by

$$C_\uparrow^\dagger = \begin{pmatrix} \tau^- & 0 & 0 & 0 \\ 0 & \tau^- & 0 & 0 \\ 0 & 0 & \tau^- & 0 \\ 0 & 0 & 0 & \tau^- \end{pmatrix}, \qquad C_\downarrow^\dagger = \begin{pmatrix} 0 & 0 & 0 & 0 \\ \tau_z & 0 & 0 & 0 \\ 0 & 0 & 0 & 0 \\ 0 & 0 & \tau_z & 0 \end{pmatrix}, \tag{4.62}$$

where $\tau^- = (\tau_x - i\tau_y)/2$, 0 is a 2×2 zero matrix, and $\tau = (\tau_x, \tau_y, \tau_z)$ are the Pauli matrices,

$$\tau_x = \begin{pmatrix} 0 & 1 \\ 1 & 0 \end{pmatrix}, \qquad \tau_y = \begin{pmatrix} 0 & -i \\ i & 0 \end{pmatrix}, \qquad \tau_z = \begin{pmatrix} 1 & 0 \\ 0 & -1 \end{pmatrix}, \qquad \tau^- = \begin{pmatrix} 0 & 0 \\ 1 & 0 \end{pmatrix}. \tag{4.63}$$

Let's check over two elements of the creation operator defined in Eq.(4.62), say $C_\uparrow^{\dagger(4,3)} = \langle\Uparrow\uparrow\downarrow |C_\uparrow^\dagger| \downarrow\Uparrow\rangle = 1$ and $C_\downarrow^{\dagger(4,2)} = \langle\Uparrow\uparrow\downarrow |C_\uparrow^\dagger| \uparrow\Uparrow\rangle = -1$.

We have:

$$C_\uparrow^\dagger| \downarrow\Uparrow\rangle = C_\uparrow^\dagger|0\rangle_\uparrow|1\rangle_\downarrow| \Uparrow\rangle \tag{4.64}$$

Following Eq.(4.61), this gives:

$$C_{\uparrow}^{\dagger}|\downarrow\Uparrow\rangle = C_{\uparrow}^{\dagger}|0\rangle_{\uparrow}|1\rangle_{\downarrow}|\Uparrow\rangle = (-1)^{0}|1\rangle_{\uparrow}|1\rangle_{\downarrow}|\Uparrow\rangle = |\uparrow\downarrow\Uparrow\rangle \tag{4.65}$$

where 0 in $(-1)^0$ indicates that there is no electron to the left of the created electron. Thus, indeed: $C_{\uparrow}^{\dagger(4,3)} = \langle\Uparrow\uparrow\downarrow|C_{\uparrow}^{\dagger}|\downarrow\Uparrow\rangle = +1$

Similarly,

$$C_{\downarrow}^{\dagger}|\uparrow\Uparrow\rangle = C_{\uparrow}^{\dagger}|1\rangle_{\uparrow}|0\rangle_{\downarrow}|\Uparrow\rangle \tag{4.66}$$

which gives:

$$C_{\downarrow}^{\dagger}|\uparrow\Uparrow\rangle = C_{\downarrow}^{\dagger}|1\rangle_{\uparrow}|0\rangle_{\downarrow}|\Uparrow\rangle = (-1)^{1}|1\rangle_{\uparrow}|1\rangle_{\downarrow}|\Uparrow\rangle = -1|\uparrow\downarrow\Uparrow\rangle \tag{4.67}$$

where 1 in $(-1)^1$ indicates that there is an electron to the left of the created electron. Thus, indeed: $C_{\downarrow}^{\dagger(4,2)} = \langle\Uparrow\uparrow\downarrow|C_{\downarrow}^{\dagger}|\uparrow\Uparrow\rangle = -1$. The annihilation (destruction) operators $C_{\uparrow}$ and $C_{\downarrow}$ are obtained by a simple transposition of the corresponding creation matrices.

The interaction term of the Kondo lattice model on a single site writes:

$$\mathcal{H}_J = J\hat{\mathbf{S}}_c \cdot \hat{\mathbf{S}}_f = J(S_c^x \cdot S_f^x + S_c^y \cdot S_f^y + S_c^z \cdot S_f^z) \tag{4.68}$$

with

$$S_c^{x,y,z} = \frac{1}{2}\sum_{\sigma\sigma'} c_{\sigma}^{\dagger}\tau_{\sigma\sigma'}^{x,y,z}c_{\sigma'},$$

and

$$S_f^{x,y,z} = \frac{1}{2}\sum_{\sigma\sigma'} f_{\sigma}^{\dagger}\tau_{\sigma\sigma'}^{x,y,z}f_{\sigma'},$$

with the Pauli matrices elements $\tau_{\sigma\sigma'}^{x,y,z}$, where, for example, $\tau_{\uparrow\downarrow}^{x} = \tau_{12}^{x}$, so that

$$J(S_c^x \cdot S_f^x + S_c^y \cdot S_f^y + S_c^z \cdot S_f^z) = \frac{J}{4}\sum_{\sigma\sigma'\sigma''\sigma'''}(\tau_{\sigma\sigma'}^{x}\tau_{\sigma''\sigma'''}^{x} + \tau_{\sigma\sigma'}^{y}\tau_{\sigma''\sigma'''}^{y} + \tau_{\sigma\sigma'}^{z}\tau_{\sigma''\sigma'''}^{z})c_{\sigma}^{\dagger}c_{\sigma'}f_{\sigma''}^{\dagger}f_{\sigma'''} \tag{4.69}$$

Using these matrices and the interaction term of the Kondo lattice model (4.60), one obtains the single site Hamiltonian matrix H_J, which has only six nonzero elements:

$$\begin{aligned}\langle\uparrow\Uparrow|H_J|\uparrow\Uparrow\rangle = \frac{J}{4},\ \langle\downarrow\Uparrow|H_J|\downarrow\Uparrow\rangle = -\frac{J}{4},\ \langle\uparrow\Downarrow|H_J|\downarrow\Uparrow\rangle = \frac{J}{2},\\ \langle\downarrow\Downarrow|H_J|\downarrow\Downarrow\rangle = \frac{J}{4},\ \langle\uparrow\Downarrow|H_J|\uparrow\Downarrow\rangle = -\frac{J}{4},\ \langle\downarrow\Uparrow|H_J|\uparrow\Downarrow\rangle = \frac{J}{2}.\end{aligned} \tag{4.70}$$

Let's verify one of these matrix elements, say, $\langle\uparrow\Uparrow|H_J|\uparrow\Uparrow\rangle = \frac{J}{4}$. We have to apply H_J on the basis vector $|\uparrow\Uparrow\rangle$. This will involve 16 terms of operators in the sum; only 4 of them give a nonzero result. Here they are:

$$c_{\uparrow}^{\dagger}c_{\uparrow}f_{\Uparrow}^{\dagger}f_{\Uparrow}|\uparrow\Uparrow\rangle = |\uparrow\Uparrow\rangle,\ c_{\uparrow}^{\dagger}c_{\uparrow}f_{\Downarrow}^{\dagger}f_{\Uparrow}|\uparrow\Uparrow\rangle = |\uparrow\Downarrow\rangle,$$

$$c^\dagger_\downarrow c_\uparrow f^\dagger_\Uparrow f_\Uparrow |\uparrow\Uparrow\rangle = |\downarrow\Uparrow\rangle,\ c^\dagger_\downarrow c_\uparrow f^\dagger_\Downarrow f_\Uparrow |\uparrow\Uparrow\rangle = |\downarrow\Downarrow\rangle. \tag{4.71}$$

Now we have to compute the corresponding coefficients in the sum made of multiplication of Pauli matrices elements, where

$$\begin{aligned}
\tau^x_{\uparrow\uparrow}\tau^x_{\uparrow\uparrow} + \tau^y_{\uparrow\uparrow}\tau^y_{\uparrow\uparrow} + \tau^z_{\uparrow\uparrow}\tau^z_{\uparrow\uparrow} = 0\cdot 0 + 0\cdot 0 + 1\cdot 1 = 1\\
\tau^x_{\uparrow\uparrow}\tau^x_{\downarrow\uparrow} + \tau^y_{\uparrow\uparrow}\tau^y_{\downarrow\uparrow} + \tau^z_{\uparrow\uparrow}\tau^z_{\downarrow\uparrow} = 0\cdot 1 + 0\cdot i + 1\cdot 0 = 0\\
\tau^x_{\uparrow\downarrow}\tau^x_{\uparrow\uparrow} + \tau^y_{\uparrow\downarrow}\tau^y_{\uparrow\uparrow} + \tau^z_{\uparrow\downarrow}\tau^z_{\uparrow\uparrow} = 1\cdot 0 - i\cdot 0 + 0\cdot 0 = 0\\
\tau^x_{\downarrow\uparrow}\tau^x_{\downarrow\uparrow} + \tau^y_{\downarrow\uparrow}\tau^y_{\downarrow\uparrow} + \tau^z_{\downarrow\uparrow}\tau^z_{\downarrow\uparrow} = 1\cdot 1 + i\cdot i + 0\cdot 0 = 0
\end{aligned} \tag{4.72}$$

which indeed gives $\langle\uparrow\Uparrow |H_J| \uparrow\Uparrow\rangle = \frac{J}{4}$.

Apart from the complication with signs (4.61), there are no other essential differences from a simple spin-chain case. The anticommutativity of the c operators is incorporated into single-site matrices (4.62). What remains is to define these operators on the whole system of four DMRG blocks. To satisfy Eq. (4.61), the matrix of the operator, acting on a given block, should include information about the number of electrons on the blocks "to the left". This can be achieved by introducing a diagonal single-site matrix P, which counts the number of electrons in each state, and gives +1 if the number is even, and -1 if the number is odd. The diagonal of the P matrix in the basis $\{|\eta_k\}$ is then $(1,-1,-1,1,1,-1,-1,1)$. Now the operator acting on a given block i, $i = 1, 2, 3$ or 4, can be defined on the whole system of four blocks so that it satisfies anticommutation relations with other operators. At the first DMRG step, the following operator matrices are introduced [151]:

$$\begin{aligned}
\tilde{C}^\dagger_{1\sigma} = C^\dagger_\sigma \otimes \delta_2 \otimes \delta_3 \otimes \delta_4,\ \tilde{C}^\dagger_{2\sigma} = P_1 \otimes C^\dagger_\sigma \otimes \delta_3 \otimes \delta_4,\\
\tilde{C}^\dagger_{3\sigma} = P_1 \otimes P_2 \otimes C^\dagger_\sigma \otimes \delta_4,\ \tilde{C}^\dagger_{4\sigma} = P_1 \otimes P_2 \otimes P_3 \otimes C^\dagger_\sigma.
\end{aligned} \tag{4.73}$$

where $\sigma = \uparrow, \downarrow$, $P_1 = P_2 = P_3 = P$ are just single-site P matrices, and δ_i are 8×8 unit matrices, acting on corresponding blocks. The destruction operator matrices are simple transpositions of the corresponding $\tilde{C}^\dagger_{i\sigma}$. The KLM Hamiltonian can be rewritten as

$$\mathcal{H} = -t \sum_{\sigma=\uparrow,\downarrow} \sum_{i=1}^{3} \left(\tilde{C}^\dagger_{i\sigma} \tilde{C}_{i+1\sigma} - \tilde{C}_{i\sigma} \tilde{C}^\dagger_{i+1\sigma} \right) + \sum_{i=1}^{4} (H_J)_i, \tag{4.74}$$

where $(H_J)_i$ are single-block matrices (in the first iteration they are all given by Eq.(4.70). Now the following DMRG algorithm is not different from a simple application to any non-fermionic spin-chain. The Hamiltonian of the whole system is diagonalized, the reduced density matrix of the left side is constructed, diagonalized and truncated leaving the states with largest eigenvalues. These chosen states make up the transformation matrix O, which is used to rotate and truncate all left-side matrices into the new basis. The truncated matrices are acting on a block number 1 in the next iteration. They are used to create a new Hamiltonian Eq.(4.74), where matrices on blocks 2 and 3 are just single-site matrices an those acting on blocks 1 and 4 are the truncated matrices of the previous iteration. E.g., the new $(H_J)_1$ matrix is a truncation of the left-side Hamiltonian of the previous step:

$$(H_J)_1 \to O \left((H_J)_1 \otimes \delta_2 - t \sum_\sigma (\tilde{C}^\dagger_{1\sigma} \tilde{C}_{2\sigma} - \tilde{C}_{1\sigma} \tilde{C}^\dagger_{2\sigma}) + \delta_1 \otimes (H_J)_2 \right) O^T \tag{4.75}$$

Similarly the new $\tilde{C}^{\dagger}_{2\sigma}$ matrix is needed as a connection between the first block and the second block, so it corresponds to the $c^{\dagger}$ matrix of the electron, residing on the rightmost spin of the block. Consequently

$$\tilde{C}^{\dagger}_{2\sigma} \leftarrow O(P_1 \otimes C^{\dagger}_{\sigma})O^T, \tag{4.76}$$

where $C^{\dagger}_{\sigma}$ is a single-site matrix, given by Eq. (4.62). Evidently, the only extra element of this implementation of the fermionic DMRG algorithm as compared to the simple-spin chain, is the necessity to keep the P matrix of the first block. It is clearly obtained as

$$P_1 \leftarrow O(P_1 \otimes P_2)^T. \tag{4.77}$$

Commutativity of the number operator with the KLM Hamiltonian leads to the block diagonal matrix (with respect to the particle number), which eventually means that the P matrix is always diagonal with either +1 or -1 on the diagonal.

There exists one problem, common to the infinite system DMRG, applied to fermionic chains: it is usually impossible to keep constant filling the c-electrons while growing the system. Even though the particle number operator $N_c = \sum_{i,\sigma} \tilde{C}^{\dagger}_{i\sigma}\tilde{C}_{i\sigma}$ commutes both with the Hamiltonian of the KLM and the DM of half-system, and it is easy to work in the subspace of a given number of particles, their number should integer at every step. As the chain grows during the iteration, the ratio between N_c and the number of system sites L can not be kept constant. The fluctuations can be a serious hindrance, e.g., to obtain accurate ground state properties close to the phase transition [151, 152]. There is no such problem in the finite system DMRG, since the system size is fixed then.

4.5 The Heisenberg model

For many magnetic materials, it is shown that the magnetic part of the Hamiltonian can be accurately represented as a set of localized spins $\vec{S}_i$ interacting with each other. A standard form of this magnetic part of the Hamiltonian can be put in the form

$$H = J\sum_{\langle ij\rangle}\{\gamma\vec{S}_i\cdot\vec{S}_j + (1-\gamma)S^z_iS^z_j\} - \sum_i \vec{H}\cdot\vec{S}_i \tag{4.78}$$

where $\langle ij\rangle$ stands for nearest-neighbors. The $\vec{S}_i\cdot\vec{S}_j$ term is called a spin exchange interaction, J is the coupling constant energy between neighbor spins, S^z_i is the z- component of a spin on site i, γ is a parameter characterizing the degree of anisotropy and $\vec{H}$ a magnetic field.

This Hamiltonian reduces to the Ising case when $\gamma = 0$ and the Heisenberg case when $\gamma = 1$. For certain highly anisotropic systems, the coupling energy can be approximated by the pure Ising form but for most systems the anisotropy, although important, is not very large and the pure Heisenberg coupling is more realistic [153].

Thus, the Heisenberg model, in spite of its simplicity as a model for many-body systems, was found to be very useful for understanding magnetism and hence has received considerable attention from experimentalists because its describes a number of materials with magnetic ions arranged in chains [154, 155, 156]. The exact energy eigenstates of an infinite chain of spins interacting with nearest neighbors via a Heisenberg interaction were

found by Bethe [157] and the ground-state energy was found later by Hulthen [158]; even the generalization of the solutions to higher dimension is not available, and thus, the problem remains open.

In order to investigate whether a purely isotropic Heisenberg interaction between nearest neighbors produce long-range order in one dimension, Lieb, Schultz and Mattis [159] were lead to construct an exactly solved model, called the XY model, which closely resemble to the Heisenberg model, and whose Hamiltonian writes as:

$$H = J \sum_i [(1+\gamma) S_i^x S_{i+1}^x + (1-\gamma) S_i^y S_{i+1}^y], \tag{4.79}$$

This model was called the XY model because the Hamiltonian only involves the x- and y-components of the spin operators. The investigation of this model strongly suggests that the isotropic Heisenberg model has no long-range order but that such order exists for any finite amount of anisotropy [159].

Another variant of the model is known as the XXZ model, with the Hamiltonian:

$$H = J \sum_i (S_i^x S_{i+1}^x + S_i^y S_{i+1}^y + \gamma S_i^z S_{i+1}^z), \tag{4.80}$$

which has XY symmetry. The behaviour of the ground state of this model as the anisotropy parameter γ is varied is well-known (see for example [160]).

Also, the effect of weak disorder in quantum spin chains has gained attention; and a wide range of models was introduced to investigate different kinds of disorder like a random transverse magnetic field in the z direction:

$$H = \sum_i h_i^z S_i^z, \tag{4.81}$$

or a random component in the planar exchange interaction,

$$H = \sum_i \delta J_i^{xy} (S_i^x S_{i+1}^x + S_i^y S_{i+1}^y), \tag{4.82}$$

and so on (see for example [160]).

In the Heisenberg model one assumes that there is a single electron localized at each site, and that the charge cannot move. Therefore, the only degrees of freedom in the Heisenberg model are the spins of each site. This can be viewed as a limiting case of the Hubbard model when we have half-filling , i.e. $n_i \equiv 1$ for all sites, hopping becoming impossible.

Although the spins in the model are localized they are meant to describe a system of mobile electrons. The model treats electrons with spin 1/2, but it can also be generalized to particles with spin $> \frac{1}{2}$. A possible generalization for these models is to extend the nearest neighbors summation to more distant neighbours.

4.5.1 Heisenberg DMRG example

In this example we will illustrate the DMRG implementation for the antiferromagnetic spin 1/2 Heisenberg chain [161]

$$H = J \sum_i S_i S_{i+1} = S_i^z S_{i+1}^z + \frac{1}{2}(S_i^+ S_{i+1}^- + S_i^- S_{i+1}^+) \tag{4.83}$$

where J is taken to be unity and

$$S_i^{\pm} = S_i^x \pm iS_i^y = \frac{1}{2}(\sigma^x \pm i\sigma^y) \qquad , \qquad S_i^z = \frac{1}{2}\sigma^z \tag{4.84}$$

where σ^x, σ^y and σ^z are the Pauli matrices given by

$$\sigma^x = \begin{pmatrix} 0 & 1 \\ 1 & 0 \end{pmatrix} \qquad , \qquad \sigma^y = \begin{pmatrix} 0 & -i \\ i & 0 \end{pmatrix} \qquad \text{and} \qquad \sigma^z = \begin{pmatrix} 1 & 0 \\ 0 & -1 \end{pmatrix} \tag{4.85}$$

The possible states for a single site are: $|d_1\rangle = |\uparrow\rangle$ and $|d_2\rangle = |\downarrow\rangle$ (this notation is borrowed from the work of A. Malvezzi [162]). Because in DMRG we deal with truncated Hilbert spaces, we will represent a block of l sites with a m-dimensional basis by $B(l;m)$ (m is the number of states kept during the renormalization process and it is obviously smaller than the full Hilbert space of the block).

We start with two blocks $B_L(1,2)$ and $B_R(1,2)$ (L for left and R for right), each contains one single site. The possible states of the block are

$$|b_1\rangle = |\uparrow\rangle, \qquad |b_2\rangle = |\downarrow\rangle. \tag{4.86}$$

Then a single site is added to each block. Let's focus on the left block, because the right one is obtained by a spatial reflection. Thus, the basis of the left enlarged block is

$$\begin{aligned} |b_1^e\rangle &= |\uparrow\uparrow\rangle \\ |b_2^e\rangle &= |\uparrow\downarrow\rangle \\ |b_3^e\rangle &= |\downarrow\uparrow\rangle \\ |b_4^e\rangle &= |\downarrow\downarrow\rangle \end{aligned} \tag{4.87}$$

The Hamiltonian H_e^L for the enlarged block $B_L(2,4)$ writes as tensor products of matrices representing each site, so that

$$H_e^L = H_B \otimes I_d + I_b \otimes H_B + \frac{1}{2}(S_b^+ \otimes S_d^- + S_b^- \otimes S_d^+) + S_b^z \otimes S_d^z \tag{4.88}$$

In Eq. (4.88) the indices b and d refer to the operators acting on the Hilbert space of the block and the site, respectively, and I is the unit matrix. H_B is a null matrix because one isolated site without external fields has the Hamiltonian equal to zero. Thus

$$\begin{aligned} H_e^L = &\begin{pmatrix} 0 & 0 \\ 0 & 0 \end{pmatrix} \otimes \begin{pmatrix} 1 & 0 \\ 0 & 1 \end{pmatrix} + \begin{pmatrix} 1 & 0 \\ 0 & 1 \end{pmatrix} \otimes \begin{pmatrix} 0 & 0 \\ 0 & 0 \end{pmatrix} \\ &+\frac{1}{2}\left[\begin{pmatrix} 0 & 1 \\ 0 & 0 \end{pmatrix} \otimes \begin{pmatrix} 0 & 0 \\ 1 & 0 \end{pmatrix} + \begin{pmatrix} 0 & 0 \\ 1 & 0 \end{pmatrix} \otimes \begin{pmatrix} 0 & 1 \\ 0 & 0 \end{pmatrix}\right] \\ &+\frac{1}{4}\begin{pmatrix} 1 & 0 \\ 0 & -1 \end{pmatrix} \otimes \begin{pmatrix} 1 & 0 \\ 0 & -1 \end{pmatrix} \end{aligned} \tag{4.89}$$

and it looks as follows:

$$H_e^L = \frac{1}{4}\begin{pmatrix} 1 & 0 & 0 & 0 \\ 0 & -1 & 2 & 0 \\ 0 & 2 & -1 & 0 \\ 0 & 0 & 0 & 1 \end{pmatrix} \tag{4.90}$$

In the same spirit, the superblock is constructed as tensor products of matrices representing the left and right blocks plus matrices of operators on rightmost and leftmost sites that connect the two blocks. Thus, The

$$H_s = H_e^L \otimes I_e^R + I_e^L \otimes H_e^R + \frac{1}{2}\left[(S_r^+)_e^L \otimes (S_l^-)_e^R + (S_r^-)_e^L \otimes (S_l^+)_e^R\right] + (S_r^z)_e^L \otimes (S_l^z)_e^R \quad (4.91)$$

where H_e^L and H_e^R are matrices representing left and right enlarged blocks(with two sites each), I_e^R and I_e^L are 4×4 unit matrices, $(S_r^+)_e^L$, $(S_r^-)_e^L$ and $(S_r^z)_e^L$ are matrices representing rightmost site operators of the left block, while $(S_l^+)_e^R$, $(S_l^-)_e^R$ and $(S_l^z)_e^R$ are matrices representing leftmost site operators of the right block. All these operators are represented in the basis of the enlarged block . The rightmost and leftmost sites are connecting the two blocks. For example, $(S_r^+)_e^L$ matrix, is given by

$$(S_r^+)_e^L = I_b \otimes S_d^+ = \begin{pmatrix} 1 & 0 \\ 0 & 1 \end{pmatrix} \otimes \begin{pmatrix} 0 & 1 \\ 0 & 0 \end{pmatrix} \quad (4.92)$$

Thus, the basis for the superblock has 16 states: $\{|\uparrow\uparrow\uparrow\uparrow\rangle, |\uparrow\uparrow\uparrow\downarrow\rangle, \cdots, |\downarrow\downarrow\downarrow\uparrow\rangle, |\downarrow\downarrow\downarrow\downarrow\rangle\}$. This means that any operator for the superblock has to be represented in this 16-states basis.

The Hamiltonian matrix of the superblock H_s is then diagonalized; the ground state vector is used to construct the density matrix ρ, following equation (4.40). Note that the diagonalization of a 16×16 matrix is quite easy task (we can do it with standard routines), and therefore we can keep applying this recipe *à la lettre*. However for realistic calculations, and in order to keep a considerable number of states m, we have to extend the superblock so it contains a number of states larger than m. This makes the diagonalization of the superblock matrix very onerous, and the recourse to other numerical methods, like Lanczos method is of great necessity. In other hand, the superblock contains basis states corresponding to many different values of total z-component spin S^z (called quantum number); hence the full matrix of the whole system can be blocked out to submatrices corresponding to different values of S^z, which may help to diminish the time consuming of the calculations.

In our example, it happens that the ground state belongs to the subspace $S^z = 0$, with the basis states:$\{|\uparrow\uparrow\downarrow\downarrow\rangle, |\uparrow\downarrow\uparrow\downarrow\rangle, |\uparrow\downarrow\downarrow\uparrow\rangle, |\downarrow\uparrow\uparrow\downarrow\rangle, |\downarrow\uparrow\downarrow\uparrow\rangle, |\downarrow\downarrow\uparrow\uparrow\rangle\}$. Thus, the matrix to be diagonalized is just a 6×6 one, instead of a 16×16 matrix, ans this will considerably speed up the calculations.

Note that ρ and H_e^L (Eq. (4.90)) have the same matrices order and also share the same block diagonal structure. ρ matrix is then diagonalized, the m eigenvectors corresponding to the largest eigenvalues are used as rows in the truncation operator matrix O (in our example $m = 2$).

After determining the basis and the transformation, the representations of all operators used to describe the enlarged block are changed to the new basis, i.e.,

$$H_e^L(B(2,2)) = O^{(1)} H_e^L(B(2,4)) O^{\dagger(1)} \quad (4.93)$$

where $H_e^L(B(2,4))$ is the Hamiltonian of the left enlarged block in the effective basis (with 4 basis states) transformed through truncation operator $O^{(1)}$ to the truncated basis (with 2 states), as $H_e^L(B(2,2))$. The index 1 in $O^{(1)}$ refers to the first step of truncation. The same

transformation is done with the other operators that will be needed for future calculations. One example is the S^+-operator, which has the following representation in the new basis

$$S_r^+(B(2,2)) = O^{(1)}(S_r^+)_e(B(2,4))O^{\dagger(1)} \tag{4.94}$$

In order to 'monitor' the accuracy of the procedure, it is useful to calculate the sum of the density matrix eigenvalues of the discarded states $(1 - \sum_{\alpha=1}^{m} w_\alpha)$. This sum measures the severity of the truncation [163]. The goal is to keep this number as small as possible. Acceptable truncation errors in actual calculations are usually kept smaller than 10^{-4} [162].

After all operators for the left block are obtained, a new enlarged block, $B(3, m \times 2)$, is constructed by adding a new site. Using tensor products of spin operator matrices in left and right blocks, a superblock Hamiltonian of 6 sites is then constructed in a $m \times 2 \times 2 \times m$-states basis. The ground state is then obtained; the density matrix constructed and the truncation operator established, i.e.,

$$H_e^L(B(3,m)) = O^{(2)}H_e^L(B(3, m \times 2))O^{\dagger(2)} \tag{4.95}$$

and, for example,

$$S_r^+(B(3,m)) = O^{(2)}(S_r^+)_e(B(3, m \times 2))O^{\dagger(2)} \tag{4.96}$$

This infinite system algorithm is then repeated until a desired length of the chain is reached. To increase the accuracy of the results we have to start the finite system algorithm which consists, as it is well explained before, in a kind of *sweeping*, i.e., incorporating(not adding) a new site to the left block and retrieving a site from the right block. The above procedure of diagonalization ,etc...is then repeatedly applied, until the right block is nothing but a single site. The structure of the superblock is then reversed: the single site is now at the left side of the superblock, while the enlarged block is at its right. The procedure of truncation is again applied. This is the finite system algorithm. The ground state values and other measurements are picked up as the left block size is the same as the right block. Four to five sweeps are, in general, needed to achieve the convergence. The accuracy of results is also increased by keeping more and more states.

4.6 Dynamic quantities

One scheme to calculate expectation values of dynamic operators was proposed by Wang, Hallberg, and Naef [28]. Following their ideas, we show how to obtain dynamic quantities in the zero temperature limit.

For any approximate ground state $|\psi_0\rangle$ of the Hamiltonian H we may construct an orthogonal basis in a Lanczos procedure. We specialize to calculating fermionic correlators

$$C(t) = \langle\psi_0|\{A^\dagger(t), A(0)\}|\psi_0\rangle. \tag{4.97}$$

We usually seek the Fourier transform

$$C(\omega) = \int_{-\infty}^{\infty} dt\, e^{i\omega t}\langle\psi_0|\{A^\dagger(t), A(0)\}|\psi_0\rangle \tag{4.98}$$

and inserting the Heisenberg time evolution we find

$$\begin{aligned} C(\omega) &= \int_{-\infty}^{\infty} dt\, e^{i\omega t}\langle\psi_0|\{e^{iHt}A^\dagger e^{-iHt}, A(0)\}|\psi_0\rangle \\ &= \langle\psi_0|A^\dagger \int_{-\infty}^{\infty} dt\, e^{i(\omega-E_0+H)t}A + A\int_{-\infty}^{\infty} dt\, e^{i(\omega+E_0-H)t}A^\dagger|\psi_0\rangle \\ &= 2\pi\langle\psi_0|A^\dagger\delta(\omega+E_0-H)A + A\delta(\omega-E_0-H)A^\dagger|\psi_0\rangle. \end{aligned} \tag{4.99}$$

Additionally we use the identity

$$\frac{1}{x+i\eta} = \frac{1}{x} - i\pi\delta(x), \qquad \eta\to 0^+, \tag{4.100}$$

to rewrite the δ-functions

$$\delta(\omega\pm(E_0-H)) = -\frac{1}{\pi}\lim_{\eta\to 0^+}\mathrm{Im}\frac{1}{\omega\pm(E_0-H)+i\eta} \tag{4.101}$$

so that

$$C(\omega) = -2\lim_{\eta\to 0^+}\mathrm{Im}\langle\psi_0|A^\dagger\frac{1}{\omega+E_0-H+i\eta}A + A\frac{1}{\omega-E_0+H+i\eta}A^\dagger|\psi_0\rangle, \tag{4.102}$$

or finally using the notation

$$G^+(z) = \psi_0|A(z+H)^{-1}A^\dagger|\psi_0\rangle, \tag{4.103}$$

$$G^-(z) = \psi_0|A^\dagger(z-H)^{-1}A|\psi_0\rangle, \tag{4.104}$$

we find

$$C(\omega) = -2\lim_{\eta\to 0^+}\mathrm{Im}(G^-(\omega+E_0+i\eta) + G^+(\omega-E_0+i\eta)). \tag{4.105}$$

We start the Lanczos procedure by defining

$$|f_0\rangle = \begin{cases} A|\psi_0\rangle, \\ A^\dagger|\psi_0\rangle, \end{cases} \tag{4.106}$$

and iterate to find further Lanczos vectors,

$$|f_{n+1}\rangle = H|f_n\rangle - a_n|f_n\rangle - b_n^2|f_{n-1}\rangle, \tag{4.107}$$

where $n\geq 0$, $b_0=0$, and $\langle f_n|f_m\rangle = 0$ for $n\neq m$. The coefficients are

$$a_n = \frac{\langle f_n|H|f_n\rangle}{\langle f_n|f_n\rangle}, \tag{4.108}$$

$$b_n^2 = \frac{\langle f_n|f_n\rangle}{\langle f_{n-1}|f_{n-1}\rangle}. \tag{4.109}$$

In order to reexpress the Green's functions, Eq. (4.103) we first define an orthonormal basis

$$|n\rangle = \frac{|f_n\rangle}{\sqrt{\langle f_n|f_n\rangle}}. \tag{4.110}$$

Using Eq. (4.107) the Hamiltonian applied to the basis state $|n\rangle$ is

$$H|n\rangle = \sqrt{\frac{\langle f_{n+1}|f_{n+1}\rangle}{\langle f_n|f_n\rangle}}|n+1\rangle + a_n|n\rangle + b_n^2\sqrt{\frac{\langle f_{n-1}|f_{n-1}\rangle}{\langle f_n|f_n\rangle}}|n-1\rangle \tag{4.111}$$

and using the notation

$$\sqrt{\frac{\langle f_m|f_m\rangle}{\langle f_n|f_n\rangle}} = n_{m,n} \tag{4.112}$$

we find the matrix elements

$$\begin{aligned}\langle m|H|n\rangle &= n_{n+1,m}\delta_{m,n+1} + a_n\delta_{m,n} + b_n^2 n_{n-1,n}\delta_{m,n-1} \\ &= \begin{cases} n_{n+1,m}, & m = n+1, \\ a_n, & m = n, \\ b_n^2 n_{n-1,n}, & m = n-1. \end{cases}\end{aligned} \tag{4.113}$$

Thus by construction the Hamiltonian is tri-diagonal in the Lanczos basis

$$(z \pm H)_n = \begin{pmatrix} z \pm a_0 & \pm b_1^2 n_{0,1} & 0 & \cdots & 0 \\ \pm n_{1,0} & z \pm a_1 & \pm b_2^2 n_{1,2} & & \vdots \\ 0 & \pm n_{2,1} & z \pm a_2 & & 0 \\ \vdots & & & \ddots & \pm b_n^2 n_{n-1,n} \\ 0 & \cdots & 0 & \pm n_{n,n-1} & z \pm a_n \end{pmatrix}. \tag{4.114}$$

First, we rewrite Eq. (4.103) as

$$\begin{aligned} G^{\pm}(z) &= \langle f_0|(z)^{-1}|f_0\rangle \\ &= \sum_{mm'}\langle f_0|m\rangle\langle m|(z \pm H)^{-1}|m'\rangle\langle m'|f_0\rangle \\ &= \sum_{mm'}\frac{\langle f_0|f_m\rangle}{\sqrt{\langle f_m|f_m\rangle}}\langle m|(z \pm H)^{-1}|m'\rangle\frac{\langle f_{m'}|f_0\rangle}{\sqrt{\langle f_{m'}|f_{m'}\rangle}} \\ &= \langle f_0|f_0\rangle\langle 0|(z)^{-1}|0\rangle. \end{aligned} \tag{4.115}$$

Hence we need to find the first element of the inverse of the matrix $(z \pm H)$ in the basis of Eq. (4.110) (See e.g. [164] for details on inverting matrices). In order to invert the matrix in Eq. (4.110) we first consider the solution to 2nd order in the coefficients a_i and $b2^i$

$$(z \pm H)_1 = \begin{pmatrix} z \pm a_0 & \pm b_1^2 n_{0,1} \\ \pm n_{1,0} & z \pm a_1 \end{pmatrix} \Rightarrow \langle 0|[(z \pm H)_1]^{-1}|0\rangle = \frac{[C_1]_{(1,1)}}{\det(z \pm H)_1}, \tag{4.116}$$

where $[C_1]_{(1,1)}$ is the complement of $[(z \pm H)_1]_{(1,1)}$, given by the subdeterminant, in this case just a scalar

$$[C_1]_{(1,1)} = z \pm a_1, \tag{4.117}$$

so that to this order

$$\langle 0|[(z \pm H)_1]^{-1}|0\rangle = \frac{z \pm a_1}{(z \pm a_0)(z \pm a_1) - b_1^2 n_{0,1} n_{1,0}}$$

$$= \frac{1}{z \pm a_0 - \frac{b_1^2}{z \pm a_1}}, \tag{4.118}$$

where we used that $n_{i,i+1}n_{i+1,i} = 1$. Next we consider the solution to $(n+1)$'st order in the coefficients a_i and b_i^2 , given by a very similar expression,

$$\langle 0|[(z \pm H)_n]^{-1}|0\rangle = \frac{[C_n]_{(1,1)}}{\det(z \pm H)_n}, \tag{4.119}$$

with the complement given by the subdeterminant

$$[C_n]_{(1,1)} = \begin{vmatrix} z \pm a_1 & \pm b_2^2 n_{1,2} & 0 & \cdots & 0 \\ \pm n_{2,1} & z \pm a_2 & \pm b_3^2 n_{2,3} & & \vdots \\ 0 & \pm n_{3,2} & z \pm a_3 & & 0 \\ \vdots & & & \ddots & \pm b_n^2 n_{n-1,n} \\ 0 & \cdots & 0 & \pm n_{n,n-1} & z \pm a_n \end{vmatrix} \equiv \det(2:n), \tag{4.120}$$

which defines the notation $\det(2:n)$ for the subdeterminant of $(z \pm H)_n$ in Eq. (4.120). Extending in the obvious way the usage of this notation we have

$$\langle 0|[(z \pm H)_n]^{-1}|0\rangle = \frac{\det(2:n)}{\det(1:n)}, \tag{4.121}$$

The full determinant can be written

$$\begin{aligned} \det(1:n) &= (z \pm a_0)\det(2:n) \mp b_1^2 n_{0,1} \begin{vmatrix} z \pm a_1 & \pm b_2^2 n_{1,2} & 0 & \cdots & 0 \\ \pm n_{2,1} & z \pm a_2 & \pm b_3^2 n_{2,3} & & \vdots \\ 0 & \pm n_{3,2} & z \pm a_3 & & 0 \\ \vdots & & & \ddots & \pm b_n^2 n_{n-1,n} \\ 0 & \cdots & 0 & \pm n_{n,n-1} & z \pm a_n \end{vmatrix} \\ &= (z \pm a_0)\det(2:n) - b_1^2 n_{0,1} n_{1,0} \det(3:n) \\ &= (z \pm a_0)\det(2:n) - b_1^2 \det(3:n), \end{aligned} \tag{4.122}$$

and hence we find

$$\begin{aligned} \langle 0|[(z \pm H)_n]^{-1}|0\rangle &= \frac{\det(2:n)}{(z \pm a_0)\det(2:n) - b_1^2 \det(3:n)} \\ &= \frac{1}{z \pm a_0 - b_1^2 \frac{\det(3:n)}{\det(2:n)}} \end{aligned} \tag{4.123}$$

Due to the tri-diagonal structure of the Hamiltonian matrix in Eq.(4.114) we can rewrite any fraction $\det(m+1:n)/\det(m:n)$ in a completely similar way,

$$\begin{aligned} \frac{\det(m+1:n)}{\det(m:n)} &= \frac{\det(m+1:n)}{(z \pm a_{m-1})\det(m+1:n) - b_m^2 \det(m+2:n)} \\ &\qquad \frac{1}{z \pm a_{m-1} - b_m^2 \frac{\det(m+2:n)}{\det(m+1:n)}}. \end{aligned} \tag{4.124}$$

Hence by successive use of Eq. (4.124) and using Eq. (4.115) we find the final solution for arbitrary n, in particular $n \to \infty$,

$$G^+(z) = \cfrac{\langle\psi_0|AA^\dagger|\psi_0\rangle}{z + a_0 - \cfrac{b_1^2}{z+a_1-\cfrac{b_2^2}{z+\cdots}}}$$
$$G^-(z) = \cfrac{\langle\psi_0|AA^\dagger|\psi_0\rangle}{z - a_0 - \cfrac{b_1^2}{z-a_1-\cfrac{b_2^2}{z-\cdots}}} \tag{4.125}$$

The condition for this method to be feasible is that the continued fractions in Eq. (4.125) converge using a finite and manageable number of Lanczos coefficients a_i and b_2^i. If very many coefficients are needed it becomes difficult to maintain the accuracy.

In principle this procedure is independent of the method used to find the ground state [165]. In a DMRG implementation of the method above there are however technical details that need attention. The DMRG basis is usually heavily truncated compared to the complete basis. The truncation is performed to optimally describe the target state, usually the ground state. The basis may therefore not be suitable for describing excitations in the system, making it impossible to accurately describe dynamical quantities in this basis.

This apparent incompatibility can be remedied by including exited states as target states. As was pointed out by Hallberg the first few Lanczos vectors are candidates for such additional target states [166] . Hence the new normalized target states become

$$|\psi^l\rangle = \begin{cases} |\psi_0\rangle, & l = 1, \\ \frac{|f_{l-2}}{\langle f_{l-2}|f_{l-2}\rangle}, & l = 2, 3, \cdots, M \end{cases} \tag{4.126}$$

and the reduced density matrix accordingly

$$\rho_{ii'} = \sum_{l=1}^{M} p_l \psi_{ij}^l (\psi^l)_{ji'}^\dagger, \tag{4.127}$$

where p_l is the weight for target state $|\psi^l\rangle$ and $\sum p_l = 1$ to maintain the normalization.

With these additional target states excitations can be described using a standard DMRG implementation. The additional calculations amount to computing and including as target states at each step M normalized Lanczos vectors, given the ground state $|\psi_0\rangle$, the Hamiltonian H, and the operator A or $A^\dagger$. Since the precision of DMRG generally decreases when more target states are included the optimal value of M has to be determined from case to case. Including more states improves the description of excitations but lowers the general precision of DMRG.

Chapter 5

Applications and results

In this chapter, I present the results of my work on DMRG method and its applications. In the first paper, a variation of the Density Matrix Renormalization Group (DMRG) procedure, based on a simplified version of White's Density Matrix Renormalization Group (DMRG) algorithm to find the ground state of single-particle quantum mechanics is developed, to compute low states energies for two crossed chains within the simple tight–binding model suggested by P. W. Anderson. For comparison, our results obtained using the new procedure are presented along with those obtained by exact diagonalization. Some technical aspects of the implementation of the algorithm are given in detail.

In the second paper, the ground state energies and other related quantities of a spin-$\frac{1}{2}$ chain with a lacking spin site are computed using exact diagonalization method. To do this, next nearest neighbors interactions are introduced to Heisenberg model Hamiltonian, known as frustrated quantum spin chain. To investigate ground state energies of large system sizes, the DMRG method is applied. Our results are then compared to those obtained for a spin chain without a lacking spin site. Thus, the introduction of such lacking site makes the system gapless, and, actually, the first four energies have the same value. Quantum quantities such as fidelity and correlation functions are also studied and compared for both cases.

In the third paper, the density-matrix renormalization-group technique and relations arising from the conformal invariance are used to calculate finite-size estimates of the conformal anomaly c, sound velocity v_s, the anomalous dimension x^{α}_{bulk} of a 1/2-spin chain within Heisenberg model with next nearest neighbors interactions. The nature of the interactions used permits us also to simulate a disorder chain by removing a single spin site, while both parts of the chain remain connected. For this case, the above quantities are also computed and compared to those of pure case.

5.1 Density Matrix Renormalization Group Method applied to two crossed disordered chains within Anderson model

5.1.1 Introduction

The Density Matrix Renormalization Group (DMRG), developed by S. R. White in 1993 [23], is a powerful numerical method which permits us to obtain the ground-state and low-lying excited states wavefunctions of large-size systems with controlled high accuracy. S.White has considered that a system (block) must be connected to an other block (environment) to form a superblock, and therefore each part contributes to the ground state of the superblock through its own states. The basic idea of the DMRG is to use the concept of density matrix to decide which states from a given block that contribute the more to the wavefunction of the whole system. As the procedure is iterated, the size of the system is increasing while the corresponding Hilbert space is kept constant.

Technically, the algorithm consists in a warm–up phase where Hamiltonian operators for each block and connection operators in the system are renormalized and then stored to be used later. This is followed by a sweeping procedure which iterates the process on the full system until convergence is reached.

In fact, since its appearance, DMRG has proven a high level of accuracy when dealing with one–dimensional systems, in such a way that it became, in few years, a valuable numerical tool, among other numerical methods, to calculate energy spectrum and other dynamic correlation functions at finite temperatures of interacting 1–d quantum systems. Still, the DMRG is called to prove its accuracy when applied to 2–d quantum systems and, eventually, 3–d ones. Thus, various algorithms have been proposed to apply DMRG to two-dimensional quantum systems; see for example ([167],[168], [169],[170],[171] and [172]). Most of these works use mappings on to effective one-dimensional models with long-range interactions, and the standard DMRG method is applied to the effective one-dimensional systems. In this spirit, the present paper is to give a new configuration of the DMRG method to treat a diffusive problem without any mapping: a disordered two–crossed chains system within the very simple tight–binding Anderson model.

This work is based on an earlier paper [173], where M.A. Martín-Delgado et al. have given a simplified version of White's DMRG algorithm to find the ground state of single-particle quantum mechanics. They solved a discretized version of the single–particle Schrödinger equation, which allows them to obtain very accurate results for the lowest energy levels of a single particle under the action of three potentials: harmonic oscillator, anharmonic oscillator and double–well. My contribution consists in replacing the standard configuration, which consists in two connected blocks (system +environment) and where two sites are added at a time, by a five–blocks system, representing the two crossed chains, and where eight sites are added at a time.

5.1.2 DMRG applied to two crossed chains

The present implementation consists in five blocks: right, left, upper and down blocks B_ℓ^L , B_ℓ^R, B_ℓ^U and B_ℓ^D with ℓ sites (environment) plus a center block B_m^C with also m sites (system), as it is shown in Fig.(5.1).

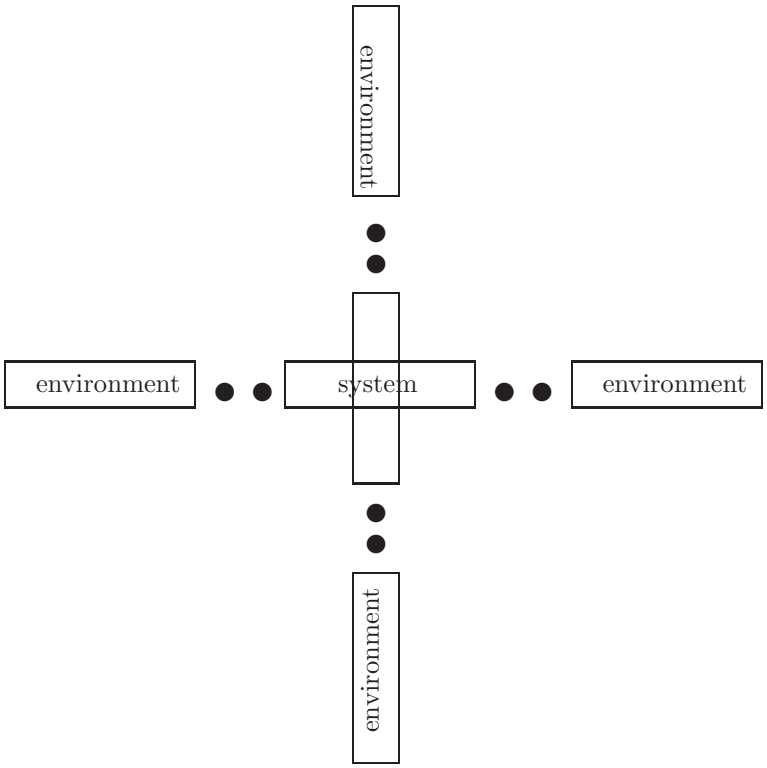

Figure 5.1: DMRG superblock configuration: five blocks and eight sites to add at each step of the procedure.

5.1.2.1 Superblock Hamiltonian

In order to treat the $N_E \geq 1$ lowest energy levels, the environment blocks B^L, B^R,B^U and B^D must contain N_E degrees of freedom. Clearly, the center block contains $2N_E - 1$ sites. Our choice for numbering sites in the superblock is such the horizontal sites are labeled with odd number from left to right, whereas the vertical sites are labeled with even number starting from up to down. The superblock Hamiltonian H_{SB} is therefore a $(6N_E + 7) \times (6N_E + 7)$ matrix given by

$$H_{SB} = \begin{pmatrix} H_{LU} & -v_L & -v_U & 0 & 0 & 0 & 0 & 0 & 0 & 0 & 0 \\ -v_L^\dagger & h_{CL} & 0 & -1 & 0 & 0 & 0 & 0 & 0 & 0 & 0 \\ -v_U^\dagger & 0 & h_{CU} & 0 & -1 & 0 & 0 & 0 & 0 & 0 & 0 \\ 0 & -1 & 0 & h_{CCL} & 0 & -v_{CL}^\dagger & 0 & 0 & 0 & 0 & 0 \\ 0 & 0 & -1 & 0 & h_{CCU} & -v_{CU}^\dagger & 0 & 0 & 0 & 0 & 0 \\ 0 & 0 & 0 & -v_{CL} & -v_{CU} & H_C & -v_{CR} & -v_{CD} & 0 & 0 & 0 \\ 0 & 0 & 0 & 0 & 0 & -v_{CR}^\dagger & h_{CCR} & 0 & -1 & 0 & 0 \\ 0 & 0 & 0 & 0 & 0 & -v_{CD}^\dagger & 0 & h_{CCD} & 0 & -1 & 0 \\ 0 & 0 & 0 & 0 & 0 & 0 & -1 & 0 & h_{CR} & 0 & -v_R^\dagger \\ 0 & 0 & 0 & 0 & 0 & 0 & 0 & -1 & 0 & h_{CD} & -v_D^\dagger \\ 0 & 0 & 0 & 0 & 0 & 0 & 0 & 0 & -v_R & -v_D & H_{RD} \end{pmatrix} \quad (5.1)$$

where H_{LU} writes

$$H_{LU} = \begin{pmatrix} H_L^{11} & 0 & H_L^{12} & 0 & \dots & H_L^{1N_E} & 0 \\ 0 & H_U^{11} & 0 & H_U^{12} & \dots & 0 & H_U^{1N_E} \\ H_L^{21} & 0 & H_L^{22} & 0 & \dots & H_L^{2N_E} & 0 \\ 0 & H_U^{21} & 0 & H_U^{22} & \dots & 0 & H_U^{2N_E} \\ \vdots & \vdots & \vdots & \vdots & \ddots & \vdots & \vdots \\ H_L^{N_E1} & 0 & H_L^{N_E2} & 0 & \dots & H_L^{N_EN_E} & 0 \\ 0 & H_U^{N_E1} & 0 & H_U^{N_E2} & \dots & 0 & H_U^{N_EN_E} \end{pmatrix} \tag{5.2}$$

H_{LU} is a $2N_E \times 2N_E$ matrix, built up by two embedded matrices H_L and H_U, each one representing the interactions inside the blocks B^L and B^U, respectively. Zeros in the matrix indicate lost links between sites. Thus, H_{LU}^{12}, for example, is equal to zero because there is no link between the first and second sites. Similarly, H_{RD} writes

$$H_{RD} = \begin{pmatrix} H_R^{11} & 0 & H_R^{12} & 0 & \dots & H_R^{1N_E} & 0 \\ 0 & H_D^{11} & 0 & H_D^{12} & \dots & 0 & H_D^{1N_E} \\ H_R^{21} & 0 & H_R^{22} & 0 & \dots & H_R^{2N_E} & 0 \\ 0 & H_D^{21} & 0 & H_D^{22} & \dots & 0 & H_D^{2N_E} \\ \vdots & \vdots & \vdots & \vdots & \ddots & \vdots & \vdots \\ H_R^{N_E1} & 0 & H_R^{N_E2} & 0 & \dots & H_R^{N_EN_E} & 0 \\ 0 & H_D^{N_E1} & 0 & H_D^{N_E2} & \dots & 0 & H_D^{N_EN_E} \end{pmatrix} \tag{5.3}$$

It represents the interactions inside the blocks B_R and B_D. The symbols h_{CL}, h_{CU}, h_{CR} and h_{CD} represent the added sites, at each iteration, to left, upper, right and down blocks, respectively. Also, h_{CCL}, h_{CCU}, h_{CCR} and h_{CCD} are the added sites to the center block. The N_E–component column vectors v_L,v_U,v_R and v_D describe the interaction between the blocks B^L, B^U ,B^R and B^R and the sites next to them in the superblock. For example, v_L writes as $(v_L^1, 0, v_L^2, 0 \dots, v_L^{N_E}, 0)$ and v_U writes as $(0, v_U^1, 0, v_U^2, \dots, 0, v_U^{N_E})$. The $(2N_E - 1)$–component column vectors v_{CL},v_{CU},v_{CR} and v_{CD} describe the interaction between the center B_C and the sites next to it in the superblock. So that, v_U, for example, writes as $(v_{CU}^1, v_{CU}^2, \cdots, v_{CU}^{N_E})$.

Then, the Hamiltonian H_{SB} in Eq.(5.1) describes the superblock

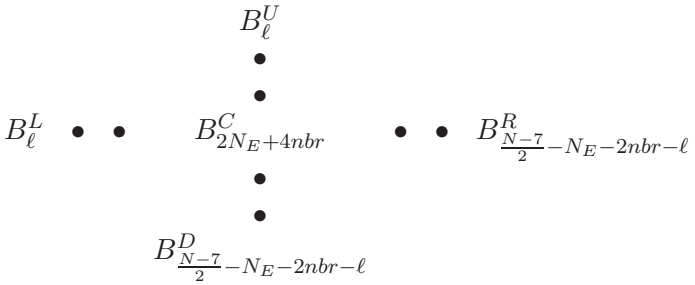

Since the blocks $B^{L,U,R,D}$ and the block B^C contain N_E and $2N_E - 1$ effective sites, respectively, we need $nbr = \frac{(N-6N_E-7)}{8}$ warm–up steps to reach the desired system length N. $H_{SB} = H_{SB}^{(\ell)}$ can be defined for $\ell = N_E, N_E + 1, \dots, N_E + nbr$.

5.1.3 DMRG truncation

As in the previous section, we have to obtain the N_E lowest eigenstates of H_{SB}, which will be designated as

$$(a^1_{L,i}, a^1_{U,i}, ..a^{N_E}_{L,i}, a^{N_E}_{U,i}, a_{CL,i}, a_{CU,i}, a_{CCL,i}, a_{CCU,i}, \mathbf{a}_{C,i}, a_{CCR,i}, a_{CCD,i}, a_{CR,i}, a_{CD,i}, a^1_{R,i}, a^1_{D,i}.., a^{N_E}_{R,i}, a^{N_E}_{D,i})^{N_E}_{i=1}$$

where $(a^1_{L,i}, \ldots a^{N_E}_{L,i})$, $(a^1_{U,i}, \ldots a^{N_E}_{U,i})$, $(a^1_{R,i}, \ldots a^{N_E}_{R,i})$ and $(a^1_{D,i}, \ldots a^{N_E}_{D,i})$ are N_E–component vectors and $\mathbf{a}_{C,i}$ is $2N_E-1$–component vector. For $N_E = 3$, these vectors are then projected onto a set of 3 vectors of the block $B^L\bullet$, i.e., $\{(\mathbf{a}_{L,i}, a_{CL,i})\}^3_{i=1}$, a set of 3 vectors of the block $B^U\bullet$, i.e., $\{(\mathbf{a}_{U,i}, a_{CU,i})\}^3_{i=1}$ and a set of 3 vectors of the block

$$\begin{array}{ccc} & \bullet & \\ \bullet & B_C & \bullet \\ & \bullet & \end{array}$$

i.e.,$\{(a_{CCL,i}, a_{CCU,i}, \mathbf{a}_{C,i}, a_{CCR,i}, a_{CCD,i})\}^3_{i=1}$. These three sets of vectors must be orthonormalized using a Gram-Schmidt orthogonalization procedure and then dividing them by

$$\mathrm{N}^i_L = \sqrt{{a^1_{L,i}}^2 + {a^2_{L,i}}^2 + {a^3_{L,i}}^2 + a^2_{CL,i}},$$

$$\mathrm{N}^i_U = \sqrt{{a^1_{L,i}}^2 + {a^2_{L,i}}^2 + {a^3_{L,i}}^2 + a^2_{CL,i}}$$

and

$$\mathrm{N}^i_C = \sqrt{a^2_{CCL,i} + a^2_{CCU,i} + {a^1_{C,i}}^2 + {a^2_{C,i}}^2 + {a^3_{C,i}}^2 + a^2_{CCR,i} + a^2_{CCD,i}}$$

respectively. The new three sets are designated as $\left\{(\mathbf{a'}_{L,i}, a'_{CL,i})\right\}^3_{i=1}$, $\left\{(\mathbf{a'}_{L,i}, a'_{CL,i})\right\}^3_{i=1}$, and $\left\{(a'_{CCL,i}, a'_{CCU,i}, \mathbf{a'}_{C,i}, a'_{CCR,i}, a'_{CCD,i})\right\}^3_{i=1}$. If there is no symmetry in the Hamiltonian, right and down matrices have to be renormalized in the same manner. A straightforward generalization of the renormalized block Hamiltonians in [173] yields the new effective Hamiltonians, H'_L and H'_U, and vectors v'_L and v'_U; which write, for $N_E = 3$, as

$$H'_L = \begin{pmatrix} a'^1_{L,1} & a'^2_{L,1} & a'^3_{L,1} & a'_{CL,1} \\ a'^1_{L,2} & a'^2_{L,2} & a'^3_{L,2} & a'_{CL,2} \\ a'^1_{L,3} & a'^2_{L,3} & a'^3_{L,3} & a'_{CL,3} \end{pmatrix} \begin{pmatrix} H^{11}_L & H^{12}_L & H^{13}_L & -v^1_L \\ H^{21}_L & H^{22}_L & H^{23}_L & -v^2_L \\ H^{31}_L & H^{32}_L & H^{33}_L & -v^3_L \\ -v^1_L & -v^2_L & -v^3_L & h_{CL} \end{pmatrix} \begin{pmatrix} a'^1_{L,1} & a'^1_{L,2} & a'^1_{L,3} \\ a'^2_{L,1} & a'^2_{L,2} & a'^2_{L,3} \\ a'^3_{L,1} & a'^3_{L,2} & a'^3_{L,3} \\ a'_{CL,1} & a_{CL,2'} & a'_{CL,3} \end{pmatrix} \quad (5.4)$$

$$H'_U = \begin{pmatrix} a'^1_{U,1} & a'^2_{U,1} & a'^3_{U,1} & a'_{CU,1} \\ a'^1_{U,2} & a'^2_{U,2} & a'^3_{U,2} & a'_{CU,2} \\ a'^1_{U,3} & a'^2_{U,3} & a'^3_{U,3} & a'_{CU,3} \end{pmatrix} \begin{pmatrix} H^{11}_U & H^{12}_U & H^{13}_U & -v^1_U \\ H^{21}_U & H^{22}_U & H^{23}_U & -v^2_U \\ H^{31}_U & H^{32}_U & H^{33}_U & -v^3_U \\ -v^1_U & -v^2_U & -v^3_U & h_{CU} \end{pmatrix} \begin{pmatrix} a'^1_{U,1} & a'^1_{U,2} & a'^1_{U,3} \\ a'^2_{U,1} & a'^2_{U,2} & a'^2_{U,3} \\ a'^3_{U,1} & a'^3_{U,2} & a'^3_{U,3} \\ a'_{CU,1} & a'_{CU,2} & a'_{CU,3} \end{pmatrix} \quad (5.5)$$

$$
\begin{aligned}
v'_{L,i} &= a'_{CL,i}, (i = 1 \ldots 3) \\
v'_{U,i} &= a'_{CU,i}, (i = 1 \ldots 3)
\end{aligned} \tag{5.6}
$$

Similarly, the new effective Hamiltonian, H'_C , and the vectors v'_{CL} and v'_{CU}, v'_{CR} and v'_{CD} are given by

$$
H'_C = \begin{pmatrix}
a'_{CCL,1} & a'_{CCU,1} & \mathbf{a}'_{C,1} & a'_{CCR,1} & a'_{CCD,1} \\
a'_{CCL,2} & a'_{CCU,2} & \mathbf{a}'_{C,2} & a'_{CCR,2} & a'_{CCD,2} \\
a'_{CCL,3} & a'_{CCU,3} & \mathbf{a}'_{C,3} & a'_{CCR,3} & a'_{CCD,3}
\end{pmatrix}
$$

$$
\begin{pmatrix}
h_{CCL} & 0 & -v^{\dagger}_{CL} & 0 & 0 \\
0 & h_{CCU} & -v^{\dagger}_{CU} & 0 & 0 \\
-v_{CL} & -v_{CU} & H_C & -v_{CR} & -v_{CD} \\
0 & 0 & -v^{\dagger}_{CR} & h_{CCR} & 0 \\
0 & 0 & -v^{\dagger}_{CD} & 0 & h_{CCD}
\end{pmatrix}
\begin{pmatrix}
a'_{CCL,1} & a'_{CCL,2} & a'_{CCL,3} \\
a'_{CCU,1} & a'_{CCU,2} & a'_{CCU,3} \\
\mathbf{a}'_{C,1} & \mathbf{a}'_{C,2} & \mathbf{a}'_{C,3} \\
a'_{CCR,1} & a'_{CCR,2} & a'_{CCR,3} \\
a'_{CCD,1} & a'_{CCD,2} & a'_{CCD,3}
\end{pmatrix} \tag{5.7}
$$

$$
\begin{aligned}
v'_{CL,i} &= a'_{CCL,i}, (i = 1 \ldots 5) \\
v'_{CU,i} &= a'_{CCU,i}, (i = 1 \ldots 5) \\
v'_{CR,i} &= a'_{CCR,i}, (i = 1 \ldots 5) \\
v'_{CD,i} &= a'_{CCD,i}, (i = 1 \ldots 5)
\end{aligned} \tag{5.8}
$$

5.1.4 Initialization, warm–up and sweeping

In the present case, the system is enlarged by 8 sites at each step of iteration. Thus, the warm–up phase, with reflection symmetry, consists in iterating these operations:

1. The left and upper blocks are built and then enlarged by adding a single site.
2. The right and down enlarged blocks are obtained by just reflecting the left and upper blocks, respectively. In the case where there is no symmetry reflection, the former blocks (right and down ones) must be built independently.
3. The center block is built and then enlarged by adding a single site to each side (four sites).
4. All these operators must be stored to be used later.
5. The five enlarged blocks, including interactions between them, form the super-block Hamiltonian.
6. The latter Hamiltonian is diagonalized, and the N_E lowest eigenstates are obtained.
7. The new effective Hamiltonians and interaction vectors are then constructed.

8. Once the system size N is reached; then the center block continues to grow up by four sites at each iteration, whereas the left, upper, down and right blocks retrieve until the number of sites in each block is equal to N_E.

9. At each step below, the left, upper, down and right blocks used are just those stored before.

10. Then, the procedure is reversed: the left, upper, down and right blocks grow up while the center block retrieve until the number of sites in it is just 5 sites. Similarly, the center blocks used are those stored as they has grown up before.

The image of the superblock at the end of these iterations is: four blocks representing a maximum of effective sites and a center block with just 5 sites.

In order to improve accuracy of the results, a number of sweep cycles are needed, keeping fixed the system size. Due to the geometry of the present system, it was necessary for us to adjust the process of sweeping, the standard process being useless. Effectively, each sweeping cycle consists of two parts:

1. The left (right) and upper (down) blocks will retrieve down to their minimum size N_E, and the stored ones are used, while the center block grows up, using the procedure below, until its maximum number of sites is reached.

2. Then, a new set of operators corresponding to the left (right) and upper (down) blocks are generated, while the center block matrices are picked up from the stored ones.

Repeating these two steps many times, energy results will converge to the more accurate values that can be obtained by DMRG procedure.

5.1.5 Results

We consider the Anderson Hamiltonian in site representation

$$H = \sum_i \varepsilon_i |i\rangle\langle i| + \sum_{\langle i,j\rangle} V|i\rangle\langle j| \tag{5.9}$$

with orthonormal states $|i\rangle$ corresponding to electrons located at sites i. V is the constant nearest-neighbor transfer integral with unit value and ε_n a site-diagonal random variable governed by a *normal* probability distribution.*i.e*

$$P(\varepsilon_n) = \begin{cases} 1/W & |\varepsilon_n| \leq W/2 \\ 0 & \text{otherwise} \end{cases} \tag{5.10}$$

W is the disorder strength. Other probability distributions, such Gaussian one, can be also used.

Despite its simplicity and since it was suggested by P.Anderson [174], the model has been widely used to study spectral and localization properties of disordered structures([175],[176]), metal-insulator transition induced by disorder([177],[178]), transport in general topologically disordered media [179], multifractal aspects of wavefunctions ([180],[181]), for interacting and non interacting electron systems.

Method	N	$E_0(N)$	$E_1(N)$	$E_2(N)$
Exact Diag.	105	-0.309401076758301	$1.352328451610949 \times 10^{-2}$	$1.352328451611478 \times 10^{-2}$
DMRG	105	-0.309401076758301	$1.352328451611124 \times 10^{-2}$	$1.352328451611313 \times 10^{-2}$
Exact Diag.	425	-0.309401076758508	$8.619875459942861 \times 10^{-4}$	$8.619875459979135 \times 10^{-4}$
DMRG	425	-0.309401076758506	$8.619875460086855 \times 10^{-4}$	$8.619875460089741 \times 10^{-4}$
Exact Diag.	905	-0.309401076758518	$1.915318921536133 \times 10^{-4}$	$1.915318921562604 \times 10^{-4}$
DMRG	905	-0.309401076758502	$1.915318922078220 \times 10^{-4}$	$1.915318922102459 \times 10^{-4}$
Exact Diag.	1.465	-0.309401076758482	$7.327654175460374 \times 10^{-5}$	$7.327654175659017 \times 10^{-5}$
DMRG	1.465	-0.309401076758503	$7.327654180964834 \times 10^{-5}$	$7.327654181053537 \times 10^{-5}$
Exact Diag.	2.025	-0.309401076758501	$3.839568650589582 \times 10^{-5}$	$3.839568651057789 \times 10^{-5}$
DMRG	2.025	-0.309401076758502	$3.839568654973506 \times 10^{-5}$	$3.839568655256073 \times 10^{-5}$
Exact Diag.	2.505	-0.309401076758508	$2.510520401701136 \times 10^{-5}$	$2.510520402393568 \times 10^{-5}$
DMRG	2.505	-0.309401076758506	$2.510520404624172 \times 10^{-5}$	$2.510520404886720 \times 10^{-5}$
Exact Diag.	3.065	-0.309401076758504	$1.677677228672380 \times 10^{-5}$	$1.677677230021150 \times 10^{-5}$
DMRG	3.065	-0.309401076758505	$1.677677232041186 \times 10^{-5}$	$1.677677232175863 \times 10^{-5}$
Exact Diag.	4.025	-0.309401076758491	$9.732859440333661 \times 10^{-6}$	$9.732859445854112 \times 10^{-6}$
DMRG	4.025	-0.309401076758504	$9.732859465153467 \times 10^{-6}$	$9.732859468420359 \times 10^{-6}$

Table 5.1: The ground, first and second excited states energies $E_0(N)$,$E_1(N)$ and $E_2(N)$ for a free particle on a tight-binding model in a two–crossed chains. The value of the diagonal entries in the diagonalized matrices is 2.0.

We begin with an ordered structure *i.e.* $\varepsilon_i = \varepsilon$. Unfortunately there is no theoretical results to compare with; hence it is necessary to obtain the ground state and few excited states energies by exact diagonalization.

Thus, results for the ground state, first and second excited states, obtained with both methods, are given in Table (5.1). The number of targeted states is $N_E = 3$. Five sweeps are generally sufficient to reach convergence. As it can be seen from the table, a high degree of agreement exists between exact diagonalization results and our DMRG results for the ground state; it ranges from complete agreement(in the order of computational material) for a system size equal to 105 sites (15 digits) to 12 digits when the size of the system exceeds 4.000 sites. For first and second excited states energies, the agreement is still significant, but in a bit less degree. In fact, for a system of 105 sites, which is relatively small, the agreement between the methods is up to 13 digits and it is apparently kept at this level in the case of a system size exceeding 4.000 sites. Certainly, the decaying accuracy of results as the system size increases is still a general behavior of DMRG method, though results do not make it so clear. It is essentially due to our limiting computational facilities to deal with much larger systems.

By introducing disorder, *i.e.* ε_i are randomly distributed, the symmetry of left, right, up and down blocks is lost, and we have to renormalize all blocks separately. As it is just a matter of comparison of our results with those obtained by exact diagonalization, we restrict our study to a single value of W, taken to be equal to $W = 2.0$. Table (5.2) displays results of the first three lowest energies of a disordered structure obtained by both exact diagonal-

ization and DMRG procedure. From the table we can see an accurate results obtained by our calculations compared to those obtained by exact diagonalization(up to 12 digits for a system with 2425 sites), although the size of the structures is not so big to be considered as representing real materials. This is due in first place to computational restrictions, which were, let's remind, the major instigator to explore other ways in dealing with such huge systems. Nevertheless, regarding the behavior of our results for those relatively small sizes, we can think that accuracy, by its decreasing aspect when system size increases, will not be completely lost before a considerable size is reached.

In other hand, this procedure enables us to obtain the ground state of a non-interacting disordered system by just multiplying the ground state value by the number of sites of the system(one electron per site). This value could be a rough estimation of energy scale for the ground state of an interacting disordered system.

Method	N	$E_0(N)$	$E_1(N)$	$E_2(N)$
Exact Diag.	105	−2.33492839367123	−2.31256015487412	−2.27633450482704
DMRG	105	−2.33492839248340	−2.31256015458150	−2.27633450453549
Exact Diag.	425	−2.62707526909553	−2.51368257944855	−2.49551862249973
DMRG	425	−2.62707353842147	−2.51368257944855	−2.49551862249973
Exact Diag.	825	−2.74034137548984	−2.66488808899811	−2.62707526909553
DMRG	825	−2.74034137548807	−2.66484686948334	−2.62707526909553
Exact Diag.	1.225	−2.68329769657425	−2.66115344781251	−2.63257708999018
DMRG	1.225	−2.68329769655407	−2.66115344781251	−2.63257708999017
Exact Diag.	2.425	−2.64472106170087	−2.63084212954662	−2.61585544521942
DMRG	2.425	−2.64472106170071	−2.63084212954661	−2.61585544521941
Exact Diag.	3.225	−2.74712495427613	−2.61737491050982	−2.59050557867426
DMRG	3.225	−2.74712485946028	−2.61736733389125	−2.59050557867427

Table 5.2: The ground, first and second excited states energies $E_0(N)$,$E_1(N)$ and $E_2(N)$ for disordered structure within tight-binding model in a two–crossed chains. The disorder strength W is equal to 2.0.

5.1.6 Conclusion

In this paper, we presented a DMRG procedure extension to compute low states energies of a two disordered crossed chains within the tight–binding model suggested by P.Anderson. The purpose of this work was to try to bring a different insight on a major challenging problem vis-à-vis the application of the DMRG procedure to systems with geometry other than 1–d. Instead of the standard two–blocks configuration, we have adopted a five–blocks configuration (four environment blocks and a system block in–between), with a bit different way to achieve warm–up phase and sweep cycles. Results obtained have shown that the new procedure works with a high precision within a certain accuracy. They have also shown a "decaying accuracy as size increases" behavior, proper to standard DMRG.

5.2 Ground state properties of a spin chain within Heisenberg model with a lacking spin site

5.2.1 Introduction

The cristallographic image used to represent condensed materials is more pedagogical than realistic; for real materials are not so perfect as it is presented. The disorder effects range from substitutional disorder, where the atomic(ionic) order is interrupted by strange atoms or lacking sites, to topological disorder, where eventually atomic (ionic) positions lose their periodicity. Another kind of distortion is the non magnetic impurities. Their presence in magnetic materials is very affecting the electronic properties of such materials and can eventually lead to quantum phase transitions.

In fact, the physics of random quantum spin systems has attracted the interest of theoretical and experimental studies[182, 183]. To take into account this distortion in materials, physicists have elaborated during the last decades many models that capture the essential of those models physics, with care of simplicity. For one-dimensional quantum magnetic systems, the Heisenberg model is one of the most fundamental models and the most widely studied by way of numerical calculations. Thus, spin chains with: random bonds [184, 185, 186], frustrated term[187], biquadratic term [188], including all variations that can be explored, are studied. Also, spin chains with a spin impurity that have a different spin magnitude are investigated[189]. Spin chains with single [190] as well as randomly distributed [186] impurities and disorder [191, 192] are explored. The Kondo model [193] is used to describe a magnetic impurity with spin S interacting locally with a non-interacting conduction electron sea(*e.g* rare earth metal alloys and actinide elements).

In the present paper, we study a spin chain with a single site nonmagnetic atom inserted. It could be also a lacking site. Adding a single non-magnetic impurity to a spin chain compound breaks the chains up into two segments. Our idea is to introduce next nearest neighbors interactions to maintain connection between spin sites at left and right of the "missing" spin. In fact, nonmagnetic ions that may be present in a magnetic material serve, among other functions, to stabilize the material and to provide connection to nearby spins with one another [194]. Therefore, the spin-1/2 Heisenberg model with next nearest neighbors interactions writes as

$$H = \sum_{i}^{N} [J_1 S_i.S_{i+1} + J_2 S_i.S_{i+2}] \tag{5.11}$$

where S_i denotes the spin $S = 1/2$ operator for lattice site i. This model with antiferromagnetic interactions (J_1, $J_2 > 0$) is well studied[195, 196, 197, 198, 187]. Thus, the pure spin chain is well known to display a quantum phase transition (Kosterlitz-Thouless transition)[199] from a gapless, translationally invariant state with algebraic spin correlations (the spin fluid phase) to dimer gapful state with exponentially decaying correlations at $\alpha_c \simeq 0.24113$, where $\alpha = \frac{J_2}{|J_1|}$. At $\alpha = 0.5$ (the Majumdar-Ghosh point)[187], the ground state is exactly solvable. It is a doubly degenerate dimer product of singlet pairs on neighboring sites. In general, the ground state is doubly degenerate for $\alpha > \alpha_c$. For large J_2 ($\alpha > 0.5$) an incommensurate phase appears in the ground state phase diagram[198, 200].

The major part of this work is to compute ground state and eventually first excited states energies and their corresponding eigenstates of the above Hamiltonian. Physical quantities are then computed through appropriate formulas. Computational physics provides us with a panoply of numerical methods that ranges from the obvious complete diagonalization to variational methods with more or less accuracy and different areas of excellency. We have chosen two of them: exact diagonalization and Density Matrix Renormalization Group (DMRG.)

5.2.2 Exact diagonalization results

5.2.2.1 ground state energy

The exact diagonalization technique is a direct method that provides us with the whole spectrum of a system Hamiltonian and the corresponding eigenvectors. Unfortunately, the order of matrices to be diagonalized for the Heisenberg model grows as 2^N; N being the number of sites. Therefore, system sizes treated by such method are very restricted and can go, using different symmetries, to more or less twenty sites; which is far from to be the thermodynamic limit. Fortunately, the study of such systems do not require the whole spectrum, and generally a set of low lying states, including the ground state and some few excited states are sufficient to describe their properties. Therefore, numerical methods had been elaborated by physicists to focus on those restricted parts of the spectrum with more or less accuracy; such as the earlier Lanczos method and the recently developed method, the DMRG. Nevertheless, the exact diagonalization still have its relevance, especially for those properties that do not depend on system size.

Thus, we diagonalize matrices for spin chains with $N = 6, 8, 10, 12$ using periodic boundary conditions. The use of these boundaries is governed by the fact that changing the position of the lacking site in the chain does not affect the energy spectrum of a chain with a single lacking site. The value of J_2 goes from 0.05 to 0.55 with a step of 0.05; for it is useful to sweep a large interval where the well-known system undergo quantum phase transitions. This permits to us to figure out how the system is affected when a spin site is missed. The value of J_1 is taken to be unity.

Figures 5.2(5.3) display the first three lowest energies as function of J_2, for a spin chain without(with) a lacking site, respectively. The chain length is $N = 10$ and J_2 values go from 0.2 to 0.3. The latter interval is thought to contain a critical point of the system [201, 199]. In figure 5.2, one can see a nonvanishing gap that appears, as it is the case when $J_2 = 0.00$. One also see that the gap is constant until J_2 is around 0.25. Beyond this value the gap is decreasing. Taking into account works that confirm the existence of such a critical point at this value, one can think that the behavior of the gap could be a signature of a spin system that crosses a critical point, but, in fact, it is not. In the other hand, figure 5.3 shows that a spin system with a missing site have no gap at all. Actually, the first four low lying energies, including the ground state have the same value.

Now, we want to see the variation of the ground state energy as a function of the system size, as the value ofJ_2 is also changing. Thus, figures 5.4(5.5) display the ground state energy for both spin system without (with) a lacking site. Both figures show a linear dependency of the ground state energy (E_0) on the system size. This implies a slope dependency on J_2

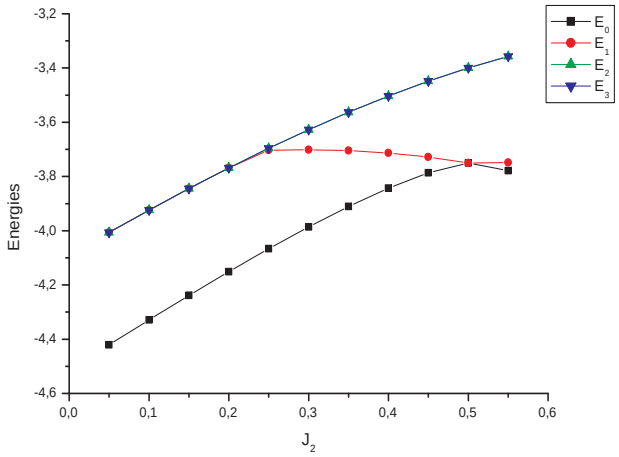

Figure 5.2: First three lowest energies as a function of J_2 for a spin chain without a lacking site spin.

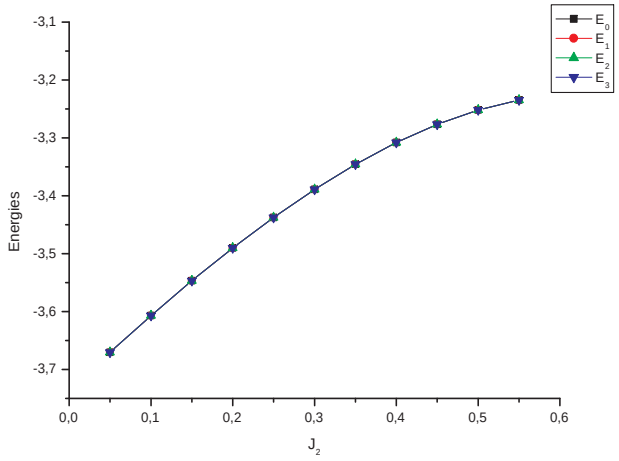

Figure 5.3: First three lowest energies as a function of J_2 for a spin chain with a lacking site spin.

and then the E_0 formula for both systems could be written as

$$E_0 = A(J_2)N \tag{5.12}$$

N being the size of the chain. To show this slope dependency on J_2, we represent on figure 5.6 the variation of $A(J_2)$ for both systems(without(with) a lacking site). One can see for both systems the non linearity of slope dependency on J_2. It seems that for a system without lacking site the slope dependency is a non analytic function around the value $J_2 = 0.5$, which is the Majumdar-Gosh point(another critical point). A polynomial fit with the latter point $J_2 = 0.5$ avoided gives

$$A(J_2) = -0,3095 + 0,16139J_2 + 0,16408J_2^2 - 0,73624J_2^3 + 0,53559J_2^4 \tag{5.13}$$

for a system without missing site, and

$$A(J_2) = -0,32159 + 0,17716J_2 - 0,06593J_2^2 - 0,03391J_2^3 \tag{5.14}$$

for a system with a lacking site.

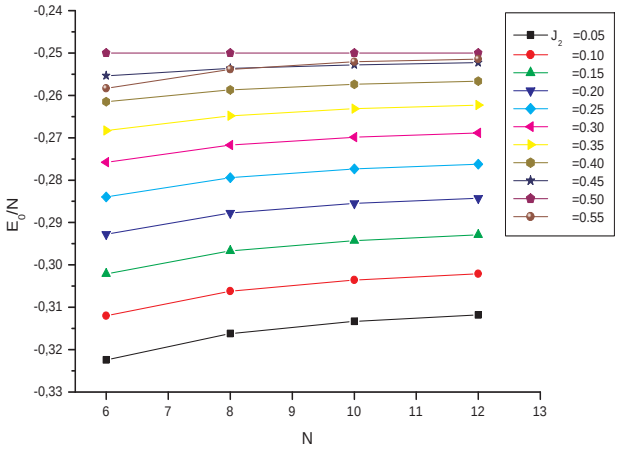

Figure 5.4: Exact ground state eigenvalue for a spin chain without a lacking site *vs* the system size N, as the value of J_2 varies.

To study the dependency of the ground state energy on both N and J_2 around the critical point $J_2 = 0.25$, we plot in the figure 5.6 the variation of $A(J_2)$ for both spin chains. The linearity of $A(J_2)$ suggests that E_0 for both systems may write as

$$E_0 \sim J_2 N \tag{5.15}$$

Actually, for a system without lacking site

$$E_0 = -2.07548J_2N \tag{5.16}$$

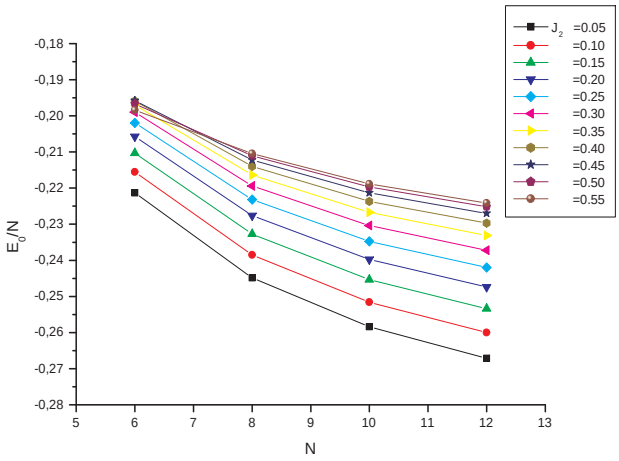

Figure 5.5: Exact ground state eigenvalue for a spin chain with a lacking site *vs* the system size N, as the value of J_2 varies.

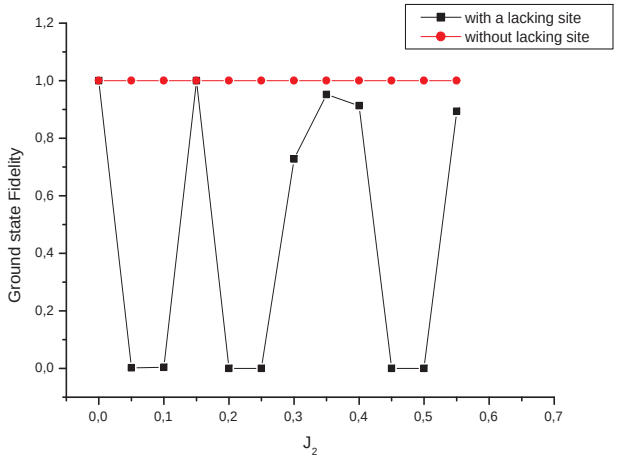

Figure 5.6: Variation of the slope $A(J_2)$ for both spin chains (with and without a lacking spin site). J_2 value ranges from 0.05 to 0.55. Results are obtained using exact diagonalization technique.

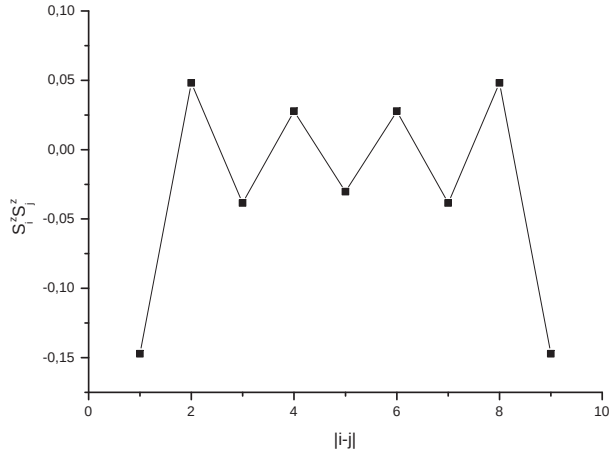

Figure 5.7: Variation of the slope $A(J_2)$ around the critical point $J_2 = 0.25$ for both spin chains (with and without a lacking spin site).Results are obtained using exact diagonalization technique.

and

$$E_0 = -1.74506 J_2 N \tag{5.17}$$

for a spin system with lacking site. These results confirm other works suggesting a critical exponent equal to 1.0 for J_2 [202].

5.2.2.2 quantum fidelity

In the other hand, the obtaining of the ground state eigenvector by exact diagonalization allows us to compute some quantities that characterize behaviours of such systems. The most in sight are the fidelity quantity and correlations functions.

In quantum physics, an overlap between two quantum states usually denotes the transition amplitude from one state to the another. That is the overlap gives unity if two states are exactly the same, while zero if they are orthogonal. Thus, one use the ground state fidelity as a measure of similarity between states. It is defined as the overlap between $|\Psi_0(\lambda))\rangle$ and $|\Psi_0(\lambda+\delta))\rangle$ [201], *i.e.*

$$F_0(\lambda, \delta) = |\langle \Psi_0(\lambda) | \Psi_0(\lambda+\delta)\rangle|, \tag{5.18}$$

where $\Psi_0(\lambda)$ is the ground state wavefunction of the Hamiltonian corresponding to the parameter λ and δ is a small quantity. In our case, λ is represented by J_2, and $\delta = 2.5\times10^{-4}$.

We can observe in figure 5.8 that the ground state fidelity for spin system without lacking spin site is almost a constant and equals to unity for a wide range of the parameter J_2. Our results confirm the fact that critical points of the quantum phase transitions can not be well characterized by the ground state fidelity for a finite size system ($N = 10$, in our case). In other hand, for a spin system with a lacking site, fidelity alternates unity and

zero values, as J_2 varies. This is a signature of loss of orthogonality between neighboring states over some regions in the interval of J_2. Therefore, the missing spin site breaks the similarity between neighboring states.

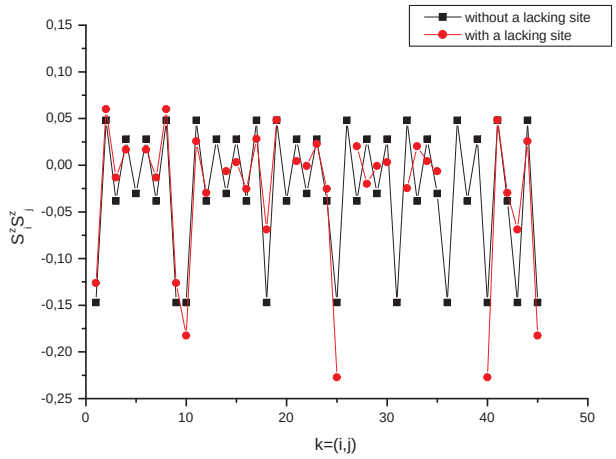

Figure 5.8: Ground state fidelity for both 10-sites spin chains (with and without a lacking spin site.

5.2.2.3 correlation functions

We compute also the correlation function $S_i^z S_j^z$ as function of the distance between spin sites $|i-j|$. The results for a spin system of size $N = 10$ without lacking site are shown in figure 5.9. One can see the alternation of signs between odd and even sites: this is a signature of the antiferromagnetic nature of the system. One can see also that results are symmetric: this is a signature of the periodic boundary conditions applied. We also have to note that the above function present a translational symmetry: they do not depend on position of the spin sites but just on distance between them. This why we have used the absolute value of distance in figure 5.9.

On the contrary, the system with a missing site do not keep this symmetry. To show this, we have displayed in figure 5.10 the correlation functions for both systems (with and without lacking site) as they vary with the distance $i-j$. The numbers on x-axis denote the distance between sites in the following order:$k \equiv (i,j)$ where $i = 1, N-1 \text{and} j = i+1, N$. As an example: $k = 4$ represents the distance between $i = 1$ and $j = 5$, where $k = 12$ represents the distance between $i = 2$ and$j = 4$. For the system without lacking site, the same values are reproduced along the x-axis, whereas the values of $S_i^z S_j^z$ are changing for the system with a missing site. This can be explained as a breaking of the translational symmetry for that quantity.

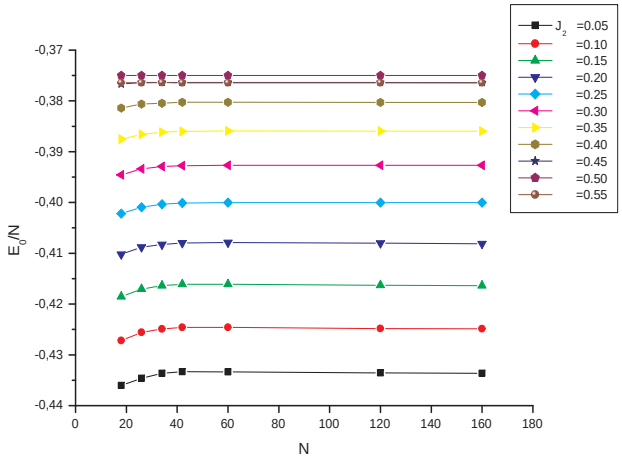

Figure 5.9: Correlation function $S_i^z S_j^z$ as function of the distance between spin sites $|i-j|$ for both 10-sites spin chains (with and without a lacking spin site).

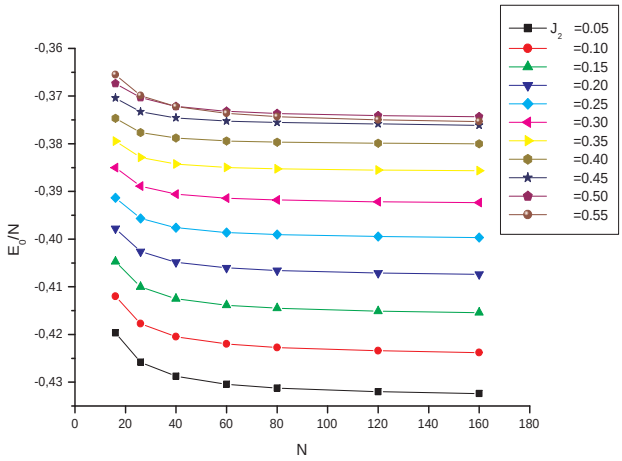

Figure 5.10: Correlation function $S_i^z S_j^z$ as function of the distance between spin sites $|i-j|$ for both 10-sites spin chains (with and without a lacking spin site).

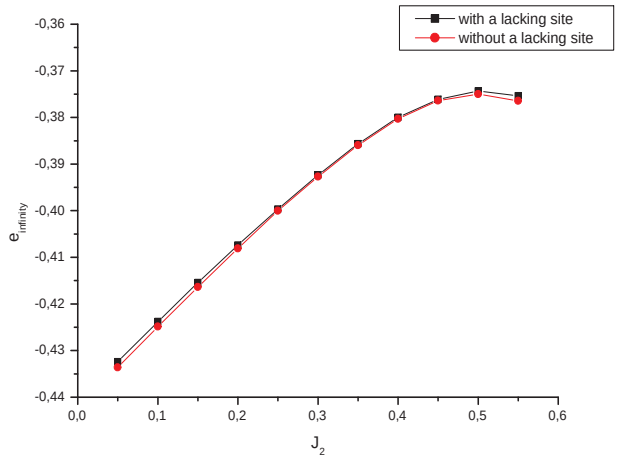

Figure 5.11: Ground state energy for a spin chain without a lacking site, as the chain size N and J_2 vary.

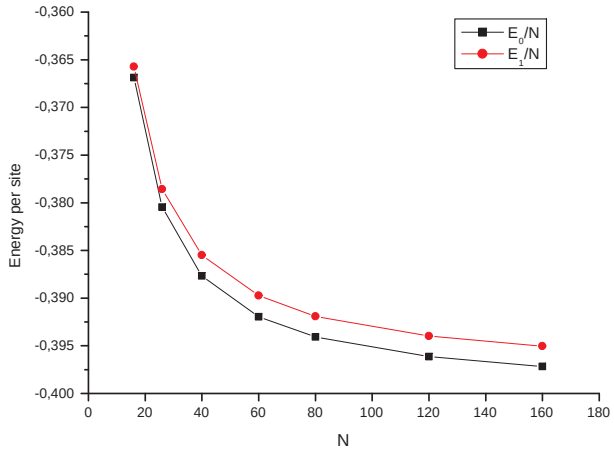

Figure 5.12: Ground state energy for a spin chain with a lacking site, as the chain size N and J_2 vary.

5.2.3 DMRG results

The Density Matrix Renormalization Group (DMRG), developed by S. R. White in 1992 [24], is a powerful numerical method which allows us to obtain the ground-state and low-lying excited states wavefunctions of large-size systems with controlled high accuracy. The basic idea of DMRG algorithm consists in increasing the size of the system while the corresponding Hilbert space is kept constant, using the concept of matrix density to determine what states to be kept. More technical details about the method can be abundantly found in literature, (see for example: [28], [203] and [204]).

As the present spin system contains next nearest neighbors interactions, the use of the DMRG technique requires more computational effort to take into account those interactions; which means more states to be kept to reach the desired accuracy.

Figures 5.11 and 5.12 display the ground state energies for two spin systems without and with lacking site, respectively, as N and J_2 vary. The utmost sizes of spin chains considered are equal to $N = 30$, with values of J_2 that go from 0.05 to 0.55 by a step of 0.05.

Our results for both systems confirm the linear dependency of the ground state energy to system size, with a slope that varies in function of the J_2 value. The latter results suggest, as already stated, that ground state energy could be written as

$$E_0 = A(J_2)N \tag{5.19}$$

In order to find out the function that represents the variation of $A(J_2)$, we plot the latter in figure 12 for both systems. For a spin system with a lacking site, the function $A(J_2)$ is analytic along the interval of J_2. It reaches a maximum for the value $J_2 = 0.5$ and a polynomial fit gives

$$A(J_2) = -0,44417 + 0,20302J_2 - 0,25835J_2^2 + 0,73757J_2^3 - 0,96477J_2^4 \tag{5.20}$$

For the spin system without a lacking site, the function $A(J_2)$ seems to be more or less abrupt around the value $J_2 = 0.40$, with also a maximum at $J_2 = 0.5$. This point is thought to be a critical point, and it seems to be characterized here by a maximum of $A(J_2)$. A polynomial fit gives (with the abrupt region smoothed)

$$A(J_2) = -0,43686 + 0,16432J_2 + 0,01212J_2^2 - 0,01237J_2^3 - 0,34502J_2^4 \tag{5.21}$$

Around the critical point $J_2 = 0.25$ the $A(J_2)$ function shows a linear dependency on J_2. Using a linear fit the ground state energy for a spin system without lacking site can be written as

$$E_0 = -1.59864J_2N \tag{5.22}$$

and

$$E_0 = -1.531757J_2N \tag{5.23}$$

for a spin system with a lacking site.

5.2.4 Conclusion

The present paper treats spin chains with next nearest neighbors interactions. Ground states and few low lying eigenvalues are computed using exact diagonalization technique. Results are then compared with those for a spin chain that "misses" a single spin site. It could be a non magnetic impurity or just a lacking site, as it is often the case in real materials. Other physical quantities, such as quantum fidelity and correlation functions are also computed. In fact, extrapolations of results suggest that both systems are gapped. The gap of a spin system with a lacking site increases as the system size increases, while for a system without lacking site the gap tends to a certain value as the system size goes to thermodynamic limit. The introduction of such distortion affects also the behavior of the eigenstates; since the quantum fidelity alternates zero and one values; which is a signature of loss of similarity of neighbor states. The computation of correlation functions have showed that a lacking site breaks the translational symmetry of a pure spin chain, as it is, actually, well known.

Using DMRG technique we have computed ground state energies for relatively large chains. This allows us to achieve a ground state energy finite-size scaling that give us formulas for ground state energy as function of J_2 and N (spin chain size).

5.3 Results of entanglement entropy of the spin-$\frac{1}{2}$ Heisenberg chains with and without a single lacking spin site with next nearest neighbors interactions: DMRG study

5.3.1 Introduction

Consider a one-dimensional system with size L and composed by two subsystems A and B of sizes l_A and $l_B = L - l_A$, respectively. The von Neumann entropy, used to quantify the bipartite entanglement between the subsystem A and the rest of the system (subsystem B), is defined as $S(L, l_A) = -Tr(\rho_A \log_2 \rho_A) = -\sum_{i=1}^{k} \lambda_i \log_2(\lambda_i)$, where the λ_i are the eigenvalues of the reduced density matrix ρ_A [205], and Tr is the trace of an operator. The reduced density matrix ρ_A is defined as $\rho_A = Tr_{(L-l_A)}|G_S\rangle\langle G_S|$, $|G_S\rangle$ being the ground state of the whole system. For the critical one-dimensional systems the entanglement entropy behaves as [206, 207, 208]

$$S(L, l_A) = \frac{c}{3\eta}\log_2\left(\frac{\eta L}{\pi}\sin(\frac{\pi l_A}{L})\right) + c_1 - (1-\eta)s_b \tag{5.24}$$

where c is the conformal anomaly (central charge), s_b is the boundary entropy, c_1 is a non-universal constant and $\eta = 1(2)$ is set for systems under periodic (open) boundary conditions.

It is useful to plot $S(L, l_A)$ as function of $\log_2\left(\frac{\eta L}{\pi}\sin(\frac{\pi l_A}{L})\right)$ in order to estimate c by a numerical fit. Another way, suggested by J. C. Xavier [209], to extract the conformal anomaly from Eq.(5.24) without any fit parameter, considers two systems with sizes L and L'; both systems are composed of two subsystems of sizes $l_A = L/2$ and $l'_A = L'/2$, respectively. Thus, from Eq.(5.24), it is possible to estimate c by

$$c(L, L') = 3\eta\frac{S(L, L/2) - S(L', L'/2)}{\log_2(L/L')} \tag{5.25}$$

The estimation of the conformal anomaly c can be used to determine other physical quantities such as sound velocity v_s and anomalous dimensions x^{α}_{bulk}.

In fact, it was shown, in the context of the conformal field theory [210, 211], that the conformal anomaly c can be extracted from the large-L behavior of the ground state energy $E_0(L)$, which behaves as [212, 213]

$$\frac{E_0}{L} = e_\infty + \frac{f_\infty}{L} - \frac{v_s \pi c}{6\delta L^2} \tag{5.26}$$

where the constant $\delta = 1(4)$ for the systems under periodic (open) boundary conditions, v_s is the sound velocity, e_∞ is the bulk ground state energy per site, and f_∞ is the surface free energy, which vanishes for the systems under periodic boundary conditions (PBC).

Also, a relation have been established between the anomalous dimension x^{α}_{bulk} (surface exponents x^{α}_{s}) and the structure of the higher energy states of the system. Thus, the energy spectrum of the Hamiltonian for different sectors are given by [214, 215],

$$E^{\alpha}_{m,m'}(L) - E_0(L) = \frac{2\pi v_s}{\eta L}(x + m + m') \tag{5.27}$$

where $m, m' = 0, 1, 2, ...$, the constant $\eta = 1(2)$ and $x = x^{\alpha}_{bulk}(x^{\alpha}_{s})$ for the systems with periodic (open) boundary conditions.

The present paper is dedicated to compute the values of the above three quantities for a 1/2-spin chain within the simple Heisenberg model, including next nearest neighbors interactions with periodic boundary conditions (PBC). The Hamiltonian of the system writes as

$$H = \sum_{i}^{L} [J_1 S_i.S_{i+1} + J_2 S_i.S_{i+2}] \tag{5.28}$$

where S_i denotes the spin $S = 1/2$ operator for lattice site i and (J_1, $J_2 > 0$) for antiferromagnetic interactions.

The reason behind this choice is two-fold:

-Estimating the above quantities for a well studied [195, 196, 197, 198, 187] model, where, in fact, the pure spin chain is well known to display a quantum phase transition (Kosterlitz-Thouless transition)[199] from a gapless, translationally invariant state with algebraic spin correlations (the spin fluid phase) to dimer gapful state with exponentially decaying correlations at $\alpha_c \simeq 0.24113$, where $\alpha = \frac{J_2}{|J_1|}$. At $\alpha = 0.5$ (the Majumdar-Ghosh point)[187], the ground state is exactly solvable. It is a doubly degenerate dimer product of singlet pairs on neighboring sites. In general, the ground state is doubly degenerate for $\alpha > \alpha_c$. For large J_2 ($\alpha > 0.5$) an incommensurate phase appears in the ground state phase diagram[198, 172].

-Simulating a disordered chain by removing out a single spin site from the chain, while the two parts of the chain are still connected due to next nearest neighbors interactions. The *lacking site* could be also a non-magnetic atom inserted among magnetic ones. In fact, nonmagnetic ions that may be present in a magnetic material serve, among other functions, to stabilize the material and to provide connection to nearby spins with one another [194].

In general, the physics of random quantum spin systems has attracted the interest of theoretical and experimental studies [182, 183], and, consequently, various models that capture the essential of those models physics have been established. Thus, spin chains with: random bonds [184, 185, 186], frustrated term [187], biquadratic term [188], including all variations that can be explored, are studied. Also, spin chains with a spin impurity that have a different spin magnitude are investigated[189]. Spin chains with single [190] as well as randomly distributed [186] impurities and disorder [191, 192] are explored. Also, the Kondo model [193] is used to describe a magnetic impurity with spin S interacting locally with a non-interacting conduction electron sea(*e.g* rare earth metal alloys and actinide elements).

As it may be understood, this is a matter of diagonalizing Hamiltonians matrices in order to obtain ground state energies for long spin chains. Unfortunately, with exact diagonalization one can deal just with small system sizes, since the Hilbert space grows exponentially with the system size. Therefore, it is necessary to use the Density Matrix Renormalization Group (DMRG). The latter, developed by S. R. White in 1992 [23], is a powerful numerical method which permits us to obtain the ground-state and low-lying excited states wavefunctions of large-size systems with controlled high accuracy [28, 203, 166]. It allows also to estimate the entanglement entropy, and, therefore, the conformal anomaly c and other related quantities, of critical systems through Eq.(5.24).

5.3.2 Results

Before presenting the numerical results, let's see how the ground energy per site, for both pure and lacking antiferromagnetic spin-1/2 Heisenberg chains with next nearest interactions, behaves as the system gets larger with periodic boundaries condition (PBC). In figure (5.13), we present the variation of E_0/L as function of L, for $J_2 = 0.2$. We can see that for both systems, E_0/L tends to a constant value for each of them, but in different ways. We have estimated the two values as: $E_0/L = -0.408$ for a pure chain, where $E_0/L = -0.407$, for a spin chain with a lacking site. In the rest of this paper, E_0/L could be considered as e_∞. These results are obtained using DMRG method, and will be useful to determine other parameters.

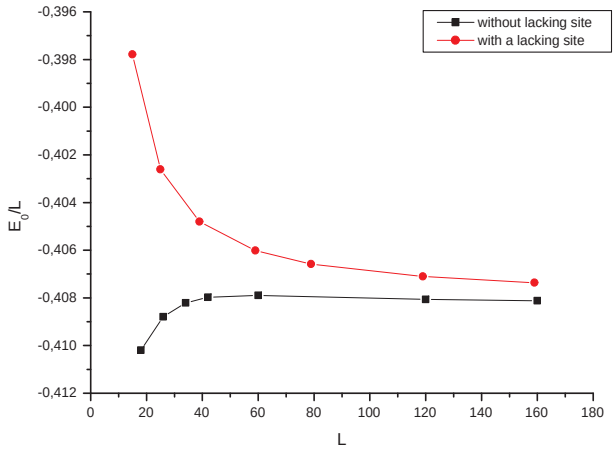

Figure 5.13: $\frac{E_0}{L}$ vs L for spin chains with and without a single lacking spin site.

Figure (5.14) displays the entanglement entropy $S(L, l_A)$ as function of the length l_A for a 160-sites pure spin chain with PBC. Three curves corresponding to $J_2 = 0.20, 0.25, 0.50$, are then presented. We see that for all three values of J_2, corresponding curves have two branches; one for even l_A and one for odd l_A. This situation, called even-odd oscillations, is already obtained for anisotropic spin-1/2 Heisenberg chains with OBC (open boundaries conditions) for only nearest neighbor sites, but in a reversed way: even l_A are down, where odd l_A are up [209]. At MG point ($J_2 = 0.5$) the entanglement entropy has two constant branches: one equal to zero for odd l_A, and the other equal to 0.69315 for even l_A. This strange behavior has already started for $J_2 = 0.40$, and it seems not useful to use entanglement entropy equation to fit our results beyond this value.

In figure (5.14), we present the entanglement entropy $S(L, l_A)$ as function of the length l_A for a 160-sites spin chain with PBC, and where a single spin site is omitted. At first glance, the even and odd l_A branches are now reversed. Also, at MG point ($J_2 = 0.5$) the entanglement entropy changes completely from constant lines to certain slopes. But the main result is that there is no symmetry between left and right parts of each branch of

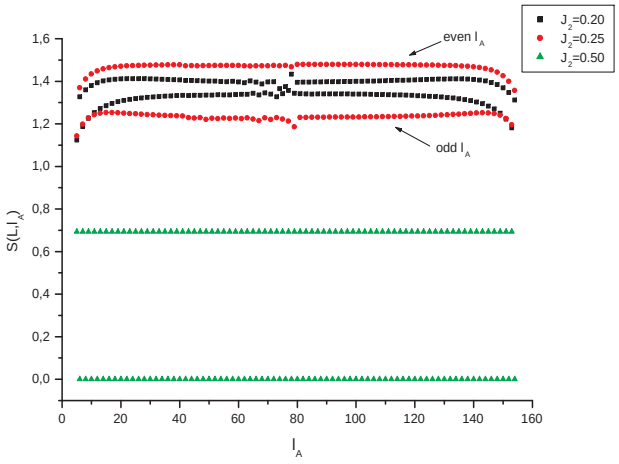

Figure 5.14: The entanglement entropy $S(L, l_A)$ vs l_A for the antiferromgnetic spin-1/2 Heisenberg pure chain. .

the entanglement entropy, *i.e.* $S(L, l_A) \neq S(L, L - l_A)$. It is surely a consequence of the translational symmetry breaking in the spin chain. Consequently, it is not suitable for us, also in this case, to deal with the above analytic expression of the entanglement entropy (Eq. 5.24) for all J_2 values to fit our results.

In Table 5.3, we present values of c^{PBC}, in unit of η, against J_2 values; for it is a confused matter for us to decide which η we should take. These values are obtained using the method suggested by J.C. Xavier [209]. The striking fact is that the values of c^{PBC} are negative, which is a bit surprising. Thus, we will use absolute values of c^{PBC} as we compute other quantities.

With the conformal anomaly c^{PBC} values in hand, we can extract the finite size estimate of sound velocity v_s from Eq.(5.26), as:

$$v_s(L) = \frac{6\,L}{\pi c^{PBC}}(L\,e_\infty - E_0(L)) \tag{5.29}$$

In Table 5.4 we present the sound velocity values for a pure spin chain for different values of L (chain size) and J_2.

Sound velocity values permit us, using Eq.(5.27), to extract the finite-size estimates of the anomalous dimension exponent through equation

$$x(L) = \frac{\eta L(E_1(L) - E_0(L))}{2\pi v_s}, \tag{5.30}$$

where $E_1(L)$ is the ground state energy in the sector with total spin $S = 1$. Unfortunately, it is not possible to compute this quantity, for, as the reader may note, there is no limit value for sound velocity, as the system get larger, to which our results tend.

There are two possible reasons for this failure: our DMRG results are not so much accurate, due to small number of states taken in the renormalization procedure.

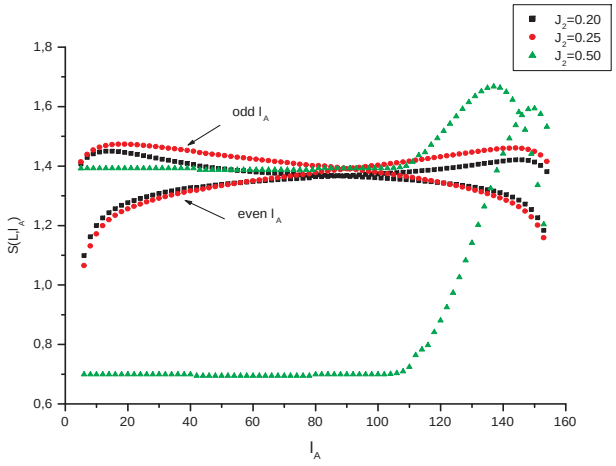

Figure 5.15: The entanglement entropy $S(L, l_A)$ vs l_A for the antiferromagnetic spin-1/2 Heisenberg chain with a single lacking spin site.

The equation of entanglement entropy used do not fit with our system, where next nearest neighbors are introduced. To the best of my knowledge, there are no results published dealing with this situation.

J_2	c^{PBC}
0.05	-0.104281
0.10	-0.229420
0.15	-0.229420
0.20	-0.250276
0.25	-0.166851
0.30	-0.052141
0.35	-0.385843

Table 5.3: Finite-size estimates of the conformal anomaly c^{PBC} in unit of η. $L' = 160$ and $L = 120$.

J_2	$L=18$	$L=26$	$L=32$	$L=42$	$L=60$	$L=120$	$L=160$
0.05	−10.511	−19.496	−34.297	−51.757	−105.79	−426.35	−759.48
0.10	−15.827	−30.274	−49.748	−74.619	−152.34	−616.97	−1100.48
0.15	−8.7075	−15.585	−24.695	−36.371	−74.307	−304.92	−545.71
0.20	−1.97802	−1.49757	−0.69346	0.10242	1.01272	−2.74935	−8.89223
0.25	3.4965	8.8755	16.406	25.844	53.170	212.59	377.64
0.30	2.51876	5.71625	10.058	15.574	31.969	127.69	226.90
0.35	28.413	62.044	108.11	166.31	340.49	1359.77	2415.95

Table 5.4: Sound velocity v_s of a pure spin chain in unit of $1/\eta$ as L and J_2 vary.

5.3.3 Conclusion

The present paper is an attempt to apply the results of conformal field theory, through which estimates of conformal anomaly c^{PBC}, sound velocity v_s and anomalous dimension can be obtained, to antiferromagnetic spin-$\frac{1}{2}$ Heisenberg spin chains with and without a single lacking site, with next nearest neighbors interactions. We have also used the DMRG method to compute ground state energies for relatively long spin chains. Results obtained show that equation for entanglement entropy used below do not fit completely with those corresponding to a spin chain with a single lacking site. This suggests an eventual modification of the expression.

For a pure spin chain, results show that up to $J_2 = 0.35$ the above expression can be used to extract the conformal anomaly. Unfortunately, the obtained results do not show any tendency to limit values as the system get larger, as it is the case of sound velocity.

Chapter 6

Conclusion

In this thesis, I have traced back to its origin a new powerful numerical method, the DMRG, invented by S. White in the beginning of the 1990's to overcome the lack of accuracy that faced Wilson numerical renormalization group when applied to quantum systems. In fact, K. Wilson, inspired by renormalization group methods in particle physics, has succeeded to solve the Kondo problem (resistance minimum). This success has opened the door to the application of the numerical renormalization group to condensed matter problems, especially to more realistic models for magnetic impurities. Unfortunately, this method have failed to give accurate results for models other than impurities problems. Since then, many efforts were made by condensed matter experts to overcome this failure; and one of them have really succeeded to do it. Indeed, S. White, who already worked with K. Wilson, had the idea of introducing the concept of density matrix as a criterion of choosing states to be kept at each renormalization step; and it works!

Since then, an avalanche of applications of this new method to various quantum models have been triggered. The efforts have a twofold goal: in one hand, developing the method itself by trying to extend it to higher dimension systems, combining it with other numerical methods for the calculations of dynamical properties, the study of systems at finite temperature and time-dependent problems, etc; and in the other hand, applying the DMRG to quantum models where the prohibitive numerical cost was established. This made out of the DMRG method one of the most powerful tools for treatment of low-lying states properties of quantum systems, especially one dimensional ones.

Here, I have exposed three works: in the first one, I have extended a simple version of the DMRG method to treat two crossed chains within the simple tight-binding model for disordered systems, suggested by Anderson. My intention was to show that DMRG can be applied to systems other than one dimension. The application gives good results, though it is just a toy model that has no concrete application in real physics; since for such systems, one needs the whole spectrum and not just the low-lying energies. .

The second application is the use of the DMRG method to calculate the ground state energy of spin chains within Heisenberg models, where a single spin site is lacking. To avoid the chain splitting, I have introduced next-nearest neighbors interactions. An extra computing effort, and obviously a extra time were needed to achieve it. The results are then compared to those of spin chains without lacking spin sites.

In my third application, I have attempted to apply the results of conformal field theory, through which estimates of conformal anomaly c^{PBC}, sound velocity v_s and anomalous

dimension can be obtained, to antiferromagnetic spin-$\frac{1}{2}$ Heisenberg spin chains with and without a single lacking site, with next nearest neighbors interactions.

As it has been said, the domain of DMRG application is very vast (there were attempts to apply it even to social and cultural issues!), and then opportunities to explore more and more physical situations through appropriate models are still available. In this spirit, I plan to focus my attention in applying DMRG to realistic disordered systems with different kind of disordered (magnetic impurities, lacking sites, etc). The most in sight is to compute the ground state of spin chains with more than one lacking spin site.

I hope that as you finish reading this thesis, you have taken the pleasure to discover a flourishing new numerical method, and you are, at least, aware that it is time to learn more about it, and eventually apply it in your research works.

Appendix A

Density Matrix for Single Particle Systems

Here we show, in the case of a single particle, that the density matrix is equivalent to a simple projection of the wavefunction, used in the superblock method for the tight-binding chain described in Sect.4.

Consider a wavefunction $\psi(k)$, where k runs over the sites of the system, $k = 1, \cdots, L$. We will call sites $1, \cdots, l$ the left block, labeled by i, and sites $l+1, \cdots, L$ the right block, labeled by j. In order to write a single-particle wavefunction in a product form

$$|\psi\rangle = \sum_{ij} \psi_{ij} |i\rangle |j\rangle, \tag{A.1}$$

it is necessary to construct an enlarged basis which includes zero and two particle states. Specifically, we use the basis

$$\begin{array}{c} |0\rangle_L \\ |1\rangle_L = c_1^\dagger |0\rangle_L \\ \vdots \\ |l\rangle_L = c^\dagger |l\rangle_L \end{array} \tag{A.2}$$

for the left block, and similarly for the right block. Here $c_i^\dagger$ creates a particle at site i. Then the wavefunction $\psi(k)$ can be written in matrix form as

$$\psi = \begin{pmatrix} 0 & \psi(l+1) & \cdots & \psi(L) \\ \psi(1) & & & \\ \vdots & & 0 & \\ \psi(l) & & & \end{pmatrix} \tag{A.3}$$

In this matrix, the upper left zero represents the amplitude in the state $|0\rangle_L \otimes |0\rangle_R$. This state is included in the basis but since there is one particle, its coefficient is always zero. The rest of the first column represents the states $|i\rangle_L \otimes |0\rangle_R$, and similarly the rest of the first row represents $|0\rangle_L \otimes |j\rangle_R$. The large lower right block of zeros represents two particle states.

Then the density matrix $\rho_{ii'}$ in matrix form is

$$\rho = \psi\psi^\dagger = \begin{pmatrix} w_R & 0 & 0 & \cdots & 0 \\ 0 & \psi_1\psi_1 & \psi_1\psi_2 & \cdots & \psi_1\psi_l \\ 0 & \psi_2\psi_1 & \psi_2\psi_2 & \cdots & \psi_2\psi_l \\ \cdots & \cdots & \cdots & \ddots & \cdots \\ 0 & \psi_l\psi_1 & \psi_l\psi_2 & \cdots & \psi_l\psi_l \end{pmatrix} \tag{A.4}$$

where $w_R = 1 - w_L = 1 - \sum_{i=1}^{l} |\psi_i|^2$ is the probability that the particle is in the right block. This density matrix has two nonzero eigenvalues, with corresponding eigenvectors $(1\ \ 0 \cdots 0)^T$ and $w_L^{-1/2}(\psi_1 \cdots \psi_l)^T$. The first eigenvector does not need to be explicitly treated.

1

Bibliography

[1] Inroduction to the theory of quantized Fields, N.N. Bogoliubov and D.V. Shirkov.

[2] K.G. Wilson, The renormalization group: critical phenomena and the Kondo problem, Rev. Mod. Phys. 47, 4, 773-840 (1975).

[3] Philippe Nozieres. In M. Krusius and M. Vuorio, editors, Proc. 14th Int. Conf. Low Temperature Physics, page 339, Amsterdam, 1975. North-Holland.

[4] A. C. Hewson, *The Kondo problem to Heavy problem* (Cambridge Univ. Press, Cambridge 1993).

[5] W. J. de Haas, J. H. de Boer and van den Berg, Physica 1, 1115(1934).

[6] J. Kondo. Progr. Theor. Phys., 37:32, 1964.

[7] Hohenberg, P.C. Kohn, W. (1964). Phys. Rev. B 136, 864.

[8] H. R. Krishna-murthy, J.W. Wilkins and K. G. Wilson, Phys. Rev. B 21, 100(1980); *ibid*. 211 1044 (1980).

[9] L. P. Kadanoff: Physics 2 (1965) 263.

[10] K. G. Wilson and J. Kogut: Phys. Rep. 12 C (1974) 75

[11] T. W. Burkhardt and J. M. J. van Leeuwen: Real-Space Renormalization, Topics in Current Physics vol.30, (Springer, Berlin, 1982).

[12] L.P. Kadanoff, Variational principles and approximate renormalization group calculations, Phys. Rev. Lett. 34, 16, 1005-8, (1975)

[13] L.P. Kadanoff, A. Houghton, Numerical evaluation of the critical properties of the two dimensional Ising model, Phys. Rev. B 11, 1, 377-386 (1975)

[14] N. Goldenfeld, Renormalization Group in Critical Phenomena (Addison-Wesley, Reading) (1994).

[15] Bray, J.W. and Chui, S.T., Phys. Rev. B 19, 4876 (1979).

[16] T. Xiang and G.A. Gehring, J.Magn. Magn. Mater. 104-107, 861 (1992); T. Xiang and G.A. Gehring (unpublished).

[17] P.A. Lee, Phys. Rev. Lett. 42, 1492 (1979).

[18] C. Y. Pan and X. Chen, Phys. Rev. B 36, 8600 (1987)

[19] M. D. Kovarik, Phys. Rev. B 41, 6889 (1990)

[20] S.R. White, How it all began, in Density-Matrix Renormalization ed. por I. Peschel et al. (Dresden conference in 1998), Springer (1999).

[21] S.R. White and R.M. Noack. Density Matrix Formulation for Quantum Renormalization Groups. Phys. Rev. Lett. 69, 2863 (1992).

[22] R.P. Feynman, Statistical Mechanics: A Set of Lectures, Benjamin (1972).

[23] S. R. White, Phys. Rev. B 48 10345 (1993)

[24] S.R. White. Real-Space Quantum Renormalization Groups. Phys. Rev. Lett. 68, 3487 (1992).

[25] M. Boman and R.J. Bursill. Phys. Rev. B57, 15167 (1998).

[26] Y. Honda and T. Horiguchi. Phys. Rev. E56, 3920 (1997).

[27] L.G. Caron and S. Moukouri. Phys. Rev. Lett. 76, 4050 (1996).

[28] I. Peschel, X. Wang, M. Kaulke and K. Hallberg, eds., *Density-matrix renormalization: a new numerical method in physics* (Springer-Verlag, Berlin, Heidelberg, 1999).

[29] S. Kneer, Diploma Thesis, Universitat Wurzburg (1997)

[30] G. Bediirftig, B. Brendel, H. Frahm and R.M. Noack, Phys. Rev. B 58, 10225 (1998).

[31] X.Q. Wang and S. Mallwitz, Phys. Rev. B 48, R492 (1996).

[32] S.J. Qin,X.Q. Wang, Lu Yu, Phys. Rev. B 56, R14251 (1997).

[33] S.R. White, Phys. Rev. Lett.77, 3633 (1996).

[34] S. Liang, Phys. Rev. B 49, 9214 (1994).

[35] A. Klümper, R. Raupach and F. Schönfeld. Phys. Rev. E56, 3920 (1997).

[36] S. R. White and D. A. Huse: Phys. Rev. B48 (1998) 3844

[37] E. S. Sorensen and I. Affleck: Phys. Rev. Lett 71 (1993) 1633; Phys. Rev. B49 (1994) 15771; Phys. Rev. B 49, 13235 (1994).

[38] K. Hida: J. Phys. Soc. Jpn. 64 (1995) 4896.

[39] S. R. White and I. Affleck, Phys. Rev. B 54 (1996).

[40] H. Otsuka, Phys. Rev. B 53 (1996) 14004.

[41] C. C. Yu and S. R. White: Phys. Rev. Lett. 71 (1993) 3866.

[42] R. M. Noack, S. R. White and D. J. Scalapino: Phys. Rev. Lett 73 (1994) 882.

[43] N. Shibata, T. Nishino, K. Ueda and C. Ishii: Phys. Rev. B53 (1996) R8828.

[44] T.-K. Ng, S. Qin and Z.-B. Su, Phys. Rev. B 54, 9854 (1996).

[45] R. J. Bursill, T. Xiang and G. A. Gehring, J. Phys. A - Math. Gen. 28, 2109 (1995).

[46] G. Fáth and J. Sólyom, Phys. Rev. B 51, 3620 (1995).

[47] U. Schollwck and T. Jolicoeur, Europhys. Lett. 30, 493 (1995).

[48] U. Schollwck, O. Golinelli and T. Jolicoeur, Phys. Rev. B 54, 4038 (1996).

[49] X. Wang, S. Qin and L. Yu, Phys. Rev. B 60, 14529 (1999).

[50] Y. Kato and A. Tanaka, J. Phys. Soc. Jpn. 63, 1277 (1994).

[51] R. Bursill, G. A. Gehring, D. J. J. Farnell, J. B. Parkinson, T. Xiang and C. Zeng, J. Phys. C 7, 8605 (1995).

[52] R. Chitra, S. Pati, H. R. Krishnamurthy, D. Sen and S. Ramasesha, Phys. Rev. B 52, 6581 (1995).

[53] , S. Pati, R. Chitra, D. Sen, H. R. Krishnamurthy and S. Ramasesha, Europhys. Lett. 33, 707 (1996)

[54] , S. Pati, R. Chitra, D. Sen, S. Ramasesha and H. R. Krishnamurthy, J. Phys. Cond. Mat. 9, 219 (1997).

[55] S. Watanabe and H. Yokoyama, J. Phys. Soc. Jpn. 68, 2073 (1999).

[56] R. Roth and U. Schollwck, Phys. Rev. B 58, 9264 (1998).

[57] Jie Ren and Shiqun Zhu, Phys. Rev. A 77, 034303 (2008).

[58] S. Qin, T.-K. Ng and Z.-B. Su, Phys. Rev. B 52, 12844 (1995).

[59] E. Polizzi, F. Mila and E. S. Sorensen, Phys. Rev. B 58, 2407 (1998).

[60] . Legeza and J. Sólyom, Phys. Rev. B 59, 3606 (1999).

[61] A. Juozapavicius, S. Caprara and A. Rosegren, Phys. Rev. B 60, 14771 (1999).

[62] K. Hida, J. Phys. Soc. Jpn. 65, 895 (1996), J. Phys. Soc. Jpn. 66, 330 (1997), J. Phys. Soc. Jpn. 66, 3237 (1997), Phys. Rev. Lett. 83, 3297 (1999).

[63] F. Schnfeld, G. Bouzerar, G. S. Uhrig and E. Mller-Hartmann, Eur. Phys. J. B 5, 521 (1998).

[64] K. Hida, J. Phys. Soc. Jpn. 68, 3177 (1999).

[65] S. K. Pati, S. Ramasesha and D. Sen, Phys. Rev. B 55, 8894 (1997), J. Phys. Condens. Mat. 9, 8707 (1997).

[66] L. Campos Venuti, E. Ercolessi, G. Morandi, P. Pieri and M. Roncaglia, *Spin chains in an external magnetic field. Closure of the Haldane gap and effective field theories*, cond-mat/9908044.

[67] J. Lou, X. Dai, S. Qin, Z. Su and L. Yu, Phys. Rev. B 60, 52 (1999).

[68] E. S. Srensen and I. Affleck, Phys. Rev. B 51, 16115 (1995).

[69] R. J. Bursill, R. H. McKenzie and C. J. Hamer, Phys. Rev. Lett. 83, 408 (1999).

[70] 32 A. Drzewiński and J. M. J. van Leeuwen, Phys. Rev. B 49, 403 (1994), A. Drzewiński and R. Dekeyser, Phys. Rev. B 51, 15218 (1995).

[71] R. J. Bursill and F. Gode, J. Phys. Condens. Mat. 7, 9765 (1995).

[72] K. A. Hallberg, P. Horsch and G. Martínez, Phys. Rev. B 52, R719 (1995).

[73] K. Hallberg, X. Q. G. Wang, P. Horsch and A. Moreo, Phys. Rev. Lett. 76, 4955 (1996).

[74] T. Hikihara and A. Furusaki, Phys. Rev. B 58, R583 (1998).

[75] C. Zhang, E. Jeckelmann, and S. R. White, Phys. Rev. Lett. 80, 2661 (1998).

[76] A. Weie, H. Fehske, G. Wellein, and A. R. Bishop, Phys. Rev. B 62, R747 (2000).

[77] B. Friedman, Phys. Rev. B 61, 6701 (2000).

[78] Y. Nishiyama, Eur. Phys. J. B 12, 547 (1999).

[79] H. Wong and Zhi-De Chen, Phys. Rev. B 77, 174305 (2008).

[80] T. Sugihara, Nuclear Physics B (Proc. Suppl.) 140 (2005) 791?793.

[81] S. Rapsch, U. Schollwck and W. Zwerger, Europhys. Lett., 46 (5), pp. 559-564 (1999).

[82] T. D. Khner, S. White and H. Monien, Phys. Rev. B 61, 12474 (2000).

[83] N. Shibata and K. Ueda, J. Phys.: Condens. Matter 11 (1999) R1-R30.

[84] T. Xhiang: Phys. Rev. 53 (1996) R10445.

[85] S. Nishimoto, E. Jeckelmann, F. Gebhard and R. M. Noack, Phys. Rev. B 65, 165114-1 (2002).

[86] T. Xiang, J. Lou and Z. Su, Phys. Rev. B 64, 104414 (2001).

[87] S. R. White, Phys. Rev. Lett. 77, 3633 (1996).

[88] S. Liang and H. Pang, Phys. Rev. B 49,9214 (1994).

[89] P. Henelius, Phys. Rev. 60, 9561 (1999).

[90] S. Moukouri, L. G. Caron, Phys. Rev. B 67, 092405 (2003).

[91] K. Okunishi and T. Nishino, Prog. Theor. Phys. 103 (2000) 541.

[92] T. Nishino, K. Okunishi, Y. Hieida, N. Maeshima and Y. Akutsu, Nucl. Phys. B 575 (2000) 504.

[93] M. Suzuki and M. Inoue: Prog. Theor. Phys. 78 (1987) 787.

[94] T. Nishino: J. Phys. Soc. Jpn. 64 (1995) 3598.

[95] R. J. Bursill, T. Xiang and G. A. Gehring, J. Phys: Condens. Matter 8 (1996) L583.

[96] X. Wang and T. Xiang, Phys. Rev. B 56 (1997) 5061.

[97] T. Xiang, Phys. Rev. B 58 (1998) 9142.

[98] N. Shibata, J. Phys. Soc. Jpn. 66 (1997) 2221.

[99] N. Shibata, B. Ammon, M. Troyer, M. Sigrist and K. Ueda, J. Phs. Soc. Jpn, 67, (1998) 1086-1089.

[100] N. Shibata, J. Phys. A: Math. Gen. 36 (2003) R381-R410.

[101] Hanbin Pang, H. Akhlaghpour, and M. Jarrell, Phys. Rev. B 53, 5086 (1996).

[102] E. Jeckelmann, Phys. Rev. B 66, 045114 (2002), E. Jeckelmann, Prog.Theor. Phys.Suppl. No. 176, (2008).

[103] P. Schmitteckert, Phys. Rev. B 70, 121302(R) (2004).

[104] U. Schollwck, Rev. Mod. Phys. 77, 259 (2005).

[105] M. A. Cazalilla, J. B. Martson, Phys. Rev. Lett 88, 256403 (2002).

[106] S. R. White and A. E. Feiguin, Phys. Rev. Lett 93, 076401 (2004).

[107] Luis G. G. V. Dias da Silva, F. Heidrich-Meisner, A. E. Feiguin, C. A. Bsser, G. B. Martins, E. V. Anda and E. Dagotto,Phys. Rev. B 78, 195317 (2008).

[108] C. Guo,A. Weichselbaum, S. Kehrein, T. Xiang and J. von Delft, Phys. Rev. B 79, 115137 (2009).

[109] S. Langer, F. Heidrich-Meisner, J. Gemmer,I. P. McCulloch and U. Schollwck, Phys. Rev. B 79, 214409 (2009).

[110] K. A. Al-Hassanieh, A. E. Feiguin, J. A. Riera, C. A. Busser, and E. Dagotto, Phys. Rev. B 73, 195304 (2006).

[111] S. Kirino, T. Fujii, J. Zhao and K. Ueda, J. Phys. Soc. Jpn. 77, 084704-1, (2008).

[112] G. Fano, F. Ortolani, and L. Ziosi, J. Chem. Phys. 108, 9246 (1998).

[113] G. L. Bendazzoli and S. Evangelisti, G. Fano, F. Ortolani, and L. Ziosi, J. Chem. Phys. 110, 1277 (1999).

[114] M. Das and S. Ramasesha , J. Chem. Sci., Vol. 118, No. 1, (2006) 67?78.

[115] M. Chandross and J. C. Hicks, Syhthetic Metals 102 (1998) 928-929.

[116] S. Daul,1 I. Ciofini, C. Daul, S. R. White, International Journal of Quantum Chemistry, Vol. 79, 331?342 (2000).

[117] D. Bohr, P. Schmitteckert and P. Wlfle, Europhys. Lett., 73 (2), pp. 246?252 (2006).

[118] Daniel J. García, K. Hallberg and M. J. Rozenberg, PRL 93, 246403 (2004).

[119] S. Nishimotoa,F. Gebhard and E. Jeckelmann, Physica B 378?380 (2006) 283?285.

[120] N. Shibata and D. Yoshioka, Phys. Rev. Lett 85, 5755 (2001).

[121] J. Dukelsky and G. Sierra, Phys. Rev. Lett 83, 172 (1999).

[122] I. P. McCulloch and M. Gulácsi, Europhys. Lett., 57 (6), pp. 852?858 (2002).

[123] A. I. Tóth, C. P. Moca, . Legeza and G. Zaránd, Phys. Rev. B 78, 245109 (2008).

[124] G. Fáth and M. Sarvary, Physica A 348, 611-629 (2005).

[125] M. A. Martín-Delgado and G. Sierra: Int. J. Mod. Phys A11 (1996) 3145

[126] M. A. Martín-Delgado, J. Rodriguez-Laguna and G. Sierra: Nuc. Phys. B473 (1996) 685.

[127] M.A. Martín-Delgado, J. Rodriguez-Laguna and G. Sierra, Nucl. Phys. B 601 [FS] (2001) 569?590.

[128] F. Verstraete, D. Porras, and J. I. Cirac, Phys. Rev. Lett 93, 227205 (2004).

[129] S. Rommer and S. stlund, Phys. Rev. B 55, 2164 (1997).

[130] I. P. McCulloch, J. Stat. Mech: Theor. Exper, doi:10.1088/1742-5468/2007/10/P10014.

[131] H. Saberi, A. Weichselbaum and J. von Delft, Phys. Rev. B 78, 035124 (2008).

[132] F. Verstraete and J. I. Cirac, Phys. Rev. B 73, 094423 (2006).

[133] A. Holzner, A. Weichselbaum and J. von Delft, Phys. Rev. B 81, 125126 (2010).

[134] J. Hubbard, Proc. Roy. Soc. A276, 238 (1963); A277, 237 (1964).

[135] P. W. Anderson, Phys. Rev. 115, 2 (1959).

[136] E. H. Lieb and F. Y. Wu, Phys. Rev. Lett. 20, 1445 (1968).

[137] H. Schulz, J. Phys. C: Solid State Phys. 18, 581 (1985).

[138] M. Imada, A. Fujimori, and Y. Tokura, Rev. Mod. Phys. 70, 1039 (1998).

[139] B. Brendel, *Numerical and analytical analysis of low-dimensional strongly correlated electron systems*, Ph.D. dissertation , Würzburg (1999), unpublished thesis.

[140] S. Andergassen et al, Phys. Rev B 73, 045125 (2006).

[141] R. Noack, S. R. White and D. J. Scalapino, Physica C 270, 281-296 (1996).

[142] S. Danl, Ph.D. dissertation, Universit de Fribourg, 1998, unpublished thesis.

[143] J. M. Carter and A. MacKinnon, Phys. Rev B 72, 024208 (2005)..

[144] B. J. Powell, An introduction to e.ective low-energy Hamiltonians in condensed matter physics and chemistry, arXiv:0906.1640 v6.

[145] Eric Jeckelmann, Phys. Rev. Lett. 89, 236401 (2002).

[146] Dan Bohr, M.Sc. Thesis, Technical University of Denmark , (2004) unpublished thesis.

[147] A. L. Fetter and J. D. Walecka, *Quantum theory of many-particle systems* (McGraw-Hill, New York, 1971).

[148] L. Onsager, Phys. Rev. 65 (1944) 117.

[149] Ausrius Juozapavicius, Doc. Dissertation, Royal institute of Technology, Stockholm, Sweden (2001) unpublished thesis.

[150] J. R. Schrieffer and P. A. Wolff, Phys. Rev. 149, 491 (1966).

[151] S. Caprara and A. Rosengren, Europhys. Lett. 39, 55 (1997).

[152] S. Moukouri and L. G. Garon, Phys. Rev. B 52, R15723 (1995).

[153] J. C. Bonner and M. E. Fisher, Phys. Rev, Vol. 135, A640 (1964).

[154] J. Sølyom and T.A.L. Ziman, Phys. Rev. B 30, 1980 (1984).

[155] R. Botet, R. Jullien and M. Kolb, Phys. Rev. B 28, 3914 (1983).

[156] M. Niel et al., Physics 86-88B, 702 (1977).

[157] H. Bethe, 2. Physik 71, 205 (1931).

[158] L. Hulthn, Arkiv. Mat. Astron. Fysik 26 A, No. ll(1938).

[159] E. Lier, T. Schultz, and D. Mattis, Annals of Physics: 16, 407-466 (1961).

[160] Curtis A. Doty and Daniel S. Fisher, Phys. Rev B, 45 2167 (1992).

[161] M. Laukamp, *Computational Study of ZN-doped Quantum Spin Chains and Ladders*, PhD thesis (1998).

[162] Andr L. Malvezzi, Brazilian Journal of Physics, vol. 33, no. 1, March, (2003).

[163] O. Legeza and G. Fáth, Phys. Rev. B 53, 14349 (1996)

[164] J. Eising, *Linear Algebra*, Institut for Matematik -Danmarks Tekniske Universitet, 2nd edition, 1997.

[165] E. R. Gagliano and C. A. Balseiro, , Phys.Rev.Lett. 59(26), 2999-3002 (1987)

[166] K. Hallberg, Phys.Rev.B. 52(14), 9827-9830 (1995).

[167] Naokazu Shibata,J.Phys.A: Math Gen, vol 36,issue 37 (2003).

[168] T.Xiang et al., Phys. Rev. B 64, 104414 (2001).

[169] Tomotoshi Nishino, J. Phys.Soc.Japan, vol 65,issue 4 (1996)

[170] S. Moukouri et al., Phys. Rev. B 67, 092405 (2003).

[171] P. Henelius, Phys. Rev. B 60 9561 (1999).

[172] S.White, Phys. Rev. Lett. 77, 3633 (1996).

[173] M.A. Martin-Delgado, G. Sierra and R.M. Noack, J.Phys.A: Math Gen, vol 32,issue 33 (1999).

[174] P. Anderson, Phys. Rev. 109, 1492 (1958).

[175] B.I. Shklovskii et al., Phys. Rev. B 47, 11487 (1993)

[176] V. Uski, Phys.Rev.B 62 R7699 (2000).

[177] D. Belitz and T. R. Kirkpatrick, Rev. Mod. Phys. 66,261 (1994).

[178] E. Abrahams, et al., Phys. Rev. Lett. 42, 673 (1979).

[179] Lee P A and Stone D A Phys. Rev. Lett.55 1622 (1985).

[180] M. Schreiber, Phys. Rev. B 31, 6146 (1985).

[181] C.M. Soukoulis, E.N. Economou, Phys. Rev. Lett 52, 565 (1984).

[182] M. Hase, I. Terasaki, Y. Sasago, K. Uchinokura, and H. Obara, Phys. Rev. Lett. 71 4059 (1993).

[183] Y. Uchiyama, Y. Sasago, I. Tsukada, K. Uchinokura, A. Zheludev, T. Hayashi, N. Miura, and P. Boni, Phys. Rev. Lett. 83 632 (1999).

[184] J.C Bonner and M.E. Fishers, Phys. Rev. 135 A640 (1964).

[185] K.Hida, J. Phys. Soc. Jpn. 65 330 (1996).

[186] K.Hida, J. Phys. Soc. Jpn. 65 895 (1996).

[187] K. Majumda and D. K. Ghosh, 1969a, J. Math. Phys. 10 (1969) 1388; ibid 1399.

[188] C. K. Lai, J. Math. Phys. 15 (1974) 1675; B. Sutherland, Phys. Rev. B 12 3795 (1975).

[189] M. Kaburagi et al, J. Phys Soc. Jpn. 72 Suppl. B pp. 135 (2003).

[190] T. A. Costi, P. Schmitteckert, J. Kroha and P. Wolfle, Phys. Rev. Lett. 73 (1994) 1275; S. Eggert and I. Affleck, Phys. Rev. Lett. 75 (1995) 934; E. S. Srensen and I. Affleck, Phys. Rev. B 51 (1995) 16115; X. Q. Wang and S. Mallwitz, Phys. Rev. B 53 (1996) R492; W. Wang, S. J. Qin, Z. Y. Lu, L. Yu and Z. B. Su, Phys. Rev. B 53 (1996) 40.

[191] P. Schmitteckert and U. Eckern, Phys. Rev. B 53 (1996) 15397.

[192] C. Schuster and U. Eckern, Ann. Phys. (Leipzig)8 (1999)5,507.

[193] K. Wilson, Rev. Mod. Phys. 47 (1975) 773.

[194] D.C. Mattis, *The theory of magnetism made simple*,World scientific,(2006)

[195] F. D. Haldane, Phys. Rev. B 25, R4925 (1982).

[196] T. Tonegawa and I. Harada, J. Phys. Soc. Jpn. 56, 2153 (1987).

[197] K. Nomura and K. Okamoto, Phys. Lett. A 169, 433(1992).

[198] R. Bursill, G. A. Gehring, D. J. J. Farnell, J. B. Parkinson, T. Xiang, and C. Zeng, J. Phys: Condens. Matter 7, 8605 (1995).

[199] K. Okamoto and K. Nomura, Phys. Lett. A 169 (1992) 433; K. Nomura and K. Okamoto, J. Phys. Soc. Japan 62 (1993) 1123; K. Nomura and K. Okamoto, J. Phys. A 27 (1994) 5773

[200] S. R. White and I. Affleck, Phys. Rev. B 54, 9862 (1996).

[201] P. Zanardi and N. Paunkovic, Phys. Rev. E 74, 031123(2006)

[202] A. Langari and S. Mahdavifar, Phys. Rev. B 73, 1 (2006).

[203] G.Chiara et al, J. Comput.Theor.Nanosci, 5, 1277-1288 (2008).

[204] K. Hallberg, Adv. Phys, vol 55, issue 5-6,477-526 (2006).

[205] G. Benenti, G. Casati, and G. Strini, *Principles of Quantum Computation and Information*, Vol.2 (World Scientific, 2007).

[206] P. Calabrese and J. Cardy, J. Stat. Mech. P06002 (2004).

[207] C. Holzhey, F. Larsen, and F. Wilczek, Nucl. Phys. B424, 443 (1994).

[208] I. Affleck and A. W. W. Ludwig, Phys. Rev. Lett. 67, 161 (1991).

[209] J. C. Xavier, Phys. Rev. B 81, 244404 (2010).

[210] P. Ginsparg, *Applied Conformal Field Theory* (Elsevier Science Publisher, 1989).

[211] P. Di Francesco, P. Mathieu, and D. Senechal, *Conformal Field Theory* (Springer, 1999).

[212] H. W. J. Blöte, J. L. Cardy, and M. P. Nightingale, Phys. Rev. Lett. 56, 742 (1986).

[213] I. Affleck, Phys. Rev. Lett. 56, 746 (1986).

[214] J. Cardy, J. Phys. A: Math. Gen. 17, L385 (1984).

[215] J. Cardy, Nucl. Phys. B270, 186 (1986).

Abstract: In 1982, K. Wilson was awarded the Nobel prize for his work on the Kondo problem. He was able to solve it through renormalization group method. Unfortunately, the results were not so encouraging, due to their weak accuracy when used to quantum systems. Many attempts were made by physicists: one of them was Steve White, who succeded, after many attempts, to localize the source of failure of Wilson method. In fact, S. White suggested, in a famous paper published in 1993, to use the density matrix concept, which, apparently, helps to choose the ''best'' states that can represent a block as part of a superblock. And it works!

Since then, the Density Matrix Renormalization Group (DMRG) has become a powerful tool to investigate the ground state properties of a large panel of quantum systems. The method was also combined to other numerical methods to better understand the behaviour of those systems.

Like any other numerical method, DMRG has its own limitations: the most in sight is that it was firstly designed to deal with 1-dimensional systems; even though, attempts were, later, made to extend it to higher dimensions.
Keywords: **Renormalization group, disordered systems, spin chains.**

Résumé: En 1982, Kenneth Wilson a reçu le prix Nobel pour avoir résolu, à l'aide de la méthode de groupe de renormalisation, le problème de Kondo. Malheureusement, les résultats n'étaient pas si encourageants une fois la méthode appliquée à des systèmes quantiques, à cause de leurs faibles précisions. Pour y remédier, plusieurs physiciens se sont mis à la besogne. Parmi eux, Steve White, qui est parvenu, après plusieurs tentatives, à déceler la source du problème. En effet, S. White a suggéré en 1993, dans un article, devenu célébre depuis, d'utiliser le concept de la matrice densité, qui permet de choisir les états représentant le mieux un bloc de spins, lors de la construction d'un superbloc.

Depuis, la méthode de groupe de renormalisation par la matrice densité est devenue un outil puissant dans l'étude des propriétés de l'état fondamental d'une panoplie de systèmes quantiques. La méthode est aussi combinée à d'autres méthodes numériques pour mieux comprendre le comportement physique de ces systèmes.

Comme toute méthode numérique ayant ses propres limites, la présente méthode ne fait pas exception. En effet, son application exclusive à des systèmes unidimensionnels était de sa propre nature, et présentait un inconvénient majeur pour le traitement des systèmes plus réalistes; bien que beaucoup d'effort a été fait dans ce sens.
Mots clés: **Groupe de renormalisation, système désordonné, chaines de spins.**

ملخص :

في سنة 1982 حصل كينيث ولسون على جائزة نوبل للفيزياء على أعماله في حل مسألة كوندو مستعينا بطريقة زمرة أعادة التسوية . لسوء الحظ لم تكن النتائج مشجعة عند تطبيق هذه الطريقة في دراسة الأنظمة الفيزيائية الكمية بسبب قلة دقتها .لذلك انكب كثير من العاملين في الحقل على ايجاد الحل .و لقد كان من بين هؤلاء ستيف وايت الذي استطاع أن يحدد مكمن الخلل في طريقة ويلسون فقام باقتراح أن يستعان بمبدأ مصفوفة الكثافة الذي يمكن من أختيار أفضل للمدارات التي تمثل مجموعة من السبينات عند تركيب مجموعة أكبر منها.

منذ ذلك الحين أصبحت هذه الطريقة من بين أقوى الطرائق في دراسة خصائص المدار القاعدي لكثير من الأنظمة الفيزيائية الكمية . كأي طريقة رقمية أخرى فأن هذه الطريقة لها حدود تطبيقاتها و المتمثلة أساسا في كونها أعدت لدراسة أنظمة أحادية البعد رغم أن جهودا بذلت من أجل تعميم تطبيقها على أنظمة ثنائية أو ثلاثية الأبعاد
الكلمات المفتاحية: زمرة اعادة التسوية, الأنظمة العشوائية, سلسلة السبينات.

Journal of Magnetism and Magnetic Materials 323 (2011) 1855–1859

Contents lists available at ScienceDirect

Journal of Magnetism and Magnetic Materials

journal homepage: www.elsevier.com/locate/jmmm

Ground state properties of a spin chain within Heisenberg model with a single lacking spin site

M. Mebrouki

Laboratoire de Physique Théorique, École préparatoire sciences et techniques, B.P. 230, 13000 Tlemcen, Algeria

ARTICLE INFO

Article history:
Received 5 August 2010
Received in revised form
9 February 2011
Available online 22 February 2011

Keywords:
Heisenberg model
Next nearest neighbors interactions
Exact diagonalization
Density matrix
Spin impurity

ABSTRACT

The ground state and first excited state energies of an antiferromagnetic spin-$\frac{1}{2}$ chain with and without a single lacking spin site are computed using exact diagonalization method, within the Heisenberg model. In order to keep both parts of a spin chain with a lacking site connected, next nearest neighbors interactions are then introduced. Also, the Density Matrix Renormalization Group (DMRG) method is used, to investigate ground state energies of large system sizes; which permits us to inquire about the effect of large system sizes on energies. Other quantum quantities such as fidelity and correlation functions are also studied and compared in both cases.

© 2011 Elsevier B.V. All rights reserved.

1. Introduction

Random effects in low-dimensional antiferromagnetic quantum spin systems have attracted the interest of theoretical and experimental studies in the last decades; see for example [1,2]. Since then, physicists have elaborated theoretical models that capture the essential of physics within a simple fashion. One of the most fundamental and widely studied model, theoretically and later numerically, is the Heisenberg model. In this context, spin chains with random bonds [3–5], frustrated term [6], biquadratic term [7], including all variations that can be explored, are studied. Spin chains with a spin impurity that has a different spin magnitude are also investigated [8]. Spin chains with single [9] as well as randomly distributed [5] impurities and disorder [10,11] are explored. The Kondo model [12] is used to describe a magnetic impurity with spin S interacting locally with a non-interacting conduction electron sea (e.g. rare earth metal alloys and actinide elements).

In the present paper we study a spin chain with a single site non-magnetic atom inserted. It could be also a lacking site. Adding a single non-magnetic impurity to a spin chain compound breaks the chains up to two segments. Our idea is to introduce next nearest neighbors interactions to maintain connection between spin sites at left and right of the "missing" spin. In fact, non-magnetic ions that may be present in a magnetic material serve, among other functions, to stabilize the material and to provide connection to nearby spins with one another [13]. Therefore, the spin-$\frac{1}{2}$ Heisenberg model with next nearest neighbors interactions writes as

$$H=\sum_{i}^{N}[J_1 S_i\cdot S_{i+1}+J_2 S_i\cdot S_{i+2}] \tag{1}$$

where S_i denotes the spin $S=1/2$ operator for lattice site i. Note that for a site with no spin all connection operators with its neighboring sites are omitted in the Hamiltonian.

This model with antiferromagnetic interactions (J_1, $J_2>0$) is well studied [14–17,6]. In fact, the pure spin chain is well known to display a quantum phase transition (Kosterlitz–Thouless transition) [18] from a gapless, translationally invariant state with algebraic spin correlations (the spin fluid phase) to dimer gapful state with exponentially decaying correlations at $\alpha_c\simeq 0.24113$, where $\alpha=J_2/|J_1|$. At $\alpha=0.5$ (the Majumda–Ghosh point) [6], the ground state is exactly solvable. It is a doubly degenerate dimer product of singlet pairs on neighboring sites. In general, the ground state is doubly degenerate for $\alpha>\alpha_c$. For large J_2 ($\alpha>0.5$) an incommensurate phase appears in the ground state phase diagram [17,19].

The major part of our task is to compute ground state and eventually first excited states energies and their corresponding eigenstates of the above Hamiltonian. Physical quantities are then computed through appropriate formulas. Computational physics provides us with a panoply of numerical methods that range from the obvious complete diagonalization to variational methods with more or less accuracy and different areas of excellency. We have

E-mail address: m_mebrouki@yahoo.fr

0304-8853/$ - see front matter © 2011 Elsevier B.V. All rights reserved.
doi:10.1016/j.jmmm.2011.02.022

chosen two of them: exact diagonalization and Density Matrix Renormalization Group (DMRG).

2. Exact diagonalization results

2.1. Ground state energy

The exact diagonalization technique is a direct method that provides us with the whole spectrum of a system Hamiltonian and the corresponding eigenvectors. Unfortunately, the order of matrices to be diagonalized for the Heisenberg model grows as 2^N; with N being the number of sites. Therefore, system sizes treated by such method are very restricted and can go, using different symmetries, to more or less 20 sites; which are far from approaching the thermodynamic limit. Fortunately, the study of such systems do not require the whole spectrum, and generally a set of low-lying states, including the ground state and some few excited states are sufficient to describe their properties. Therefore, numerical methods had been elaborated by physicists to focus on those restricted parts of the spectrum with more or less accuracy; such as the earlier Lanczos method and the recently developed method, the DMRG. Nevertheless, the exact diagonalization still have its relevance, especially for those properties that do not depend on the system size.

Thus, we diagonalize matrices for spin chains with $N=6$, 8, 10, 12 using periodic boundary conditions. The use of these boundaries is governed by the fact that changing the position of the lacking site in the chain does not affect the energy spectrum of a chain with a single lacking site. The value of J_2 goes from 0.05 to 0.55 with a step of 0.05. This is useful to sweep a large interval where the well-known system undergoes quantum phase transitions. This allows us to figure out how the system is affected when a spin site is missed. The value of J_1 is taken to be unity.

Figs. 1 and 2 display the first four lowest energies in function of J_2, for a spin chain without (with) a lacking site, respectively. The chain length is taken to be $N=10$ and J_2 values go from 0.05 to 0.55. The latter interval is thought to contain a critical point of the system [20,18]. In Fig. 1, one can see a nonvanishing gap that appears, as it is the case when $J_2=0.00$. One can also see that the gap is constant until J_2 is around 0.25. Beyond this value the gap is decreasing. Taking into account works that confirm the existence of such a critical point at this value, one can think that the behavior of the gap could be a signature of a spin system that crosses a critical point. In the other hand, Fig. 2 shows that a spin system with a missing site has no gap at all. Actually, the first four low-lying energies including the ground state have the same value. This degeneracy may be due to the frustration of having a short chain (nine sites) with an odd number of spin sites.

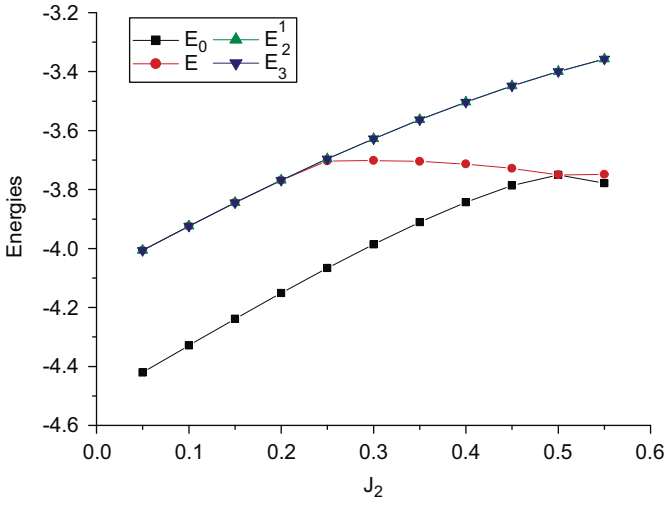

Fig. 1. First four lowest energies as a function of J_2 for a spin chain without a lacking site spin, obtained by exact diagonalization.

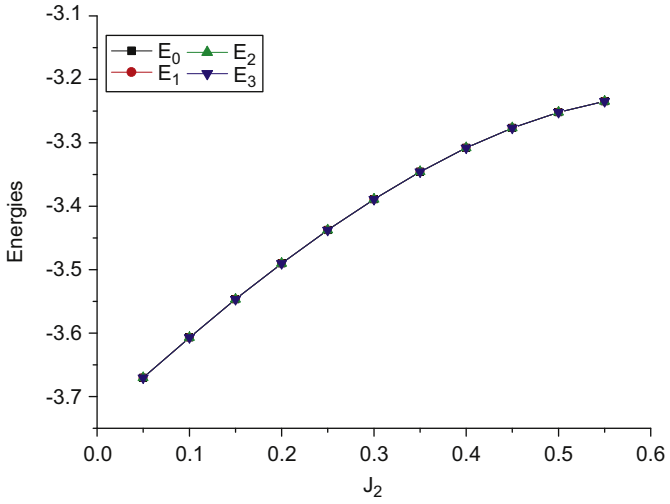

Fig. 2. First four lowest energies as a function of J_2 for a spin chain with a lacking site spin, obtained by exact diagonalization.

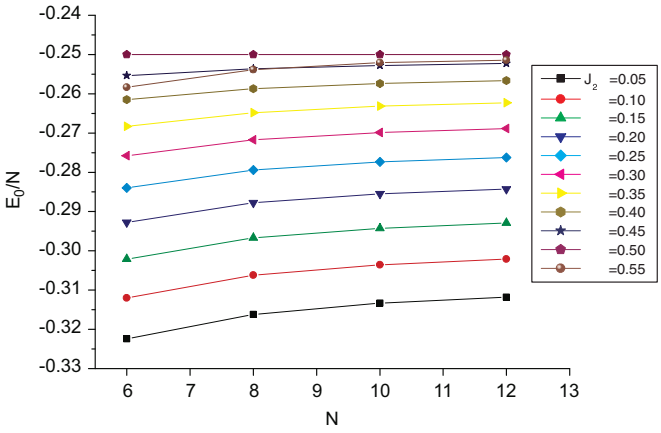

Fig. 3. Exact ground state eigenvalue per site for a spin chain without a lacking site as a function of J_2, obtained by exact diagonalization.

Now, we want to check the variation of the ground state energy per site E_0/N in function of J_2. Thus, Figs. 3 and 4 display E_0/N for spin chains without (with) a lacking site, as J_2 varies from 0.05 to 0.55. Both figures show that, for relative small system sizes (up to 12 sites), the ground state energy per site is increasing (decreasing) as the system size increases. The figures show also that the increasing (decreasing) rate of E_0/N depends on the value of J_2. We remark also that E_0/N increases as J_2 increases to reach a maximum value when $J_2=0.5$ (Majumdar–Gosh point), then it decreases.

As the above results are obtained for small system sizes, this seems to be not so sufficient to make us deciding about the large-N variation of the E_0/N. Therefore, we need to use the DMRG method, which enables us to compute the ground state energy for more long spin chains. This will be explained after we investigate quantum fidelity and correlation functions.

2.2. Quantum fidelity

Obtaining of the ground state eigenvector by exact diagonalization allows us to compute some quantities that characterize behaviors of such systems. The most in sight are the fidelity quantity and correlations functions.

In quantum physics, an overlap between two quantum states usually denotes the transition amplitude from one state to the another. That is the overlap gives unity if two states are exactly the same, while zero if they are orthogonal. Thus, one use the ground state fidelity as a measure of similarity between states. It is defined as the overlap between $|\Psi_0(\lambda)\rangle$ and $|\Psi_0(\lambda+\delta)\rangle$ [20], i.e.

$$F_0(\lambda,\delta) = |\langle \Psi_0(\lambda)|\Psi_0(\lambda+\delta)\rangle| \quad (2)$$

where $\Psi_0(\lambda)$ is the ground state wavefunction of the Hamiltonian corresponding to the parameter λ and δ is a small quantity. In our case, λ is represented by J_2, and $\delta = 2.5 \times 10^{-4}$.

We observe in Fig. 5 that the ground state fidelity for a spin system without lacking spin site is almost a constant and equals to unity for a wide range of the parameter J_2. Our results confirm the fact that critical points of the quantum phase transitions cannot be well characterized by the ground state fidelity for a finite-size system ($N=10$, in our case). In the other hand, for a spin system with a lacking site, fidelity alternates unity and zero values, as J_2 varies. This is a signature of loss of orthogonality between neighboring states over some regions in the interval of J_2. Therefore, the missing spin site breaks the similarity between neighboring states.

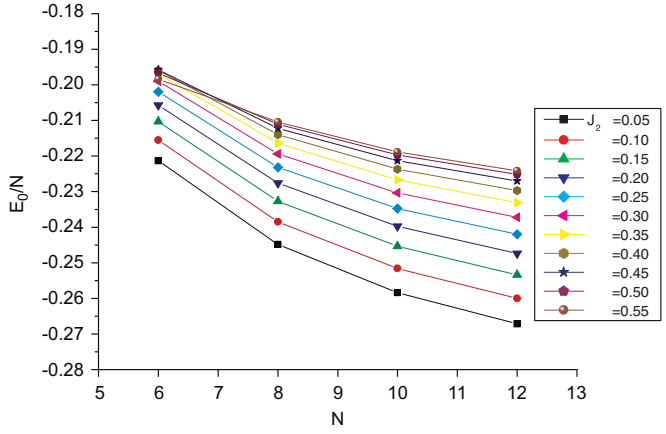

Fig. 4. Exact ground state eigenvalue per site for a spin chain with a lacking site as a function of J_2, obtained by exact diagonalization.

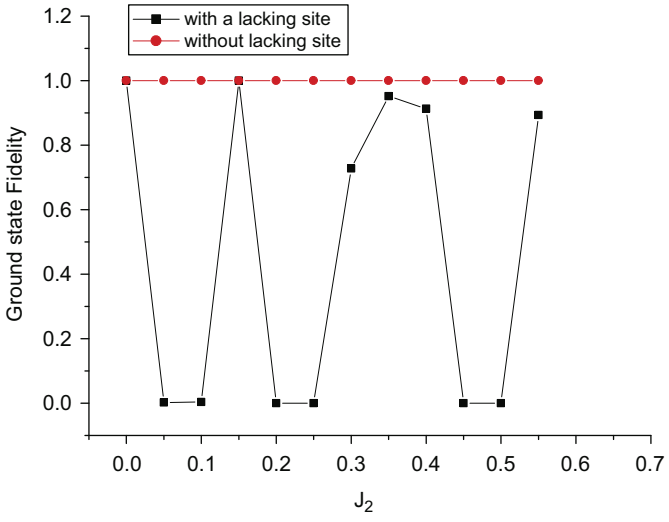

Fig. 5. Ground state fidelity for both 10-sites spin chains (with and without a lacking spin site).

2.3. Correlation functions

We compute also the correlation function $S_i^z S_j^z$ as a function of the distance between spin sites $|i-j|$. The results for a spin system of size $N=10$ without lacking site are shown in Fig. 6. One can see the alternation of signs between odd and even sites: this is a signature of the antiferromagnetic nature of the system. One can see also that results are symmetric: this is a signature of the periodic boundary conditions applied. We also have to note that the above functions present a translational symmetry: they do not depend on position of the spin sites but just on distance between them. This is why we have used the absolute value of distance in Fig. 6.

On the contrary, the system with a missing site does not keep this symmetry. To show this, we have displayed in Fig. 7 the correlation functions for both systems (with and without lacking

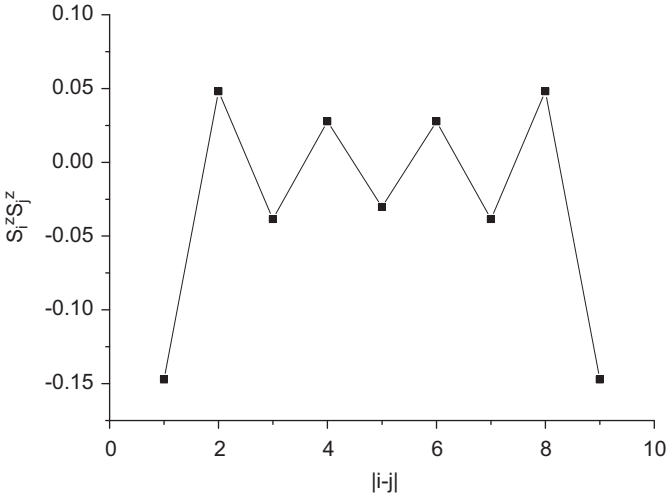

Fig. 6. Correlation function $S_i^z S_j^z$ as a function of the distance between spin sites $|i-j|$ for a 10-sites spin chains without a lacking spin site ($J_2=0.35$).

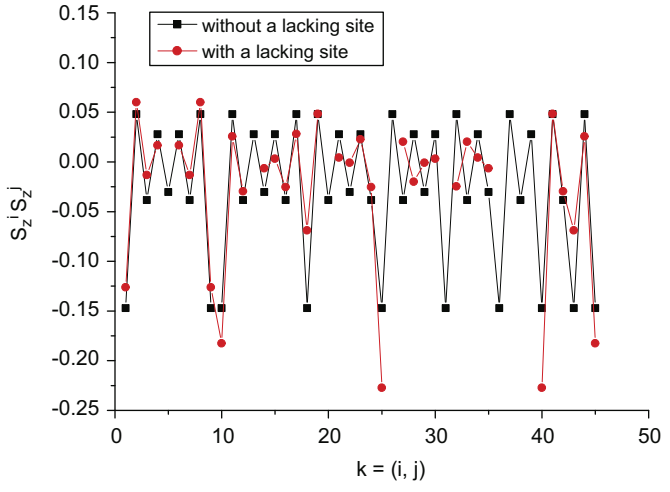

Fig. 7. *Correlation function* $S_i^z S_j^z$ as a function of the couple (i, j) number k for both 10-sites spin chains (with and without a lacking spin site). Spin on the sixth site is missing ($J_2=0.35$).

site) as they vary with the distance $i-j$. The numbers on x-axis denote the distance between sites in the following order: $k \equiv (i,j)$ where $i=1$, $N-1$ and $j=i+1$, N. As an example: $k=4$ represents the distance between $i=1$ and $j=5$, where $k=12$ represents the distance between $i=2$ and $j=4$. For a system without lacking site, the same values are reproduced along the x-axis, whereas the values of $S_i^z S_j^z$ are changing for the system with a missing site (the spin on sixth site is missing). This can be explained as a breaking of the translational symmetry for that quantity.

3. DMRG results

The Density Matrix Renormalization Group (DMRG), developed by White [21], is a powerful numerical method which allows us to obtain the ground state and low-lying excited state wavefunctions of large-size systems with controlled high accuracy. The basic idea of DMRG algorithm consists in increasing the size of the system while the corresponding Hilbert space is kept constant, using the concept of matrix density to determine what states to be kept. More technical details about the method can be abundantly found in literature, (see for example [22–24]).

As the present spin system contains next nearest neighbors interactions, the use of the DMRG technique requires more computational effort to take into account those interactions; which mean more states to be kept to reach a desired accuracy.

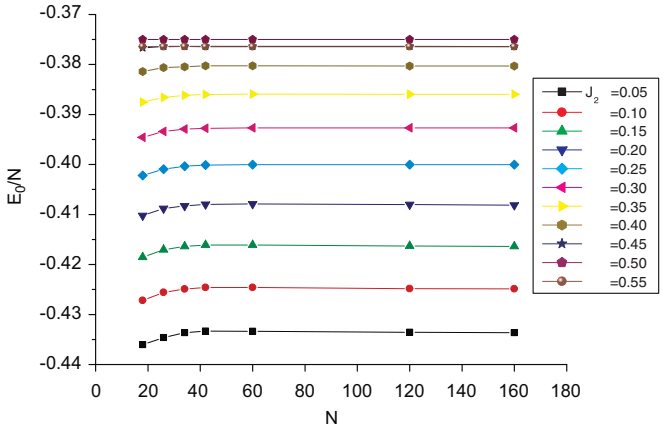

Fig. 8. Ground state energy per site for a spin chain without a lacking site as a function of J_2, obtained by DMRG method.

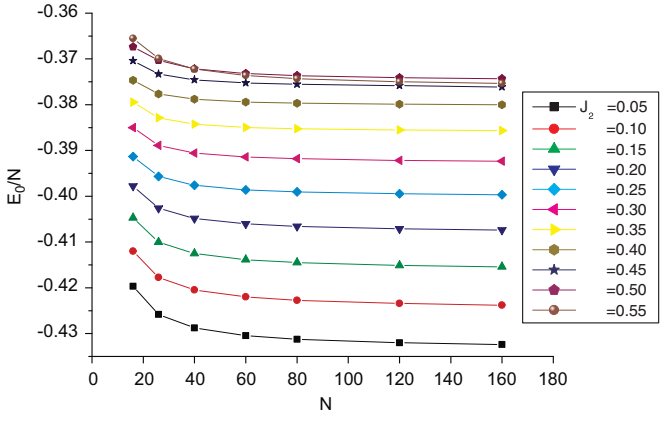

Fig. 9. Ground state energy per site for a spin chain with a lacking site as a function J_2, obtained by DMRG method.

Figs. 8 and 9 display the ground state energies per site for spin chains without (with) a lacking spin site in function J_2. The utmost sizes of spin chains considered are equals to $N=160$, with values of J_2 that go from 0.05 to 0.55 by a step of 0.05.

Our results for both systems show that, for each value of J_2, E_0/N tends to a certain constant value as N gets larger. This is shown in Fig. 10 where the value of $e_{\text{infinity}} = E_0/N$ as a function of J_2 is represented. The symbol "infinity" insinuates the idea of relatively large systems. For both systems, we can see that the J_2-dependency is almost the same, and it is likely linear around the critical point $J_2=0.25$. Note that the observation already done about the increasing (decreasing) of E_0/N as N varies for chains with (without) a spin site lacking is also confirmed with DMRG.

In order to find out a function representing the variation of e_{infinity} with J_2 for both systems, we do a polynomial fit of the above results. In fact, a polynomial fit for a spin system with a lacking site gives

$$e_{\text{infinity}}(J_2) = -0.44157 + 0.19034J_2 - 0.16388J_2^2 + 0.48493J_2^3 - 0.76037J_2^4$$

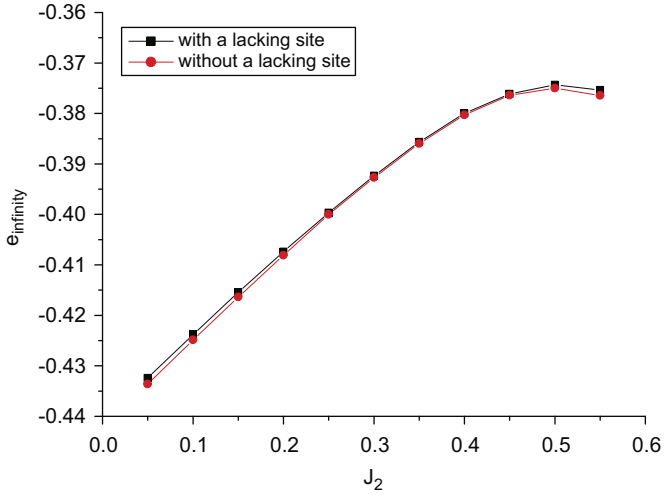

Fig. 10. Variation of e_{infinity} as a function of J_2 for both spin chains (with and without a lacking spin site). Results are obtained using DMRG method.

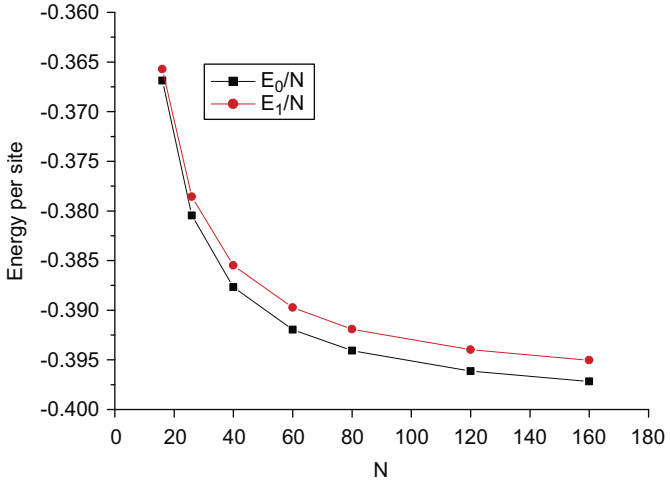

Fig. 11. Variation of E_0/N and E_1/N as a function of the system size N for a spin chain with a lacking spin site, with $J_2=0.25$. Results are obtained using DMRG technique.

For a spin chain without a lacking spin site, it gives

$$e_{\text{infinity}}(J_2) = -0.44284 + 0.19032J_2 - 0.14232J_2^2 + 0.44779J_2^3 - 0.76224J_2^4$$

Finally, we present in Fig. 11 ground state energy E_0/N and first excited energy E_1/N values for a spin chain with a lacking spin site as a function of system size N. J_2 is taken to be equal to 0.25. It is obvious from the figure that between ground state and first excited state appear an energy gap as the spin system gets longer; contrarily to what was found when we treated small sizes by exact diagonalization, and where no energy gap exists. This shows that a spin chain with a lacking site is not intrinsically gapped, as it is the case of a pure spin chain, but it is, actually, the effect of large system size which makes the system gapped.

4. Conclusion

The present paper treats spin chains with next nearest neighbors interactions. Ground states and few low-lying eigenvalues are computed using exact diagonalization technique. Results are then compared with those for a spin chain that "misses" a single spin site. It could be a non-magnetic impurity or just a lacking site, as it is often the case in real materials. Other physical quantities such as quantum fidelity and correlation functions are also computed. In fact, extrapolations of results, using DMRG technique, suggest that both systems are gapped, but they show also that the gap of a spin system without a lacking site is intrinsic, while it is an effect of large system size for a spin chain with a lacking site. The introduction of such distortion affects also the behavior of the eigenstates; since the quantum fidelity alternates zero and one values; which is a signature of loss of similarity of neighbor states. The computation of correlation functions has showed that a lacking site breaks the translational symmetry of a pure spin chain, as it is, actually, well known.

The DMRG technique has also permitted to achieve a ground state energy finite-size scaling which gives us formulas for ground state energy as a function of J_2 and N (spin chain size).

References

[1] M. Hase, I. Terasaki, Y. Sasago, K. Uchinokura, H. Obara, Phys. Rev. Lett. 71 (1993) 4059.
[2] Y. Uchiyama, Y. Sasago, I. Tsukada, K. Uchinokura, A. Zheludev, T. Hayashi, N. Miura, P. Böni, Phys. Rev. Lett. 83 (1999) 632.
[3] J.C. Bonner, M.E. Fishers, Phys. Rev. 135 (1964) A640.
[4] K. Hida, J. Phys. Soc. Jpn. 65 (1996) 330.
[5] K. Hida, J. Phys. Soc. Jpn. 65 (1996) 895.
[6] K. Majumda, D.K. Ghosh, J. Math. Phys. 10 (1969) 1388;
K. Majumda, D.K. Ghosh, J. Math. Phys. 10 (1969) 1399.
[7] C.K. Lai, J. Math. Phys. 15 (1974) 1675;
B. Sutherland, Phys. Rev. B 12 (1975) 3795.
[8] M. Kaburagi, et al., J. Phys. Soc. Jpn. 72 (Suppl. B) (2003) 135.
[9] T.A. Costi, P. Schmitteckert, J. Kroha, P. Wölfle, Phys. Rev. Lett. 73 (1994) 1275;
S. Eggert, I. Affleck, Phys. Rev. Lett. 75 (1995) 934;
E.S. Sørensen, I. Affleck, Phys. Rev. B 51 (1995) 16115;
X.Q. Wang, S. Mallwitz, Phys. Rev. B 53 (1996) R492;
W. Wang, S.J. Qin, Z.Y. Lu, L. Yu, Z.B. Su, Phys. Rev. B 53 (1996) 40.
[10] P. Schmitteckert, U. Eckern, Phys. Rev. B 53 (1996) 15397.
[11] C. Schuster, U. Eckern, Ann. Phys. (Leipzig) 8 (1999) 5.
[12] K. Wilson, Rev. Mod. Phys. 47 (1975) 773.
[13] D.C. Mattis, The Theory of Magnetism Made Simple, World Scientific, 2006.
[14] F.D. Haldane, Phys. Rev. B 25 (1982) R4925.
[15] T. Tonegawa, I. Harada, J. Phys. Soc. Jpn. 56 (1987) 2153.
[16] K. Nomura, K. Okamoto, Phys. Lett. A 169 (1992) 433.
[17] R. Bursill, G.A. Gehring, D.J.J. Farnell, J.B. Parkinson, T. Xiang, C. Zeng, J. Phys.: Condens. Matter 7 (1995) 8605.
[18] K. Okamoto, K. Nomura, Phys. Lett. A 169 (1992) 433;
K. Nomura, K. Okamoto, J. Phys. Soc. Jpn. 62 (1993) 1123;
K. Nomura, K. Okamoto, J. Phys. A 27 (1994) 5773.
[19] S.R. White, I. Affleck, Phys. Rev. B 54 (1996) 9862.
[20] P. Zanardi, N. Paunkovic, Phys. Rev. E 74 (2006) 031123.
[21] S. White, Phys. Rev. Lett. 69 (1992) 2863;
S. White, Phys. Rev. B 48 (1993) 10345.
[22] I. Peschel, X. Wang, M. Kaulke, K. Hallberg (Eds.), Density-matrix Renormalization, Springer, 1998.
[23] G. Chiara, et al., J. Comput. Theor. Nanosci. 5 (2008) 1277.
[24] K. Hallberg, Adv. Phys. 55 (5–6) (2006) 477–526.

Density Matrix Renormalization Group Method applied to two crossed disordered chains within Anderson model

Mohamed Mebrouki
Laboratoire de Physique théorique, B.P. 230, 13000 Tlemcen, Algeria

Abstract : A variation of the Density Matrix Renormalization Group (DMRG) procedure, based on a simplified version suggested by Martin-Delgado et al., is developed to compute low states energies for two crossed chains within the simple tight binding model suggested earlier by P. Anderson. For comparison, our results obtained using the new procedure are presented along with those obtained by exact diagonalization. In order to make clear the procedure, some technical aspects of the implementation of the algorithm are given in detail.
Keywords: reduced density matrix, disordered system, tight-binding model.
PACS numbers: 03.65.-w, 03.65.Ge

I. Introduction

The Density Matrix Renormalization Group (DMRG), developed by S. R. White in 1992 [1], is a powerful numerical method which permits us to obtain the ground-state and low-lying excited states wavefunctions of large-size systems with controlled high accuracy. S.White has considered that a system (block) must be connected to an other block (environment) to form a superblock, and therefore each part contributes to the ground state of the superblock through its own states. The basic idea of the DMRG is to use the concept of density matrix to decide which states from a given block that contribute the more to the wavefunction of the whole system. As the procedure is iterated the size of the system is increasing while the corresponding Hilbert space is kept constant.
Technically, the algorithm consists in a warm up phase where Hamiltonian operators for each block and connection operators in the system are renormalized and then stored to be used later. This is followed by a sweeping procedure which iterates the process on the full system until convergence is reached.
In fact, since its appearance, DMRG has proven a high level of accuracy when dealing with one-dimensional systems, in such a way that it became, in few years, a valuable numerical tool, among other numerical methods, to calculate energy spectrum and other dynamic correlation functions at finite temperatures of interacting 1-d quantum systems.

Still, the DMRG is called to prove its accuracy when applied to 2-d quantum systems and, eventually, 3-d ones.
Thus, various algorithms have been proposed to apply DMRG to two-dimensional quantum systems; see for example [2-7]. Most of these works use mappings on to effective one-dimensional models with long-range interactions, and the standard DMRG method is applied to the effective one-dimensional systems. In this spirit, the present paper is to give a new configuration of the DMRG method to treat a diffusive problem without any mapping: a disordered two-crossed chains system within the very simple tight-binding Anderson model.
Our work is based on an earlier paper [8], where M.A. Martín-Delgado et al. have given a simplified version of White's Density Matrix Renormalization Group (DMRG) algorithm to find the ground state of single-particle quantum mechanics. They solved a discretized version of the single-particle Schrödinger equation, which allows them to obtain very accurate results for the lowest energy levels of a single particle under the action of three potentials: harmonic oscillator, anharmonic oscillator and double-well.
Our contribution consists in replacing the standard configuration, which consists in two connected blocks (system + environment), by a five-blocks system, representing the two crossed chains.

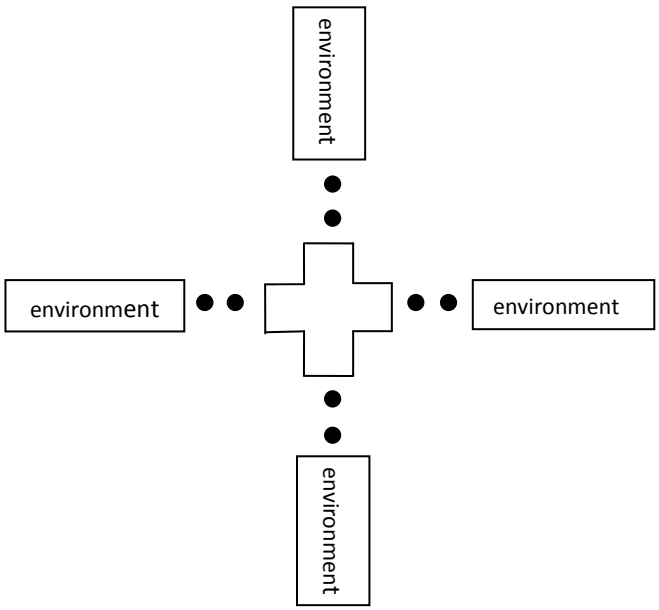

Figure 1: DMRG superblock configuration: five blocks and eight sites to add in each step of the procedure.

 © 2010 The Moroccan Statistical Physical and Condensed Matter Society

II. DMRG applied to two crossed chains

The present implementation consists in five blocks: right, left, upper and down blocks B_l^L, B_l^R, B_l^U and B_l^D with l sites (environment) plus a center block B_m^C with also m sites (system), as it is shown in figure 1.

2.1. Superblock Hamiltonian

In order to treat the $N_E \geq 1$ lowest energy levels, the environment B_l^L, B_l^R, B_l^U and B_l^D must contain N_E degrees of freedom. Clearly, the center block contains $2N_E - 1$ sites. Our choice for numbering sites in the superblock is such the horizontal sites are labeled with odd number from left to right, whereas the vertical sites are labeled with even number starting from up to down. The superblock Hamiltonian H_{SB} is therefore a $(6N_E + 7) \times (6N_E + 7)$ matrix given by

$$H_{SB}\begin{pmatrix}
H_{LU} & -v_L & -v_U & 0 & 0 & 0 & 0 & 0 & 0 & 0 & 0 \\
-v_L^\dagger & h_{CL} & 0 & -1 & 0 & 0 & 0 & 0 & 0 & 0 & 0 \\
-v_U^\dagger & 0 & h_{CU} & 0 & -1 & -v_{CL}^\dagger & 0 & 0 & 0 & 0 & 0 \\
0 & -1 & 0 & h_{CCL} & 0 & 0 & 0 & 0 & 0 & 0 & 0 \\
0 & 0 & -1 & 0 & h_{CCU} & -v_{CU}^\dagger & 0 & 0 & 0 & 0 & 0 \\
0 & 0 & 0 & -v_{CL} & -v_{CU} & H_C & -v_{CR} & -v_{CD} & 0 & 0 & 0 \\
0 & 0 & 0 & 0 & 0 & -v_{CR}^\dagger & h_{CCR} & 0 & -1 & 0 & 0 \\
0 & 0 & 0 & 0 & 0 & -v_{CD}^\dagger & 0 & h_{CCD} & 0 & -1 & 0 \\
0 & 0 & 0 & 0 & 0 & 0 & 0 & 0 & h_{CR} & 0 & -v_R^\dagger \\
0 & 0 & 0 & 0 & 0 & 0 & 0 & 0 & 0 & h_{CD} & -v_D^\dagger \\
0 & 0 & 0 & 0 & 0 & 0 & 0 & 0 & -v_R & -v_D & H_{RD}
\end{pmatrix} \quad (1)$$

where H_{LU} writes:

$$H_{LU} = \begin{pmatrix}
H_L^{11} & 0 & H_L^{12} & 0 & \cdots & H_L^{1N_E} & 0 \\
0 & H_U^{11} & 0 & H_U^{12} & \cdots & 0 & H_U^{N_E 1} \\
H_L^{21} & 0 & H_L^{22} & 0 & \cdots & H_L^{2N_E} & 0 \\
0 & H_U^{21} & 0 & H_U^{22} & \cdots & 0 & H_U^{2N_E} \\
\vdots & \vdots & \vdots & \vdots & \ddots & \vdots & \vdots \\
H_L^{N_E 1} & 0 & H_L^{N_E 2} & 0 & \cdots & H_L^{N_E N_E} & 0 \\
0 & H_U^{N_E 1} & 0 & H_U^{N_E 2} & \cdots & 0 & H_U^{N_E N_E}
\end{pmatrix} \quad (2)$$

H_{LU} is a $2N_E \times 2N_E$ matrix, built up by two embedded matrices H_L and H_U, each one representing the interactions inside the blocks B_L and B_U, respectively. Zeros in the matrix indicate lost links between sites. Thus, H_{LU}^{12}, for example, is equal to zero because there is no link between the first and second sites.

Similarly, H_{RD} writes as

$$H_{RD} = \begin{pmatrix}
H_R^{11} & 0 & H_R^{12} & 0 & \cdots & H_R^{1N_E} & 0 \\
0 & H_D^{11} & 0 & H_D^{12} & \cdots & 0 & H_D^{N_E 1} \\
H_R^{21} & 0 & H_R^{22} & 0 & \cdots & H_R^{2N_E} & 0 \\
0 & H_D^{21} & 0 & H_D^{22} & \cdots & 0 & H_D^{2N_E} \\
\vdots & \vdots & \vdots & \vdots & \ddots & \vdots & \vdots \\
H_R^{N_E 1} & 0 & H_R^{N_E 2} & 0 & \cdots & H_R^{N_E N_E} & 0 \\
0 & H_D^{N_E 1} & 0 & H_D^{N_E 2} & \cdots & 0 & H_D^{N_E N_E}
\end{pmatrix} \quad (3)$$

It represents the interactions inside the blocks B_R and B_D. The symbols h_{CL}, h_{CU}, h_{CR} and h_{CD} represent the added sites, at each iteration, to left, upper, right and down blocks, respectively. Also, h_{CCL}, h_{CCU}, h_{CCR}

 © 2010 The Moroccan Statistical Physical and Condensed Matter Society

and h_{CCD} are the added sites to the center block. The N_E-component column vectors v_L, v_U, v_R and v_D describe the interaction between the B_L, B_U, B_R and B_D and the sites next to them in the superblock. For example, v_L writes as $\left(v_L^1, 0, v_L^2, \cdots, v_L^{N_E}, 0\right)$ and v_U writes as $\left(0, v_U^1, 0, v_L^2, \cdots, 0, v_U^{N_E}\right)$. The $2N_E - 1$-component column vectors v_{CL}, v_{CU}, v_{CR}, and v_{CD} describe the interaction between the center B_C and the sites next to it in the superblock. So that, v_U, for example, writes as $\left(v_{CU}^1, v_{CU}^2, \cdots, v_{CU}^{N_E}\right)$.

Then, the Hamiltonian H_{SB} in Eq.(1) describes the superblock:

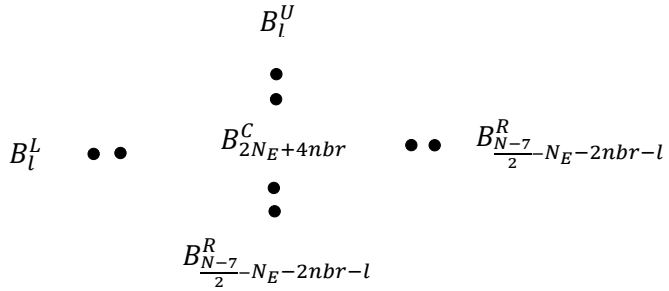

Since the blocks $B_{\{L,U,R,D\}}$ and the block B_C contain N_E and $2N_E - 1$ effective sites, respectively, we need $nbr = \frac{N-6N_E-7}{8}$ warm-up steps to reach the desired system length N. $H_{SB} = H_{SB}^{(l)}$ can be defined for $l = N_E, N_E + 1, \cdots, N_E + nbr$.

2.2 . DMRG truncation

As in the previous section, we have to obtain the N_E lowest eigenstates of H_{SB}, which will be designated as:

$$\left\{\left(a_{L,i}^1, a_{U,i}^1, \cdots, a_{L,i}^{N_E}, a_{U,i}^{N_E}, a_{CL,i}, a_{CU,i}, a_{CCL,i}, a_{CCU,i}, \boldsymbol{a}_{C,i}, a_{CCR,i}, a_{CCD,i}, a_{CR,i}, a_{CD,i}, a_{R,i}^1, a_{D,i}^1, \cdots, a_{R,i}^{N_E}, a_{D,i}^{N_E}\right)\right\}_{i=1}^{N_E}$$

where $\left(a_{L,i}^1, \cdots, a_{L,i}^{N_E}\right)$, $\left(a_{U,i}^1, \cdots, a_{U,i}^{N_E}\right)$, $\left(a_{R,i}^1, \cdots, a_{R,i}^{N_E}\right)$ and $\left(a_{D,i}^1, \cdots, a_{D,i}^{N_E}\right)$ are N_E-component vectors and $\boldsymbol{a}_{C,i}$ is $2N_E - 1$-component vector. For $N_E = 3$, these vectors are then projected onto a set of 3 vectors of the block B_L •, *i.e.*, $\left\{\left(\boldsymbol{a}_{L,i}, a_{CL,i}\right)\right\}_{i=1}^3$, a set of 3 vectors of the block B_U •, *i.e.*, $\left\{\left(\boldsymbol{a}_{U,i}, a_{CU,i}\right)\right\}_{i=1}^3$ and a set of 3 vectors of the block :

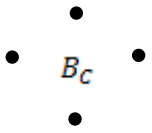

,*i.e.*, $\left\{\left(a_{CCL,i}, a_{CCU,i}, \boldsymbol{a}_{C,i}, a_{CCR,i}, a_{CCD,i}\right)\right\}_{i=1}^3$. These three sets of vectors must be orthonormalized using a Gram-Schmidt orthogonalization procedure and then dividing them by:

$$N_L^i = \sqrt{\left(a_{L,i}^1\right)^2 + \left(a_{L,i}^2\right)^2 + \left(a_{L,i}^3\right)^2 + \left(a_{CL,i}\right)^2}$$
$$N_U^i = \sqrt{\left(a_{U,i}^1\right)^2 + \left(a_{U,i}^2\right)^2 + \left(a_{U,i}^3\right)^2 + \left(a_{CU,i}\right)^2}$$

and

$$N_C^i = \sqrt{\left(a_{CCL,i}\right)^2 + \left(a_{CCU,i}\right)^2 + \left(a_{C,i}^1\right)^2 + \left(a_{C,i}^2\right)^2 + \left(a_{C,i}^3\right)^2 + \left(a_{CCR,i}\right)^2 + \left(a_{CCD,i}\right)^2}$$

respectively.

 © 2010 The Moroccan Statistical Physical and Condensed Matter Society

The new three sets are designated as $\{(\boldsymbol{a}'_{L,i}, a'_{CL,i})\}_{i=1}^{3}$, $\{(\boldsymbol{a}'_{U,i}, a'_{CU,i})\}_{i=1}^{3}$, and

$\{(a'_{CCL,i}, a'_{CCU,i}, \boldsymbol{a}'_{C,i}, a'_{CCR,i}, a'_{CCD,i})\}_{i=1}^{3}$.

If there is no symmetry in the Hamiltonian, right and down matrices have to be renormalized in the same manner. A straightforward generalization of the renormalized block Hamiltonians in [8] yields the new effective Hamiltonians, H'_L and H'_U, and vectors $v'_L$and v'_U; which write, for $N_E = 3$, as:

$$H'_L = \begin{pmatrix} a'^{\mathbf{1}}_{L,1} & a'^{\mathbf{2}}_{L,1} & a'^{\mathbf{3}}_{L,1} & a'_{CL,1} \\ a'^{\mathbf{1}}_{L,2} & a'^{\mathbf{2}}_{L,2} & a'^{\mathbf{3}}_{L,2} & a'_{CL,2} \\ a'^{\mathbf{1}}_{L,3} & a'^{\mathbf{1}}_{L,3} & a'^{\mathbf{1}}_{L,3} & a'_{CL,3} \end{pmatrix} \begin{pmatrix} H_L^{11} & H_L^{12} & H_L^{13} & -v_L^1 \\ H_L^{21} & H_L^{22} & H_L^{23} & -v_L^2 \\ H_L^{21} & H_L^{23} & H_L^{33} & -v_L^3 \\ -v_L^1 & -v_L^2 & -v_L^3 & h_{CL} \end{pmatrix} \begin{pmatrix} a'^{\mathbf{1}}_{L,1} & a'^{\mathbf{1}}_{L,2} & a'^{\mathbf{1}}_{L,3} \\ a'^{\mathbf{2}}_{L,1} & a'^{\mathbf{2}}_{L,2} & a'^{\mathbf{1}}_{L,3} \\ a'^{\mathbf{3}}_{L,1} & a'^{\mathbf{3}}_{L,2} & a'^{\mathbf{1}}_{L,3} \\ a'_{CL,1} & a'_{CL,2} & a'_{CL,3} \end{pmatrix} \tag{4}$$

$$H'_U = \begin{pmatrix} a'^{\mathbf{1}}_{U,1} & a'^{\mathbf{2}}_{U,1} & a'^{\mathbf{3}}_{U,1} & a'_{CU,1} \\ a'^{\mathbf{1}}_{U,2} & a'^{\mathbf{2}}_{U,2} & a'^{\mathbf{3}}_{U,2} & a'_{CU,2} \\ a'^{\mathbf{1}}_{U,3} & a'^{\mathbf{1}}_{U,3} & a'^{\mathbf{1}}_{U,3} & a'_{CU,3} \end{pmatrix} \begin{pmatrix} H_U^{11} & H_U^{12} & H_U^{13} & -v_U^1 \\ H_U^{21} & H_U^{22} & H_U^{23} & -v_U^2 \\ H_U^{21} & H_U^{23} & H_U^{33} & -v_U^3 \\ -v_U^1 & -v_U^2 & -v_U^3 & h_{CU} \end{pmatrix} \begin{pmatrix} a'^{\mathbf{1}}_{U,1} & a'^{\mathbf{1}}_{U,2} & a'^{\mathbf{1}}_{U,3} \\ a'^{\mathbf{2}}_{U,1} & a'^{\mathbf{2}}_{U,2} & a'^{\mathbf{1}}_{U,3} \\ a'^{\mathbf{3}}_{U,1} & a'^{\mathbf{3}}_{U,2} & a'^{\mathbf{1}}_{U,3} \\ a'_{CU,1} & a'_{CU,2} & a'_{CU,3} \end{pmatrix} \tag{5}$$

with

$$\begin{aligned} v'_{L,i=}\, a'_{CL,i}, (i = 1,2,3) \\ v'_{U,i=}\, a'_{CU,i}, (i = 1,2,3) \end{aligned} \tag{6}$$

Similarly, the new effective Hamiltonian, H'_C, and the vectors v'_{CL}, v'_{CU}, v'_{CR} and v'_{CD} are given by:

$$H'_C = \begin{pmatrix} a'_{CCL,1} & a'_{CCU,1} & \boldsymbol{a}'_{C,1} & a'_{CCR,1} & a'_{CCD,1} \\ a'_{CCL,2} & a'_{CCU,1} & \boldsymbol{a}'_{C,2} & a'_{CCR,1} & a'_{CCD,1} \\ a'_{CCL,3} & a'_{CCU,1} & \boldsymbol{a}'_{C,3} & a'_{CCR,1} & a'_{CCD,1} \end{pmatrix} \begin{pmatrix} h_{CCL} & 0 & -v_{CL}^{\dagger} & 0 & 0 \\ 0 & h_{CCU} & -v_{CU}^{\dagger} & 0 & 0 \\ -v_{CL} & -v_{CU} & H_C & -v_{CR} & -v_{CD} \\ 0 & 0 & -v_{CR}^{\dagger} & h_{CCR} & 0 \\ 0 & 0 & -v_{CD}^{\dagger} & 0 & h_{CCD} \end{pmatrix} \begin{pmatrix} a'_{CCL,1} & a'_{CCL,2} & a'_{CCL,3} \\ a'_{CCU,1} & a'_{CCU,1} & a'_{CCU,1} \\ \boldsymbol{a}'_{C,1} & \boldsymbol{a}'_{C,2} & \boldsymbol{a}'_{C,3} \\ a'_{CCR,1} & a'_{CCR,1} & a'_{CCR,1} \\ a'_{CCD,1} & a'_{CCD,1} & a'_{CCD,1} \end{pmatrix} \tag{7}$$

with

$$\begin{aligned} v'_{CL,i=}\, a'_{CCL,i}, (i = 1,\cdots,5) \\ v'_{CU,i=}\, a'_{CCU,i}, (i = 1,\cdots,5) \\ v'_{CR,i=}\, a'_{CCR,i}, (i = 1,\cdots,5) \\ v'_{CD,i=}\, a'_{CCD,i}, (i = 1,\cdots,5) \end{aligned} \tag{8}$$

2.2. Initialization, warm up and sweeping

In the present case, the system is enlarged by 8 sites at each step of iteration. Thus, the warm-up phase, with reflection symmetry, consists in iterating these operations:

1. The left and upper blocks are built and then enlarged by adding a single site.
2. The right and down enlarged blocks are obtained by just reflecting the left and upper blocks, respectively. In the case where there is no symmetry reflection, the former blocks (right and down ones) must be built independently.
3. The center block is built and then enlarged by adding a single site to each side (four sites).
4. All these operators must be stored to be used later.
5. The five enlarged blocks, including interactions between them, form the super-block Hamiltonian.
6. The latter Hamiltonian is diagonalized, and the N_E lowest eigenstates are obtained.
7. The new effective Hamiltonians and interaction vectors are then constructed.
8. Once the system size N is reached; then the center block continues to grow up by four sites at each iteration, whereas the left, upper, down and right blocks retrieve until the number of sites in each block is equal to N_E.
9. At each step below, the left, upper, down and right blocks used are just those stored before.
10. Then, the procedure is reversed: the left, upper, down and right blocks grow up while the center block retrieves until the number of sites in it is

 © 2010 The Moroccan Statistical Physical and Condensed Matter Society

just 5 sites. Similarly, the center blocks used are those stored as they have grown up before.

The image of the superblock at the end of these iterations is: four blocks representing a maximum of effective sites plus a center block with just 5 sites.

In order to improve accuracy of the results, a number of sweep cycles are needed, keeping fixed the system size. Due to the geometry of the present system, it was necessary for us to adjust the process of sweeping, the standard process being useless. Effectively, each sweeping cycle consists of two parts:

1. The left (right) and upper (down) blocks will retrieve down to their minimum size N_E, and the stored ones are used, while the center block grows up, using the procedure below, until its maximum number of sites is reached.
2. Then, a new set of operators corresponding to the left (right) and upper (down) blocks are generated, while the center block matrices are picked up from the stored ones.

After repeating these two steps many times, energy results will converge to the more accurate values that can be obtained by DMRG procedure.

III. Results

We consider the simple Anderson Hamiltonian in site representation:

$$H = \sum_i \ \varepsilon_i \ |i\rangle\langle i| + \sum_{\langle i,j\rangle} V \, |i\rangle\langle j| \tag{9}$$

with orthonormal states $|i\rangle$ corresponding to electrons located at sites i. V is the constant nearest-neighbor transfer integral with unit value and ε_i a site-diagonal random variable governed by a *normal* probability distribution *.i.e.*

$$P(\varepsilon_i) = \begin{cases} \frac{1}{W}, & |\varepsilon_i \ | \leq \frac{W}{2} \\ 0, & otherwise \end{cases}$$

W is the disorder strength. Other probability distributions, such the Gaussian one, can be also used.

Despite its simplicity and since it was suggested by P.Anderson [9], the model has been widely used to study spectral and localization properties of disordered structures [10, 11], metal-insulator transition induced by disorder [12, 13], transport in general topologically disordered media [14], multifractal aspects of wavefunctions [15, 16] for interacting and non-interacting electron systems.

We begin our investigation with an ordered structure *.i.e.* $\varepsilon_i = \varepsilon$. Unfortunately, there are no theoretical results to compare with; therefore, it is necessary to obtain the ground state and few excited states energies by exact diagonalization.

Table 1: The ground, first and second excited states energies $E_0(N)$, $E_1(N)$ and $E_2(N)$ for a free particle on a tight-binding model in a two-crossed chains, computed using exact diagonalization (ED) and DMRG method. The value of the diagonal entries in the diagonalized matrices is 2.0.

Method	N	E0(N)	E1(N)	E2(N)
ED	105	-0.309401076758301	1.352328451610949×10-2	1.352328451611478×10-2
DMRG	105	-0.309401076758301	1.352328451611124×10-2	1.352328451611313×10-2
ED	425	-0.309401076758508	8.619875459942861×10-4	8.619875459979135×10-4
DMRG	425	-0.309401076758506	8.619875460086855×10-4	8.619875460089741×10-4
ED	905	-0.309401076758518	1.915318921536133×10-4	1.915318921562604×10-4
DMRG	905	-0.309401076758502	1.915318922078220×10-4	1.915318922102459×10-4
ED	1465	-0.309401076758482	7.327654175460374×10-5	7.327654175659017×10-5
DMRG	1465	-0.309401076758503	7.327654180964834×10-5	7.327654181053537×10-5
ED	2025	-0.309401076758501	3.839568650589582×10-5	3.839568651057789×10-5
DMRG	2025	-0.309401076758502	3.839568654973506×10-5	3.839568655256073×10-5
ED	2505	-0.309401076758508	2.510520401701136×10-5	2.510520402393568×10-5
DMRG	2505	-0.309401076758506	2.510520404624172×10-5	2.510520404886720×10-5
ED	3065	-0.309401076758504	1.677677228672380×10-5	1.677677230021150×10-5
DMRG	3065	-0.309401076758505	1.677677232041186×10-5	1.677677232175863×10-5
ED	4025	-0.309401076758491	9.732859440333661×10-6	9.732859445854112×10-6
DMRG	4025	-0.309401076758504	9.732859465153467×10-6	9.732859468420359×10-6

Thus, results for the ground state, first and second excited states, obtained with both methods, are given in table 1. The number of targeted states is $N_E = 3$. Five sweeps are generally sufficient to reach convergence. As it can be seen from the table, a high degree of agreement exists between exact diagonalization results and our DMRG

 © 2010 The Moroccan Statistical Physical and Condensed Matter Society

results for the ground state; it ranges from complete agreement (in the order of computational material) for a system size equal to 105 sites (15 digits) to 12 digits when the size of the system exceeds 4000 sites. For first and second excited states energies, the agreement is still significant, but in a bit less degree. In fact, for a system of 105 sites, which is relatively small, the agreement between the methods is up to 13 digits and it is apparently kept at this level in the case of a system size exceeding 4000 sites. Certainly, the decaying accuracy of results as the system size increases is still a general behavior of DMRG method, though results do not make it so clear. It is essentially due to our limiting computational facilities to deal with much larger systems.

By introducing disorder, *i.e.* ε_i are randomly distributed, the symmetry of left, right, up and down blocks is lost, and we have to renormalize all blocks separately. As it is just a matter of comparison of our results with those obtained by exact diagonalization, we restrict our study to a single value of W, taken to be equal to $W = 2.0$. Table 2 displays results of the first three lowest energies of a disordered structure obtained by both exact diagonalization and DMRG procedure. From the table we can see an accurate results obtained by our calculations compared to those obtained by exact diagonalization (up to 12 digits for a system with $2{,}425$ sites), although the size of the structures is not so big to be considered as representing real materials. This is due in first place to computational restrictions, which were, let's remind, the major instigator to explore other ways in dealing with such huge systems. Nevertheless, regarding the behavior of our results for those relatively small sizes, we may think that accuracy, by its decreasing aspect when system size increases, will not be completely lost before a considerable size is reached.

In other hand, this procedure enables us to obtain the ground state of a non-interacting disordered system by just multiplying the ground state value by the number of sites of the system (one electron per site). This value could be a rough estimation of energy scale for the ground state of an interacting disordered system.

IV. Conclusion

In this paper, we presented a DMRG procedure extension to compute low states energies of a two disordered crossed chains within the tight-binding model suggested by P. Anderson. The purpose of this work was to try to bring a different insight on a major challenging problem vis-à-vis the application of the DMRG procedure to systems with geometry other than 1-d. Instead of the standard two-blocks configuration, we have adopted a five-blocks configuration (four environment blocks and a system block in-between), with a bit different way to achieve warm-up phase and sweep cycles. Results obtained have shown that the new procedure works with a high precision within a certain accuracy. They have also shown a "decaying accuracy as size increases" behavior, proper to standard DMRG.

The present procedure can be applied to many-body problems (spin systems, fermionic and bosonic systems) but, unfortunately, it seems to be, as we have tried it, a big memory and time consumer.

Table 2: The ground, first and second excited states energies $E_0(N)$, $E_1(N)$ and $E_2(N)$ for a free particle on a tight-binding model in a two-crossed chains, computed using exact diagonalization (ED) and DMRG method. The disorder strength W is equal to 2.0.

Method	N	E0(N)	E1(N)	E2(N)
ED	105	-2.33492839367123	-2.31256015487412	-2.27633450482704
DMRG	105	-2.33492839248340	-2.31256015458150	-2.27633450453549
ED	425	-2.62707526909553	-2.51368257944855	-2.49551862249973
DMRG	425	-2.62707353842147	-2.51368257944855	-2.49551862249973
ED	825	-2.74034137548984	-2.66488808899811	-2.62707526909553
DMRG	825	-2.74034137548807	-2.66484686948334	-2.62707526909553
ED	1225	-2.68329769657425	-2.66115344781251	-2.63257708999018
DMRG	1225	-2.68329769655407	-2.66115344781251	-2.63257708999017
ED	2425	-2.64472106170087	-2.63084212954662	-2.61585544521942
DMRG	2425	-2.64472106170071	-2.63084212954661	-2.61585544521941
ED	3225	-2.74712495427613	-2.61737491050982	-2.59050557867426
DMRG	3225	-2.74712485946028	-2.61736733389125	-2.59050557867427

V. References

[1] S. White, Phys. Rev. Lett. 69, 2863 (1992), Phys. Rev. B 48, 10345 (1993).

[2] N. Shibata, J.Phys.A: Math Gen, vol 36,issue 37 (2003).

[3] T. Xiang, J. Lou and Z. Su, Phys. Rev. B 64, 104414 (2001).

[4] T. Nishino, J. Phys. Soc. Japan, vol 65, issue 4 (1996).

 © 2010 The Moroccan Statistical Physical and Condensed Matter Society

[5] S. Moukouri, L. G. Caron, Phys. Rev. B 67, 092405 (2003).
[6] P. Henelius, Phys. Rev. B 60 9561 (1999).
[7] S. White, Phys. Rev. Lett. 77, 3633 (1996).
[8] M.A. Martín-Delgado, G. Sierra and R.M. Noack, J.Phys.A: Math Gen, vol 32,issue 33 (1999).
[9] P. Anderson, Phys. Rev. 109, 1492 (1958).
[10] B.I. Shklovskii, B. Shapiro, B. R. Sears, P. Lambrianides, and H. B. Shore, Phys. Rev. B 47, 11487 (1993).
[11] V. Uski, Phys.Rev.B 62 R7699 (2000).
[12] D. Belitz and T. R. Kirkpatrick, Rev. Mod. Phys. 66,261 (1994).
[13] E. Abrahams, P. W. Anderson, D. C. Licciardello, and T. V. Ramakrishnan, Phys. Rev. Lett. 42, 673 (1979).
[14] P. A. Lee and D. A. Stone, Phys. Rev. Lett 55, 1622 (1985).
[15] M. Schreiber, Phys. Rev. B 31, 6146 (1985).
[16] C.M. Soukoulis, E.N. Economou, Phys. Rev. Lett 52, 565 (1984).

 © 2010 The Moroccan Statistical Physical and Condensed Matter Society